To my parents, my sister,
Daniela and Prakash

"Das höchste Glück des denkenden Menschen ist es, das Erforschliche erforscht zu haben und das Unerforschliche ruhig zu verehren."

Johann Wolfgang von Goethe

Studying the Patterning Mechanisms and Cell Fates during Limb Regeneration in *Ambystoma mexicanum*

DISSERTATION

Zur Erlangung des akademischen Grades

Doctor rerum naturalium

(Dr. rer. nat.)

vorgelegt

der Fakultät Mathematik und Naturwissenschaften

der Technischen Universität Dresden

von

Dipl.-Biol. Martin Kragl

Geboren am 09.10.1978 in Erfurt

Gutachter:

Prof. Dr. Michael Brand

Prof. Dr. Kiyokazu Agata

Dr. Elly Tanaka

Summary

One of the most fascinating but least understood phenomenon that has attracted researchers for centuries is the regeneration of the urodele limb. The present thesis is a contribution to unravel fundamental mechanisms and to develop new techniques that will aid studying the mechanisms.

Limb regeneration occurs via a pool of progenitor cells collectively referred to as the blastema. The blastema forms from local tissues in the stump such as skin, muscle, bone and nerves, which respond to the dramatic changes in their environment by loosing their organization and releasing cells. These progenitors start dividing and, during the course of regeneration, replace the entire portion of what has been missing.

One fascinating aspect of urodele limb regeneration is that, when amputated at the level of the upper arm, an entire limb regenerates while, when amputated at the level of the hand, exclusively a hand forms. How do cells in the limb know which portion to reconstitute? Cells acquire this information very early, and it has been suggested that independent of the level of amputation, the first cells that arise are specified to hand fates. Followed by the sequential intercalation of progenitors of intermediate elements. It is technically challenging to verify this model, and it demands that a small amount of tissue is tested on the single cell level. We developed single cell PCR as a technique that aids to understand the early patterning events by looking at their expression of *HoxA* genes. The expression domains of *HoxA* genes mark the future upper arm, lower arm and hand elements. Although we lose this spatial information by collecting and analyzing single cells, we are able to distinguish progenitors of different elements from their combined expression of *HoxA* genes. Therefore, we can determine at what time points hand, lower arm and upper arm progenitors arise.

Another aspect of regeneration that has been investigated for decades is the influence of the different stump tissues on pattern and tissue formation. Do all progenitors contribute equally to the reconstruction the three-dimensional structure of the limb? Do cells in the blastema possess a tissue specific memory that directs a preferential contribution to certain tissue types? We addressed these two questions using transgenic animals that ubiquitously express GFP under control of the CAGGS promotor as donors of fluorescent skin, bone and muscle tissue as well as Schwann

cells, which we transplanted into wild type host. We show that these tissues integrate into the host limb and contribute progenitor cells to the blastema. This allows us to study the fate of the cells deriving from different sources. We demonstrate that bone derived cells have a priority to contribute to newly forming skeletal elements, while progeny of skin is found in a variety of other tissues including bone, tendons and connective tissue. One principle is common to both tissue types: Muscle does not arise from either of these sources. We studied the ability of the differently derived progenitor cells on patterning based on two major findings related to positional information during regeneration: 1) The identification of *Meis* and *HoxA* genes as important key determinants of positional information. 2) The ability of blastema cells to retain their identity, which becomes most obvious when cells derived from the hand level are transplanted to the upper arm region. During the course of regeneration, these cells translocate back to their level of origin and contribute to hand tissue. We show that this does not apply to cells in the blastema that originate from Schwann cells, and that this inability of retaining positional memory correlates with the fact that *Meis* and *HoxA* genes are not active in these cells. Therefore, we suggest that cells in the blastema do not equally contribute to pattern the regenerate.

I herewith declare that I have produced this thesis without the prohibited assistance of third parties and without making use of aids other than those specified; notions taken over directly or indirectly from other sources have been identified as such. This thesis has not previously been presented in identical or similar form to any other German or foreign examination board.

This work was 01.09.2003 - 29.06.2007 under the supervision of Prof. Dr. Michael Brand in Dr. Elly Tanaka's laboratory at the Max-Planck-Institute for Molecular Cell Biology and Genetics.

Dresden, 29.06.2007

TABLE OF CONTENTS

ABBREVIATIONS

7'AAD	7' aminoactinomycin
AEC	apical epidermal cap
AER	apical ectodermal ridge
A/P	anterior-posterior
BrdU	5-Bromo-2-Deoxyuridine
CAGGS	CMV enhancer fused with chicken β-actin promotor
CMV	cytomegalo virus
D/V	dorsal-ventral
Fgf	fibroblast growth factor
GFP	green fluorescent protein
PBS	phosphate buffered saline
PCR	polymerase chain reaction
P/D	proximo-distal
PFA	paraformaldehyde
RA	retinoic acid
TBS	tris buffered saline

INDEX OF TABLES

INDEX OF FIGURES

ACKNOWLEDGEMENTS

I want to thank my supervisor Elly Tanaka for introducing me to the field of regeneration and many interesting discussions. I am very grateful also for her financial support and that she made it possible for me to attend various conferences and work for 2 months in Japan. This was extremely stimulating for me. Many thanks also to the Tanaka lab. In particular, I want to thank Heino Andreas for reliable and excellent axolotl care, Dunja Knapp as she provided me with axolotls specifically labelled for Schwann cells, Akira Tazaki and Anja Telzerow for helping with and discussing about my work. My thanks go also to former members of the lab, especially Karen Echeverri and Esther Schnapp for helpful suggestions concerning my work.

I am very grateful to Kiyokazu Agata and members of his lab, especially Hiroshi Tarui, Tetsutaro Hayashi and Yutaka Imokawa. For 2 months, I could stay in this laboratory and learn how to perform single cell PCR in a high throughput way. I learned a lot during this time – thank you!!

Many thanks also to Ina Nüsslein. She helped me to establish FACS analysis and sorting of cells derived from regenerating axolotl limbs, and this work would not have been possible without her.

Many thanks to the protein expression facility, as it generates the best TAQ! Thanks also to the DNA sequencing facility for reliable and fast sequencing.

I am very greatful to Michael Brand and Kiyokazu Agata for taking the responsibility to review this thesis.

Special thanks to Karen Echeverri and Leah Herrgen for critical reading of the manuscript.

1. Introduction: Patterning Events during Regeneration

1.1 Regeneration – a phenomenon shared between various species

The ability of animals to regrow lost body parts has been known and studied since ancient times. Among the first people interested in regeneration was the greek philosopher Aristotle, who refers in his book "Generation of Animals" to the ability of lizards to regrow their tails. Regeneration is a phenomenon that is widely distributed among animals, and species that regenerate lost body parts include hydra, planarians, arthropods, teleosts and amphibians (for review, see Slack, 2003). The ability of mammals to regenerate is limited to the adult liver and infant fingertips (Hata et al., 2007, Yoshizato, 2007).

During the past decades, due to the establishment of modern molecular biology tools, regeneration became an interesting subject with regard to elucidate those mechanisms that initiate and direct the replacement of lost organs or appendages, and to understand how regeneration of damaged or defective tissue can be induced in humans.

One popular system to study this is the planarians, one of the simplest metazoans in which regeneration is manifested. Amazingly, a complete individual regenerates from a small body part, and two topics are mainly investigated in this organism. Planarians possess a very simple central nervous system (CNS), consisting of a U-shaped brain located anterior and a pair of longitudinal ventral nerve cords along the body (Agata and Watanabe, 1999). Thus, planarians are one of the most simple systems in which CNS regeneration is studied, and progress has been made in identifying key regulators. For example, a gene coding for a fibroblast growth factor receptor (FGFR)-like molecule named *Nou-darake* has been found to restrict brain formation to the head region (Cebria et al., 2002). Furthermore, the implication of molecules with regard to rebuilding correct brain function is tested in planarians. In a recent study, mRNA of a gene called *Djsnap-25* was specifically eliminated in the head region during regeneration, and the newly formed brain was normal in its morphology, however, negative phototaxis was affected in these animals (Takano et al., 2007).

Regeneration in planarians occurs through a specific population of somatic stem cells called neoblasts, which are the only mitotically active cells in planarians (Newmark and Sanchez-Alvarado, 2002). Thus, planarians may provide useful information concerning somatic tissue turnover and stem cell biology, and work on identifying the molecular networks underlying stem cell- based regeneration is in progress (Reddien et al., 2005a; Sanchez-Alvarado, 2006). For example, a recent study identified the gene *smedwi-2* to be important for regulating both regeneration and replacement of aged tissue (Reddien et al., 2005b).

The lowest vertebrates that regenerate wounded tissues and organs are the teleosts, and already more than 200 years ago Broussonet described that adult fishs can completely restore their fins after amputation. With the establishment of zebrafish as a model organism, more and more studies are directed to elucidating the underlying molecular mechanisms. For example, *Fgf20* has been identified to play a key role in initiating regeneration of the fin (Whitehead et al., 2005), and it has been demonstrated that components of the Wnt pathway are implicated in fin regeneration (e.g., Poss et al., 2000; Stoick-Cooper et. al., 2006).

Apart from fins, neural tissues are also capable of regenerating. It has been shown that the retina regenerates by a stem cell based mechanism (Otteson and Hitchcock, 2003), and amazingly, spinal cord tissue recovers after complete transection due to axonal regrowth (Becker et al., 1997). Zebrafish also have the remarkable ability to regenerate injured brain due to neural stem cells, which remain active throughout the life of the animal, and studies on these phenomena may provide insight into how mammalian CNS regeneration can be ectopically induced (Volker Kroehne, personal communication). Another relevant organ that regenerates in zebrafish is the heart, and progress is made in identifying molecular and cellular mechanisms (for review, see Poss, 2007).

However, the highest vertebrates and therefore evolutionary more closely related to humans that can regenerate are the amphibians, and urodeles such as newts and salamanders are unique in their ability to replace lost appendages and organs such as limbs, tail, gills, jaw and part of the heart. When loosing a limb, the correct amount of all tissues that also build a human limb like skin, muscle, bone and nerves regenerate. Studies on regenerating urodele limbs have a long history, and two issues were mainly investigated during the past decades aiming to understand the principles of

regeneration of such a complex structure, and gaining more insight in how damaged or defective human tissue could be cured. It has been found more than 80 years ago that tissues other than bone can replace skeletal structures during regeneration (Weiss, 1925; Bischler, 1926), and a question relevant for tissue engineering is whether a change of cell fate is a necessary feature of regeneration, or whether tissue-specific regeneration can also take place.

Furthermore, regeneration of an entire limb occurs from only a small number of cells at the site of amputation. These cells know exactly which portion to regenerate and form a hand when the hand was amputated, or form an entire limb when amutation took place at the shoulder level, which in its three dimensional morphology is an exact copy of the one being lost. What mechanism(s) drive these cells to pattern the limb, and which tissue types participate in the patterning process? These questions were extensively studied during the past decades, however, due to the lack of modern molecular biology tools they were restricted to transplantation experiments and morphological observation.

In this work, we aim to investigate several questions regarding urodele limb regeneration that had interested researchers for decades: What mechanism(s) lead(s) to the reestablishment of such a complex structure, with the correct amount of tissue regenerated and with all its elements located at the right place? What are the roles of the different tissues during regeneration regarding the patterning process and tissue formation?

We develop and work with new molecular tools directed to answer these questions, however, we also refer to earlier studies and integrate our investigations into the network of knowledge that derives from this work.

1.2 Stages of urodele limb regeneration

The vertebrate limb is a three- dimensional structure defined along three axes, the proximo-distal (P/D), dorsal-ventral (D/V), and anterior-posterior axis (A/P). From proximal to distal, it is divided into three major segments, the upper arm, lower arm and hand.

Urodele limb regeneration occurs through different morphological changes and three characteristic steps, which are 1) wound healing, 2) dedifferentiation and blastema formation, and 3) repatterning of the missing structure (Figure 1-1).

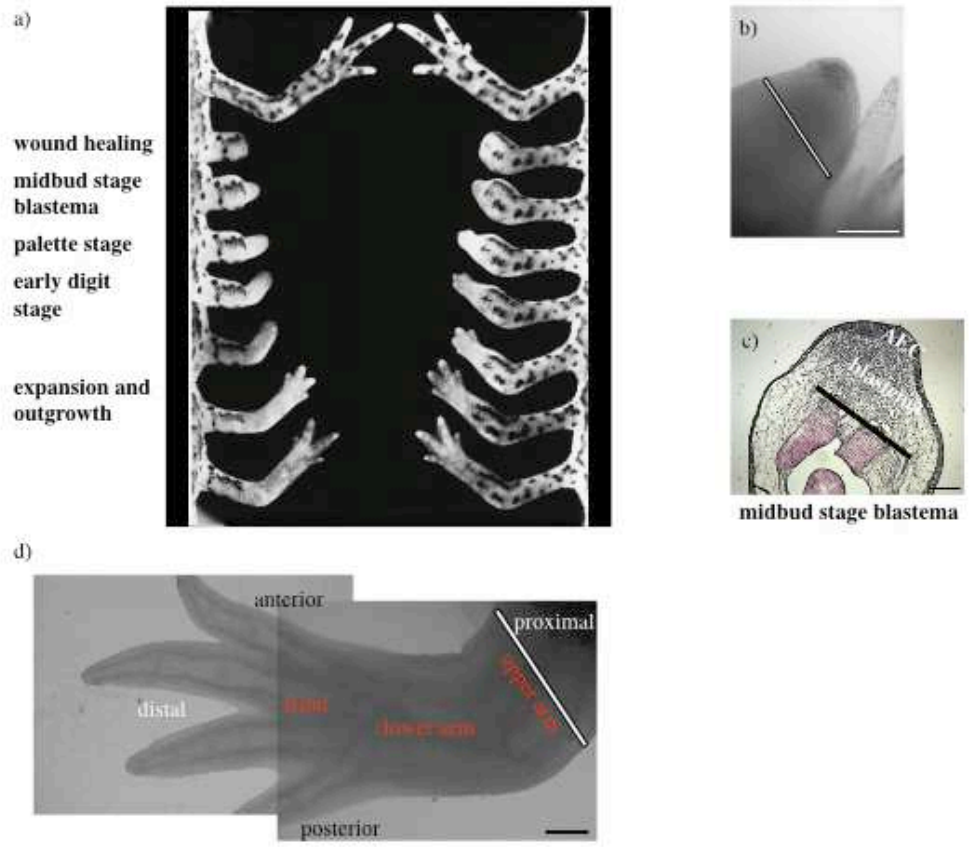

Fig. 1-1: Regeneration of the urodele limb. a) Stages of limb regeneration. Depending on size and age of the animal, the midbud stage blastema is reached between 3 and 7 days and progresses into the palette after 10-28 days, respectively. After 4-12 weeks, the entire arm has regenerated. From: Goss, 1969. b) Bright field view of the midbud stage blastema. Bar: 0.5 mm. c) Section of a midbud stage blastema stained with hematoxylin/eosin. Bar: 50 μm. d) The limb is a three dimensional structure, and a relative position of a cell within this system can be described along the proximo-distal, anterior-posterior and dorso-ventral axis. Along the proximo-distal axis are the three main elements hand, lower arm and upper arm, with the upper arm located more proximally and the hand located more distally. Dorsal is to the reader. Bar: 0.5 mm.

1.2.1 Wound healing

Within 24 hours after amputation, adjacent epithelial cells migrate over the cut surface to form a one cell layer thick epithelium called the wound epidermis (Repesh and Oberpriller, 1978). Thereafter, the wound epidermis thickens and forms the apical epidermal cap (AEC). The basal layers of the AEC are functionally and morphologically equivalent to the apical ectodermal ridge (AER) of the developing limb bud (Saunders, 1948, Christensen and Tassava, 2000). The AEC is essential for outgrowth of the regenerating limb, and its surgical removal or replacement by mature skin blocks regeneration (Stocum and Dearlove, 1974; Mescher, 1976; Tassava and Garling, 1979). It expresses mitogens of the FGF family, like FGF-1 and FGF-2, resembling the situation during limb development where the AER provides growth and proliferation factors (Boilly, 1991; Mullen, 1996; Christensen, 2002; Dungan, 2002).

1.2.2 Blastema formation

Between the stump tissue and the wound epidermis, a pool of progenitor cells forms that is collectively referred to as the blastema (Butler and O'Brien, 1942; Hay and Fischman, 1961; O'Stien and Walker, 1961). Depending on the age and size of the animals, this tissue becomes visible between 3 and 7 days. Blastema cells proliferate and will, during the course of regeneration, entirely replace the lost structure. During the early, medium and late midbud stages of regeneration, the blastema has a cone-like shape and morphologically resembles the outgrowing limb bud.

Blastema formation in urodeles occurs through a considerable extent by local dedifferentiation of fully differentiated mesenchymal tissues at the amputation plane, such as muscle, dermis, bone or Schwann cells, that give rise to proliferating mononucleate cells that populate the blastema (Thornton, 1938, 1968; Hay and Fischman, 1961; Steen, 1968; Namenwirth, 1974; Muneoka et al., 1986; Lo et al., 1993; Kumar et al., 2000, Echeverri et al., 2001). Mechanisms of dedifferentiation during blastema formation as well as the role of different tissues will be extensively discussed in chapter 3.

In addition to the AEC, the presence of innervating nerves is required for proliferation and outgrowth of the regenerate (Lloyd and Tassava, 1980; Mullen et al., 1996) and it has been recently demonstrated that deviation of a nerve so that it faces a lateral skin wound was sufficient to induce ectopic blastema formation (Endo et al, 2004). Putative candidates for nerve mitogenic factors include FGF-2, GGF-2, transferrin and substance P (Globus, 1988; Mescher, 1996; Mullen et al., 1996; Wang et al., 2000).

Nerves and AEC do not act independently on the blastema. The gene Dlx-3 is believed to be crucial for blastema growth and proliferation and is upregulated in the AEC beginning from the early stages of regeneration. Upon denervation, its expression ceases but can be rescued by ectopic supply of FGF-2, demonstrating a functional and molecular relationship between nerves and the AEC during early stages of regeneration (Mullen et al., 1996).

1.2.3 Redifferentiation and Patterning

As outgrowth of the blastema progresses, the whole structure flattens to form a palette and chondrogenic condensations become visible at this stage. Regeneration then proceeds into the digit stage, at this time point a considerable amount of cells have differentiated and the shape of the digits becomes obvious. The regenerate thickens and expands. Whereas wound healing and blastema formation are nerve dependent, redifferentiation and repatterning do not require the presence of nerves (Stocum, 1968).

In the classic view, wound healing and blastema formation are unique to regeneration, whereas redifferentiation and outgrowth of the extremity are considered to be similar to the events occurring during limb development. Among the subjects that have interested researchers most during the past decades were the exact properties of the blastema cells that lead to repatterning and the time point(s) at which cells acquire their new positional values.

1.3 Positional identity is already established at the blastema stage

Despite being considered as a pool of multipotent progenitor cells, the blastema is a highly organized tissue, and a number of experiments indicate that the essential patterning information is already established at that time when cells are still undifferentiated (Stocum, 1968; Dearlove and Stocum, 1974; Michael and Faber, 1961). For example, transplantation of the midbud stage blastema, at that time point consisting of approximately 10,000 cells, to a neutral environment such as the dorsal fin results in formation of all the limb elements that would have formed in situ (Stocum, 1968; Fig. 1-2). Recently, Echeverri and Tanaka (2005) examined the patterning information present in the midbud blastema by performing cell marking and inter-blastema transplantation experiments and concluded that P/D identity of cells could be established in the blastema by 8 days after limb amputation. In these experiments, cells in the proximal and distal region of the blastema were labeled by electroporation of fluorescent protein-encoding plasmids, and depending on where cells were labeled, they were either found in the regenerated upper arm or hand, respectively (Fig. 1-2). When fluorescent cells from the distal tip of a 4-day blastema were transplanted to the proximal region of an 8-day proximal blastema, the transplanted cells translocated to their region of origin and ultimately contributed to the regenerated hand, indicating that at this time they were already irreversibly specified to their distal cell fate. The same result was observed with cells from the tip of a proximal blastema. In contrast, proximal-to-distal transplantations resulted in loss of cells.

These experiments demonstrate that cells acquire their positional information relatively early during the course of regeneration, however, do all cells at any proximo-distal level have the same potency to alter their identity?

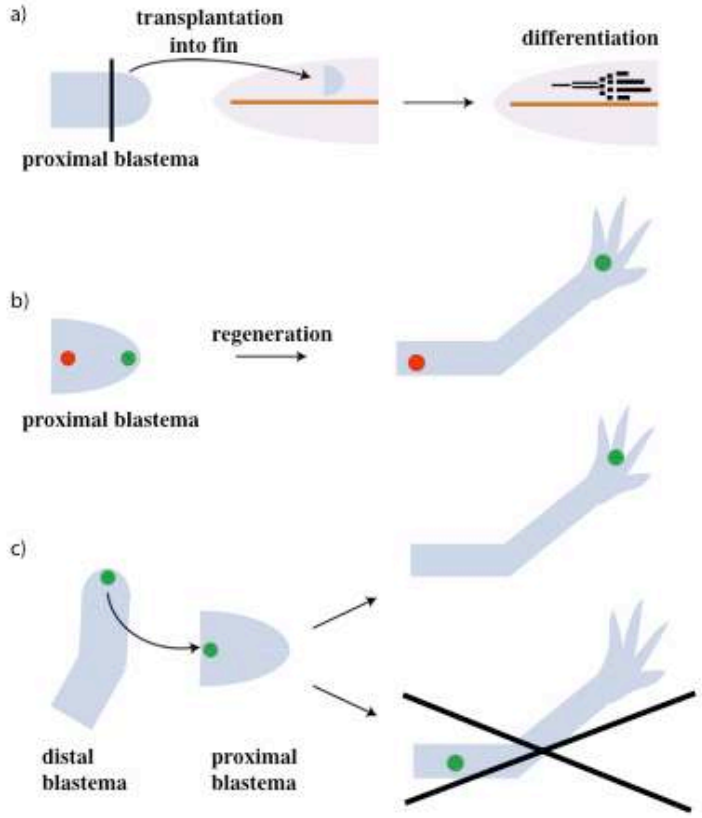

Fig. 1-2: The blastema is an autonomous system. a) If transplanted into a different environment such as the dorsal fin, it differentiates into a miniature limb (Stocum, 1968). b) Blastema cells located at different proximo-distal levels do not mix during regeneration. c) Distal blastema cells are determined to their fate. If transplanted to a more proximal level, they translocate to their level of origin during the course of regeneration (Echeverri and Tanaka, 2005).

1.4 The rule of distal transformation

In salamanders, limb regeneration is normally uni-directional, meaning that cells at the amputation plane will always regenerate limb elements more distal to that location, a phenomenon that has been termed “the rule of distal transformation” (Rose, 1962, Stocum, 1975; Maden, 1980). This was most clearly illustrated in an experiment where an “inverse” limb was created by suturing the wrist to the body (Figure 1-3). After healing, amputation resulted in a limb where the wrist element lay in the proximal position, while the upper arm was in the distal position. Such limbs regenerated a wrist from the inverted upper arm, rather than upper arm elements (Rose, 1962). This result indicates that cells at the amputation plane have an identity associated with their position along the P/D axis, a concept called positional memory (Wolpert, 1969), but then amputation can reprogram some cells or their progeny to a more distal identity. What properties in the blastema determine the differences between proximal and distal cells?

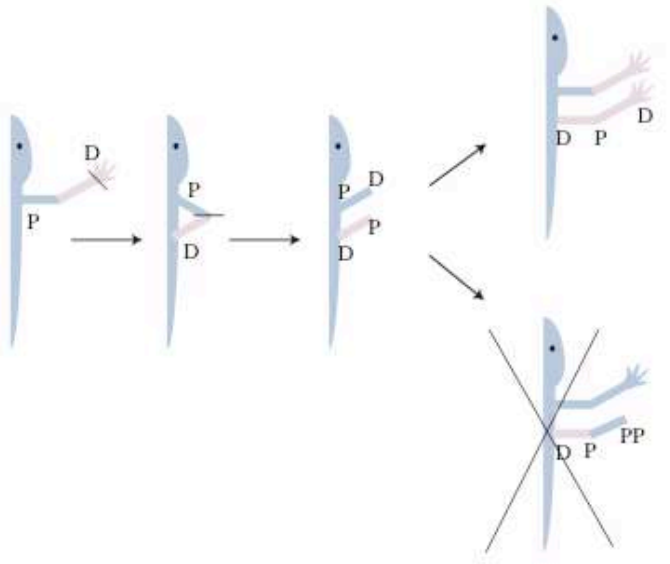

Fig. 1-3: The rule of distal transformation. When an "inverse" limb is created, more distal (D) elements regenerate from the proximal (P) site. Regeneration of more proximal (PP) elements does not occur, demonstrating that distal-to-proximal changes of cell identity do not normally occur (Rose, 1962).

1.5 Positional information exists as a graded property

A number of grafting experiments have implicated the role of local cell-cell interactions in patterning the regenerating P/D axis. When a wrist blastema is transplanted onto an upper arm stump, a normal regenerate forms in which the positions between upper arm and hand derive primarily from the upper arm stump (Stocum, 1975; Iten and Bryant, 1975; Pescitelli and Stocum, 1980). This phenomenon has been termed intercalary regeneration, where the upper arm stump intercalates the missing limb positions up to the transplanted distal blastema. Intercalary regeneration does not occur when a digit stage distal blastema or a mature hand is grafted to a proximal stump (Stocum, 1975).

Transplantation of an upper arm blastema to wrist results in growth of the upper arm from the wrist (Stocum and Melton, 1977). Notably, there is no inverse arm produced between the wrist stump tissue and the upper arm blastema as may be expected if the intercalary behavior was reciprocal. This difference in recognition has also been observed in experiments performing interblastema transplantations of cells. While distal cells, when grafted to a more proximal region, translocated back to their original level, proximal cells died when transplanted to the distal tip of the blastema (Echeverri and Tanaka, 2005). The basis of these different effects of recognition is unknown.

This ability of proximal and distal blastema tissue to recognize each other is also manifested in another way that has been termed affinophoresis. When a distal blastema is grafted onto the side of a regenerating upper arm at the junction between mature and blastema tissue, the grafted distal blastema is carried along the regenerating proximal blastema so that it ultimately produces a second hand emanating from the wrist (Crawford and Stocum, 1988) and indicates that cells from the same P/D region have a preferential affinity for like cells. This was further investigated by juxtaposing proximal and distal blastemas in hanging drop cultures (Nardi and Stocum, 1983). In such preparations, the proximal tissue engulfs the distal tissue, indicating different adhesive properties between distal and proximal cells. When distal-distal or proximal-proximal tissue is confronted, a straight border is maintained.

It has been proposed that these observations reflect the cell surface recognition processes required for intercalary regeneration. Whether these recognition events are a cause or a consequence for P/D patterning is one of the big challenges to address and mainly depends on the elucidation of the underlying molecules and genetic networks.

1.6 Regulators of proximal identity

1.6.1 Retinoic acid and regeneration

In 1978, Niazi and Saxena made an intriguing observation: When they amputated the hindlimb buds of the toad *Bufo andersoni* through the shank and treated them with retinyl palmitate, the regenerate contained duplications in the proximodistal axis. Thus, the law of distal transformation was experimentally bypassed and distal cells were respecified to obtain an identity more proximal to their origin.

When investigated on regenerating urodele limbs, Niazi and Saxena's result was reproduced and treatment with retinoids reprogrammed cells at the wound surface to become more proximal (Maden, 1982, 1983; Kim and Stocum, 1986). In the most extreme case, a complete limb containing stylopod, zeugopod and autopod was regenerated by a blastema derived from the wrist level. Treatment with a lower concentration produced limbs with only the zeugopod being duplicated, and further

dilution resulted in limbs with one single but extended zeugopod (Figure 1-4). This demonstrates that retinoids reprogram the cells at the amputation plane in a graded, concentration-dependent manner. When naturally occurring retinoids were tested regarding their potency in changing cell fate, retinoic acid (RA) was found to have the strongest effect, followed by retinol, retinyl palmitate and retinyl acetate.

Retinoids can also affect cell adhesion. In cell affinophoresis assays, RA treated distal blastemas were not engulfed by proximal ones (Figure 1-4). Furthermore, RA treated distal blastemas were not displaced during regeneration when grafted onto the dorsal site of a proximal blastema.

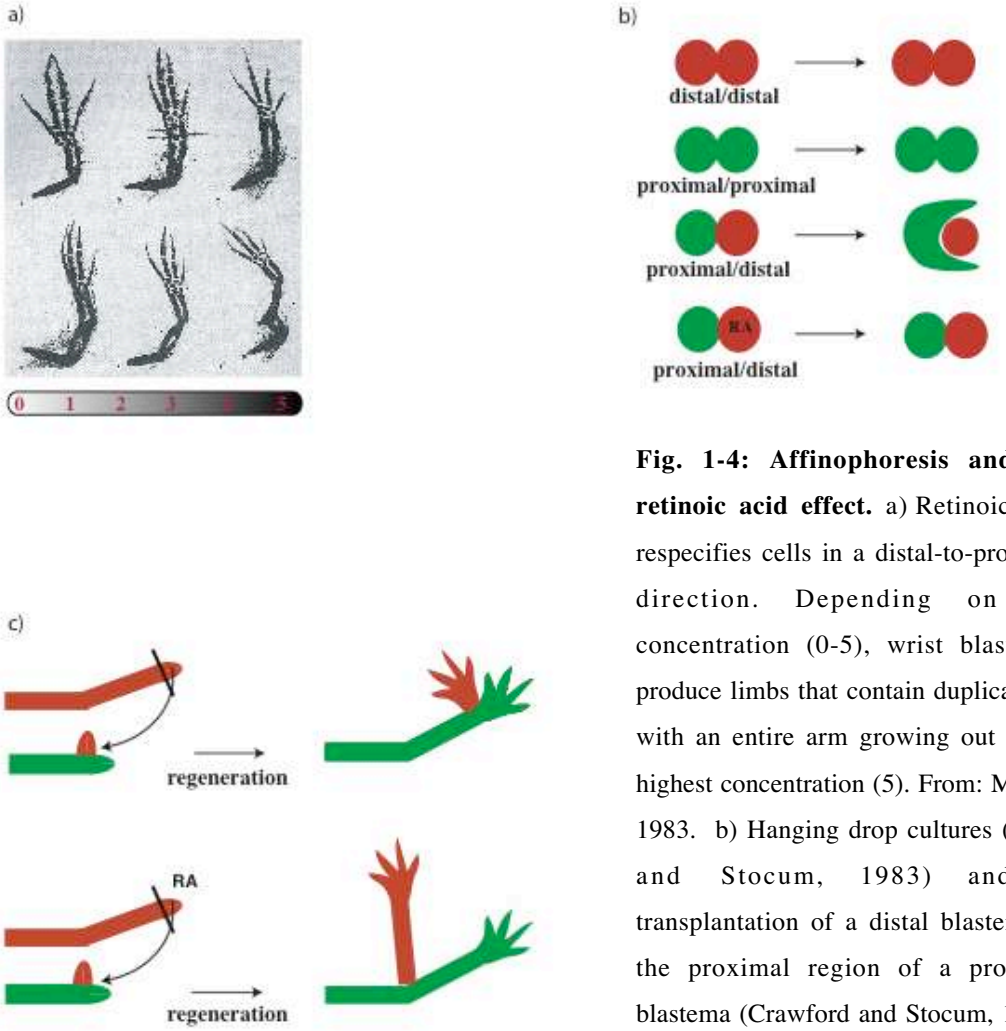

Fig. 1-4: Affinophoresis and the retinoic acid effect. a) Retinoic acid respecifies cells in a distal-to-proximal direction. Depending on the concentration (0-5), wrist blastemas produce limbs that contain duplications, with an entire arm growing out at the highest concentration (5). From: Maden, 1983. b) Hanging drop cultures (Nardi and Stocum, 1983) and c) transplantation of a distal blastema to the proximal region of a proximal blastema (Crawford and Stocum, 1988), both illustrating that positional information involves the cell surface. In the presence of RA, a distal blastema behaves as a proximal one.

1.6.2 Does endogeneous RA act as a proximalizing morphogen?

Since the degree of RA dependent duplications of limb segments during regeneration is concentration dependent, it is tempting to speculate that RA might be an endogenous morphogen. However, although retinoids were identified in the blastema, they have also been shown to influence posteriorization, ventralization, the morphology of the AEC, nerve growth into the blastema and several other processes (see Maden, 1985 for review). Therefore, it is experimentally challenging to investigate a possible role of RA for proximo-distal patterning.

However, it seems unlikely that RA participates in the patterning process. As discussed earlier, distally derived cells do not change their identity when transplanted to a more proximal level. They rather migrate to the level of their origin, demonstrating that they were not reprogrammed in a distal to proximal way upon transplantation. On the other hand, a possible role of RA in conferring proximal identity during the earliest stages of regeneration could never be ruled out completely. So far, all experiments addressing this question were performed on the midbud stage blastema, a stage in which progenitors of upper arm, lower arm and hand have already specified.

In this context, it is important to mention that five retinoic acid receptor (RAR) isoforms, α1, α2, δ1a, δ1b and δ2 were detected in the blastema, from which each is assumed to trigger different downstream events (Schilthuis et al., 1993; Gann et al., 1996). In a study to investigate which of the isoforms confers proximalization, Pecorino et al. (1996) generated chimeric RAR's for each isoform whose ligand binding domains were exchanged to a thyroid binding domain. These constructs were transfected seperately into distally derived blastemas that were grafted to a proximal stump. Upon thyroid treatment, cells transfected with the δ2 construct translocated proximally and thus violated the rule of distal transformation. All other constructs showed no response. Although the battery of genes conferring proximal translocation and being activated by the δ2 isoform remains to be elucidated, a few genes that respond to RA and are involved in conferring proximo-distal identity have been found.

1.6.3 Downstream factors of RA

In a screen aiming to identify genes that 1) are up- or downregulated by RA, 2) are differentially expressed between proximal vs. distal blastemas and 3) code for a cell surface molecule, the only candidate that met these three criteria was Prod1 (da Silva et al., 2002). Its ortholog CD59 in mammals is a cell surface antigen involved in the later steps of the complement pathway (Davies et al., 1989). Prod1 is a GPI linked cell surface protein whose expression level in a proximal blastema is 1.7 fold higher compared to that of a distal one. Interestingly, Prod1 is also expressed in a graded fashion in the mature limb, suggesting a role in the positional memory system of the limb. Treatment with phospholipase C and antibodies directed against distinct regions of the protein blocked proximal engulfment in an affinophoresis assay, demonstrating a functional and molecular link between Prod1 and positional identity (da Silva et al., 2002). Further evidence came from in vivo cell labeling experiments, which showed that distal blastema cells that had been electroporated with Prod1 migrated to a more proximal location (Echeverri and Tanaka, 2005). However, there are a lot of open questions. Although there is a proximal-to-distal graded expression of Prod1 in the mature limb, there is no evidence of such a gradient being present in the blastema. Furthermore, there is no published information about possible ligands. Also, the role of Prod1 during development is not known.

Recent studies on both limb development and regeneration have revealed a link between the proximalizing RA pathway and the homeobox containing transcription factors of the Meis family (Mercader et al., 1999, 2005). Ectopic expression of Meis1 or Meis2 abolishes the development of distal structures and leads to a proximilization of the developing limb in mouse and chicken. In the presence of RA, Meis1 and Meis2 are upregulated. During limb regeneration, Meis transcription factors are expressed in a proximal-to-distal gradient in the blastema (unpublished observations), and overexpression of Meis1 or Meis2 in distal blastema cells leads to their proximal translocation. Like Prod1 overexpressing cells, it could not be investigated whether those translocated cells also differentiated at their new location. Strikingly, in the presence of Meis antisense morpholinos, RA treated regenerating limbs did not produce duplications along the proximodistal axis, demonstrating that Meis genes act downstream of RA (Mercader et al., 2005).

It is not known which genes become upregulated by Meis transcription factors during development and regeneration and how proximal identity is established by them. Also, it remains unclear whether Meis 1, Meis2 and Prod1 act in the same RA induced pathway and, if yes, which one is upstream of the others.

1.7 Regulators of distal cell identities

While clear progress has been made on factors that can proximalize cells, very little is known about which molecular factors can confer a distal identity to blastema cells. As discussed above, some cells at the plane of injury are converted from a proximal to a distal cell identity, and this is likely to depend on the A/P or D/V confrontation of cells.

1.7.1 Fgfs

During limb development and regeneration, there are a number of molecules expressed in the AER/ AEC and the distal limb bud/ blastema, respectively, that are important for keeping limb bud/ blastema cells in a proliferative, undifferentiated state. These include FGF2, FGF4, FGF8, FGF10 and Msx1 (Christensen et al., 2001, 2002). However, experiments transplanting AER/AEC from one stage or another, or those replacing the epidermal tissue with beads soaked in FGF indicate that FGF is rather a permissive factor that interacts in an unknown way with another patterning system to generate P/D pattern (Niswander et al., 1993). In this context, it is interesting to recall that the AER, and more specifically Fgfs have been shown to restrict the RA effects in the distal region of the developing limb bud (Mercader et al., 2000).

One piece of evidence that suggests an indirect role of FGFs in distal identity came from denervated limbs. In these limbs, *Dlx3*, a gene that is normally expressed in the wound epidermis and the distal- most blastema cells and has been implicated in conferring distal identity, was absent (Cohen, 1989; Cohen and Jürgens, 1989). Interestingly, beads coated with Fgf2 could rescue *Dlx3* expression and regeneration in the absence of nerves (Mullen et al., 1996), highlighting the possibility that factors

beyond D/V and A/P confrontation, such as nerve ingrowth, could contribute to pattern the blastema.

1.7.2 HoxA genes

Thus far, the best known molecular marker of distal limb identity is HoxA13, which is expressed 24-48 hours post amputation (Gardiner et al., 1995). Based on expression and mutational analysis in mouse, HoxA13 is associated with hand identity while 3' HoxA genes such as HoxA11 and HoxA9 are associated with lower and upper arm identity, respectively (Yokouchi et al., 1995; Nelson et al., 1996).
Resembling the developing limb bud, HoxA9 is expressed throughout the blastema at the midbud stage, while HoxA13 expression is restricted to the distal blastema cells. Although RA downregulates HoxA13, it becomes rapidly activated after amputation. Therefore, it seems unlikely that endogeneous retinoids are present in the early regenerating limb (Gardiner et al., 1995; Gardiner and Bryant, 1996). However, this does not rule out the possibility that endogenous RA signalling could be repressed in distal regions but activated in proximal regions where it may be required for patterning of lower and upper arm elements. Furthermore, it could never be ruled out experimentally that a "proximal", HoxA13 negative, region exists from the beginning. The role of HoxA genes in the establishment of the proximo-distal axis will be more extensively discussed in chapter 2.

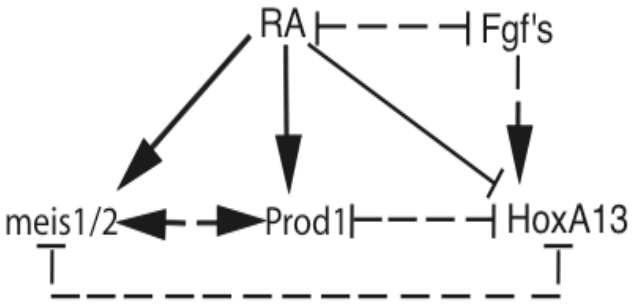

Fig. 1-5: Factors that have been identified thus far and their interactions. Dashed lines indicate that it is not known whether and how interaction takes place.

1.8 Models of limb regeneration

Undoubtedly, the patterning of the regenerating limb is a complex process where cells from different positions and identities may recognize each other, reenter the cell cycle, become distalized and reproduce the missing limb elements. Due to the early establishment of positional values, it has been experimentally challenging to investigate how the events that lead to the reestablishment of the limb occur mechanistically. In the history of limb regeneration, numerous models were proposed that attempted to explain the different phenomena on a mechanistic basis.

1.8.1 Cell-cell contacts lead to P/D outgrowth

The induction of a blastema at the cut end and thus P/D outgrowth of the regenerate crucially depends on the healing process, where cells from different D/V or A/P positions converge at the end of the limb. This requirement was uncovered when a number of researchers noticed that grafting a blastema from the right limb onto the stump of the left, contralateral limb, amazingly resulted in three full regenerating limbs at the graft site, termed supernumerary limb formation (Iten and Bryant, 1975; Tank, 1978; Maden and Goodwin, 1980; Stocum, 1982; Figure 1-6). A number of further experiments indicated that supernumerary outgrowth occurs when normally nonadjacent tissue is ectopically juxtaposed (Carlson, 1974, 1975; Papageorgiou and Holder, 1983; Maden and Mustafa, 1982; Stocum, 1980). For example, rotation of the mature skin around 180° so that cells carrying anterior, posterior, dorsal and ventral values face cells of the respective contralateral site results in supernumerary outgrowth when amputated through the region of rotation.

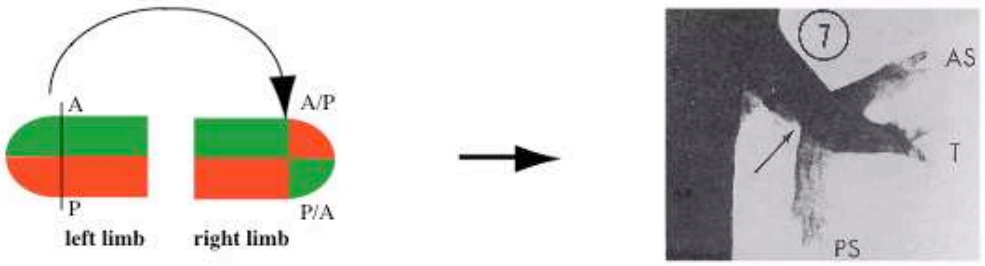

Fig. 1-6: Supernumerary outgrowth. When a blastema is placed onto the stump of the contralateral site so that anterior ant posterior sites are confronted, two extra limbs called supernumeraries (in the image shown termed as AS and PS) regenerate. From:Iten and Bryant, 1975.

1.8.2 The Polar Coordinate Model

The so called Polar Coordinate Model aimed to explain these phenomena on a basis of local cell-cell interactions and to predict the formation of ectopic limbs (French et al., 1976). It proposes that a complete set of anterior, posterior, dorsal and ventral values must be present and the juxtaposition of cells carrying all these different values leads to the stepwise intercalation of the missing elements (Figure 1-7). Supernumerary limbs form as a result of local interactions of cells with different circumferential values, and the 'complete circle rule for distal transformation' of the PCM predicts that in the case of anterior and posterior values being confronted, these local cell-cell interactions cause the intercalation of the missing dorsal and ventral values, thus generating two extra limb circumferences and leading to the outgrowth of two additional limbs.

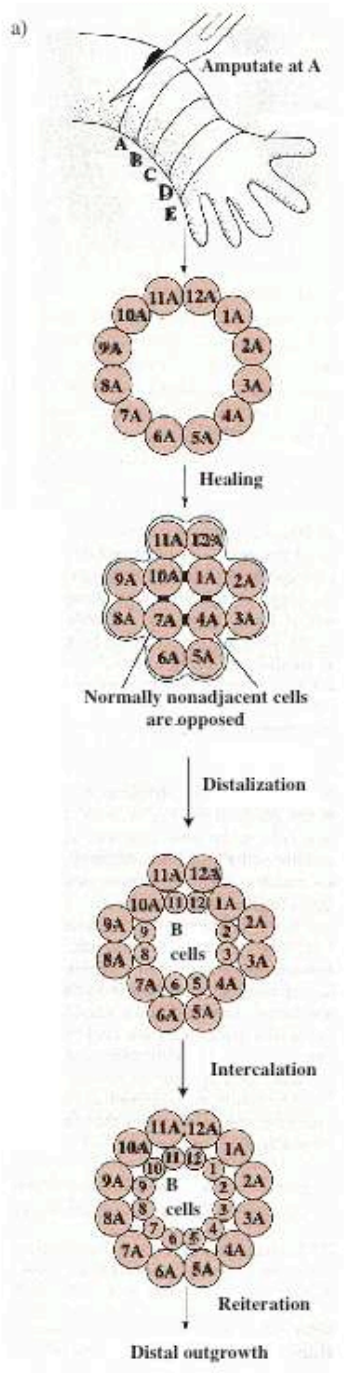

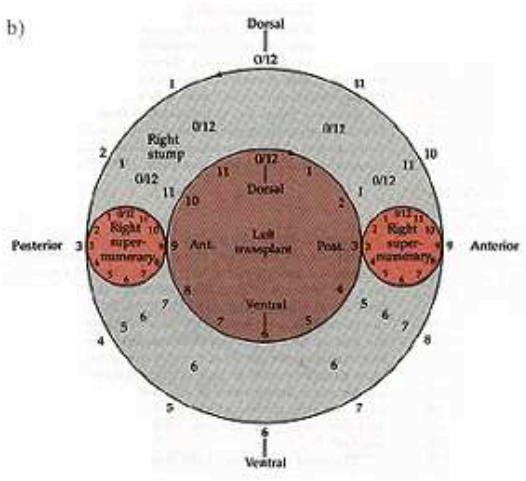

Fig. 1-7: The Polar Coordinate Model (PCM). a) The mature limb contains circumferential values (1-12) and proximo-distal values (A-E, with "A" cells carrying most proximal values). Amputation results in the juxtaposition of normally nonadjacent cells (1A, 4A, 7A, 11A), which leads to the intercalation of the next distal values ("B cells"). Repetetive rounds of intercalation lead to the regeneration of the entire limb. b)The 'complete circle rule' of the PCM explains the effect seen in a). Between juxtaposed anterior and posterior cells, dorsal and ventral values intercalate so that the limb consists of three sets of circumferential values, which regenerate three limbs (French et al., 1976).

1.8.3 The Averaging model

However, the PCM did not account for all phenomena that were observed in relation to supernumerary outgrowth. Maden (1977) proposed a distinct model where regeneration occurs as intercalation of missing values within the circumferential, proximal and distal boundaries. Contact between proximal and distal cells would result in intercalation of intermediate valued cells, which has been termed the "averaging" model (Fig. 1-8). It proposes that cells of the newly forming wound epidermis covering the amputation plane carry the most distal value. The juxtaposition of distal cells with stump cells induces the stump to dedifferentiate and produce cells with a value intermediate between the distal and stump identities. The multiple reiteration of this event results in the full complement of limb positional values.

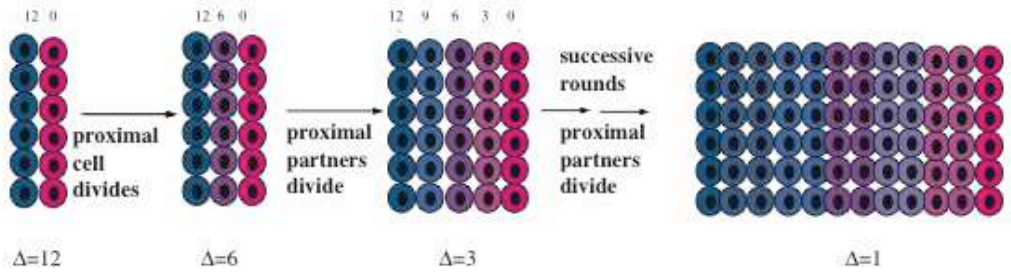

Fig. 1-8: The Averaging Model (Maden, 1977). Distal-most cells arise first and all other P/D domains become intercalated sequentially. In our example, the limb was amputated at a P/D level of 12 and regenerated the most distal cells that carry, by definition, the value 0. During the next round of cell duplication, cells of the intermediate value 6 are generated. During the following round of duplication, cells with the values 9 and 3 are produced, and these successive rounds of proliferation will last until progenitor cells of all domains have formed.

A strong point of this model is that it would explain the intercalation phenomenon. A criticism has been that it would predict intercalation in two directions when an upper arm blastema is grafted onto a wrist stump. According to this model, elements between the distal stump and the more proximal cells of the graft would intercalate in addition to the full limb regenerating from the graft. This situation has never been observed. However, confrontation of distal blastema to mature proximal tissue may

not be equivalent to confronting proximal blastema to distal mature tissue. Whereas grafting of the wrist blastema onto an upper arm stump causes the tissue to undergo the typical “dedifferentiation”, changes that are required for blastema formation, these changes do not occur in the proximal blastema to wrist graft. This connection to induction of dedifferentiation may explain why no inverse limb is produced in the latter graft. Indeed, if a mature hand is grafted onto an upper arm stump, no intercalation is observed (Stocum, 1975), indicating that mature tissue does not have the ability to initiate the intercalation event.

The wound epidermis does not necessarily need to carry the distal-most values. One could also imagine a scenario in which the first dedifferentiated cells would become specified to the most distal values by nature (Nye et al., 2003).

1.8.4 The boundary model or: Do morphogens play a role in pattern the regenerate?

Supernumerary outgrowth during regeneration of surgically manipulated limbs can also be explained by a different mechanism: The confrontation of cells carrying different identities induces them to produce one or more morphogens, a scenario similar to the two-dimensional wing disc system of *Drosophila*, where morphogens are produced along the A/P and D/V border.

One model that integrates concepts of tissue distalization with morphogen production was proposed by Meinhard who emphasized the importance of morphogen production at boundaries (Meinhard, 1983). He suggested that the mature limb is divided into three radial compartments, anterior dorsal (AD), anterior ventral (AV) and posterior (P). After limb amputation, the point where anterior dorsal, anterior ventral and posterior cells come together represents a new signaling point where a distalizing morphogen is produced that will pattern the P/D axis (Figure 1-9).

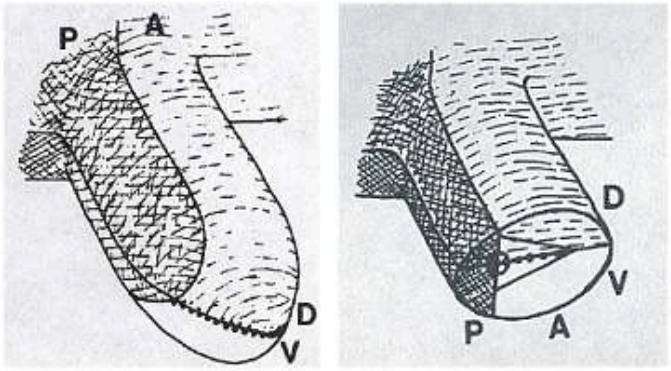

Fig. 1-9: The boundary model (Meinhardt, 1983). it postulates that the mature limb consists of three distinct compartments with posterior (P), anterior-dorsal (AD) and anterior-ventral (AV) features, respectively. According to this model, the point where AD, AV and P cells come together will form an organizing centre, from which a distalizing morphogen spreads and directs outgrowth of the regenerate (Meinhard, 1983).

Any surgical manipulation would lead to the induction of ectopic compartment boundaries that would influence the number and shape of the regenerates when amputated through the operated region. Intriguingly, this model accounts for almost all phenomena that are connected with the numerous different transplantation experiments and the resulting supernumerary formation (Maden, 1983).

1.9 How does limb regeneration occur? Discussion and outlook

The question arises whether such soluble morphogens can have a place in regeneration, where they may have to act over large distances. For example the circumference of a developing axolotl limb bud is several millimeters compared to the adult limb, which can be more than 10 times larger. One solution to this problem, at least for the P/D axis, would be for the morphogen to exert its patterning effects at the very earliest stages of limb regeneration when the blastema would be a reasonably small number of cells thick. This concept is difficult to test, as transplantation and manipulation of the early blastema is technically challenging.

However, intercalation and affinophoresis suggest a crucial role of the cell surface in this process, and the patterning of the regenerating limb can theoretically be explained without any morphogen needed. It is widely believed in the field that intercalation takes place, with the generation of the most distal progenitors first and progenitors of the intermediate elements thereafter in a sequential manner. To test this, it is crucial to

perform investigations on the very early regenerate as the essential patterning information is already established in the blastema.
Bearing in mind that the limb consists of several types of tissues, investigations towards the contribution of each tissue or cell type to the reestablishment of the three dimensional structure will have an important impact on our understanding of how limb regeneration occurs and supplement studies aiming to identify what mechanism drives the repatterning of the limb.

1.10 Towards understanding patterning during regeneration – The aims of the thesis

It is crucial to understand the early patterning events during regeneration. Therefore, in the first part of this thesis we developed single cell PCR as a new tool to analyze cells at the very early stages. We aimed to elucidate whether distal cells arise first and intermediate elements arise at later time points. This result would strengthen the hypothis that intercalation is the initial event of regeneration.
In the second part we investigated lineage dependent differences in the expression of genes associated with proximo-distal patterning. Furthermore, we addressed the question of whether cells of different lineages retain their positional memory when ectopically placed at a different proximo-distal level. Connected with that, we aimed to confirm that an endogeneous proximalizing factor, such as retinoic acid, does not play any role at any stage of regeneration. Although we concentrate on questions concerning proximo-distal patterning, our research is also directed to the question of tissue specificity and whether the blastema is a multipotent pool of cells or whether cells retain a tissue specific memory which affects their ultimate lineage.

2. Single Cell PCR as a Tool to Study the Early Patterning Events

2.1 Introduction

2.1.1 Alternative ways of generating progenitor cells

Before delving into specifics, it is helpful first to visualize some alternative possibilities of how the blastema may be formed and expand (Figure 2-1). One possibility is that a pool of progenitors of the same identity forms and then, sequentially, cells of other identities arise. Experimental studies have pointed to a cell surface based mechanism by which progenitors of the different segments intercalate, and the model in which distally specified progenitors arise first is clearly favored (for review, see Nye et al., 2003). If such a mechanism takes place, one would expect that, at a very early stage, only distal cells are found.

However, the existence of the intercalation model is not proven, and theoretically progenitor cells could become simultaneously specified to upper arm, lower arm and hand identities. In such a way, cells could be organized in their appropriate domains from the beginning, or segment addition could occur by the random generation of upper arm, lower arm and hand progenitor cells after amputation and subsequent sorting into their appropriate domains.

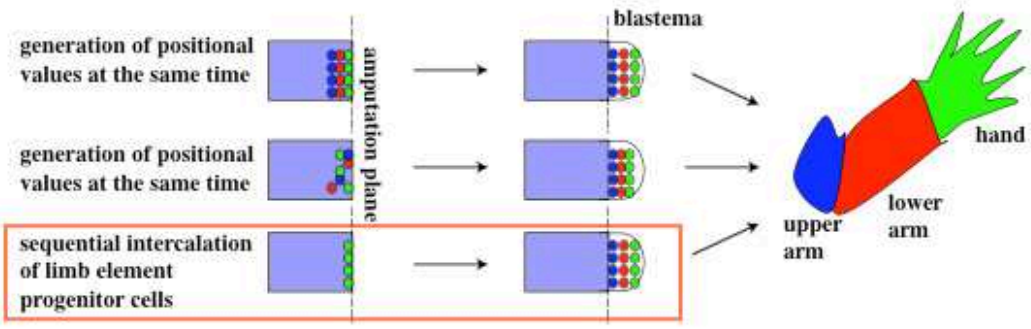

Fig. 2-1: Different possibilities of how cells in the blastema could become specified to their proximo-distal values. Theoretically, cells could be specified at the same time and either be organized into their domains from the beginning or randomly distributed and subsequently sort into their appropriate domains. However, it is widely believed that generation of positional values happens by sequential intercalation of limb progenitor cells, with distally specified progenitors arising first.

To test whether intercalation takes places, it would be optimal to analyze progenitors in the early regenerate for markers that are associated with upper arm, lower arm and hand identities.

2.1.2 Reexpression of HoxA genes: A fundamental difference to development?

Thus far, the best known molecular markers of proximo-distal limb identities are the HoxA genes (Yokouchi et al., 1995; Gardiner, 1995; Nelson et al., 1996). Based on expression and mutational analysis in mouse, *HoxA13* is associated with hand, *HoxA11* with lower arm and *HoxA9* with upper arm identities (Morgan et al., 1992; Dolle et al., 1993; Small and Potter, 1993; Davis and Capecchi, 1994; Davis et al., 1995; Yokouchi et al., 1995; Fromental-Ramain et al., 1996; Zakany and Duboule, 1996; Nelson et al., 1996, Boulet and Capecchi, 2004).

As the developing limb bud emerges, all of its cells express HoxA9. Following the principles of colinearity, sequential *HoxA11* and *HoxA13* expression start at a later stage of limb development. Their expression domains are nested, with *HoxA13* being restricted to the distal tip of the limb bud. At this time, the limb can be divided into three distinct regions: The *HoxA9* expressing domain will give rise to upper and lower arm, whereas the *HoxA9*/*HoxA11* and *HoxA9*/*11*/*13* expressing regions will form lower arm and hand elements, respectively.

Resembling the developing limb bud, *HoxA9* is expressed throughout the blastema of the midbud stage, while *HoxA13* expression is restricted to the distal blastema cells. However, the spatial and temporal reexpression of *HoxA9* and *HoxA13* during regeneration suggests a fundamental mechanistic difference to development in the initiation of P/D patterning. As soon as one day after amputation, both *HoxA13* and *HoxA9* are reexpressed in the mesenchymal tissue beneath the amputation plane. This early reexpression of *HoxA13* may reflect that the first cells that arise after amputation are specified to a distal identity. However, from these experiments it is is not clear whether all cells express *HoxA13*, or whether *HoxA9*/*11* or *HoxA9* positive cells coexist. Therefore, it is still not clear whether all progenitor cells that arise first after amputation are specified to a distal cell fate, which would strongly suggest that intercalation is the mechanism of the reestablishment of the proximo-distal axis.

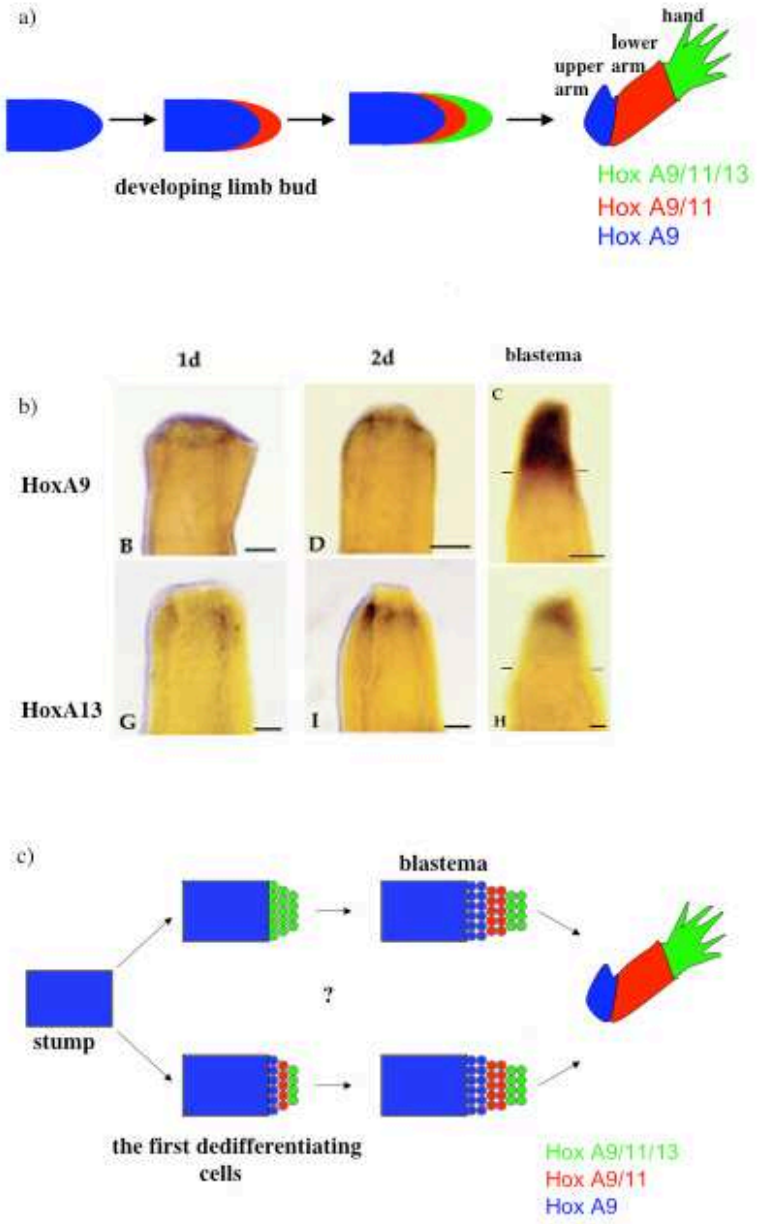

Fig. 2-2: Expression of *HoxA* genes during development and regeneration.
a) Sequence of *HoxA* expression during limb development. b) *HoxA13* is reexpressed during limb regeneration starting at 1 day after amputation. However, it is not clear whether all cells express *HoxA13*. From: Gardiner et al., 1995. c) Two possibilities of *HoxA* gene expressing populations during the early stages of limb regeneration. If all dedifferentiated cells at these stages carry a distal identity, one would expect one population of *HoxA9*$^+$*./11*$^+$*/13*$^+$ cells.

2.1.3 Single Cell PCR as a tool to test when different positional values are generated

Studies on the early regenerating limb have been challenging due to the difficult morphology of this tissue and the low number of cells, which makes surgical manipulations impossible. The expression analysis by using in situ hybridizations is also not optimal. While single cell resolution is not obtained by whole mount analysis,

and it is technically challenging to perform section in situ hybridizations on a stump that had been amputated one or two days before, as dedifferentiating tissue is very loose and cells are lost during the hybridization process. A further challenge is the performance of double- or triple in situ hybridizations, which is crucial for distinguishing between different cell populations. RT PCR from whole tissue does also not allow to distinguish between different cell populations.

Therefore, we addressed the question of different *Hox* gene expressing cell populations using single cell PCR, in which individual cells are dissociated from regenerating limbs and analyzed for their expression of *Hox* genes.

Using this technique, spatial information is lost, but it is possible to detect the existence of different segment identities using the *Hox* genes as markers. A clear advantage of this technique is that a whole battery of genes can be tested for its expression in one cell, allowing us to test whether one or several *HoxA* gene expressing populations exist at the earliest stages of limb regeneration.

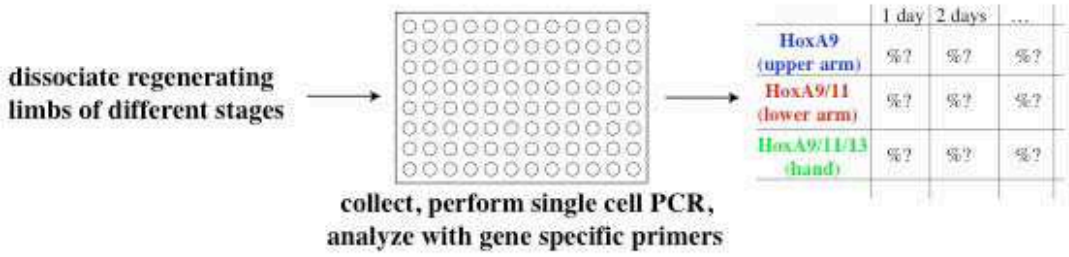

Fig. 2-3: Experimental outline aiming to identify *HoxA* expressing cell populations at different stages of limb regeneration.

Single cell PCR was first established by Brady and Iscove (1993) and has since been extensively used for medical applications such the distinction of subpopulations of cells in one tumor. Recently, it also aided in identifying different cell populations during pancreas development, early Xenopus gastrulation or planarian regeneration (Chiang et al., 2003; Wardle, 2004; Hiroshi Tarui, personal communication) and has furthered our understanding of these processes.

2.1.4 Principles of single cell PCR

Single cell PCR consists of three major steps: 1) reverse transcription, 2) polyadenylation and 3) PCR amplification of the cDNA pool.

During the reverse transcription, time and nucleotide concentration are chosen in a way that only the last 500 base pairs 5' from the polyA tail are reverse transcribed. Polyadenylation serves to add a polyA tail to the 3' end of the generated cDNA, so that each transcript, regardless of the sequence in between, has the same length and the same 5' and 3' end. This is crucial for preventing bias towards shorter transcripts and helps to conserve the relative abundance. The pool is subsequently amplified by PCR using a polyT primer in order to detect genes that were expressed. This can be done by hybridizing the DNA to a chip or by using this cDNA as a template for gene specific PCR.

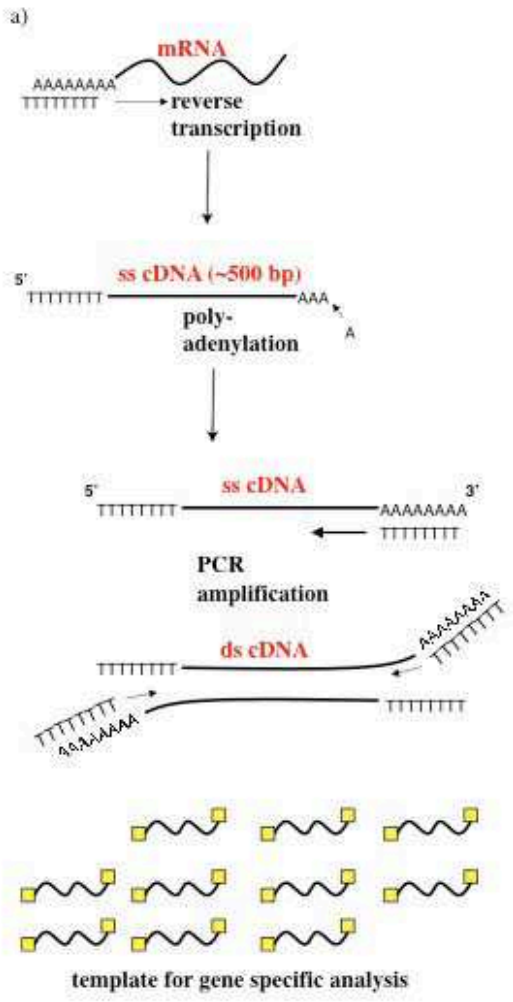

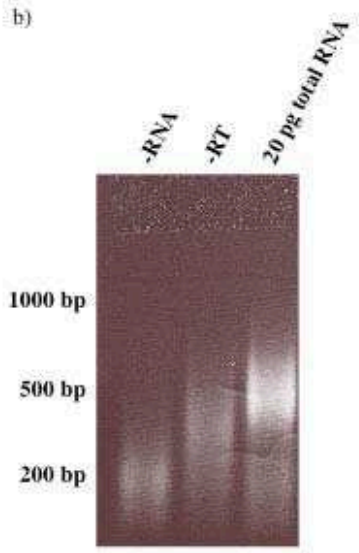

Fig. 2-4: Principles of single cell PCR. a) Single cell PCR is a three- step protocol including reverse transcription, polyadenylation and PCR amplification of the generated cDNA pool. To prevent bias towards short transcripts, the conditions during the reverse transcription are chosen to produce cDNA of 500 bp length. b) Generation of cDNA from 20pg of total RNA.

2.2 Results

2.2.1 Optimization of the protocol

To establish single cell PCR in the lab, we applied the protocol published by Brady to a dilution series of purified axolotl limb total RNA. From these dilutions, we generated cDNA's and, using them as templates, tested whether we can amplify tubulin using gene specific primers. Total RNA in one cell is estimated to be abundant at 20-25 pg (Brady and Iscove, 1993), and we aimed to amplify *Tubulin* from these amounts of RNA. Although we could detect *Tubulin* from amounts equivalent to 10 cells, amplification from 20 pg was not reproducible. Therefore, we had to further optimize the protocol in order to reach a sensitivity that allows us to detect transcripts at the single cell level.

We tested several parameters including different concentrations of dNTP's, temperatures and lengths of the poly(dT) primer during the reverse transcription, different dATP concentrations during the polyA tailing as well as several different enzymes. In our search for better parameters, we also came across a modification in the PCR program, introducing a 20 min incubation of polyA tailed cDNA's prior to amplification (Fiona Wardle, personal communication). We tested whether this step has any impact on the sensitivity of our protocol and found that it dramatically influences the amplification process in a positive way (Fig. 2-5). Therefore, it became part of the protocol.

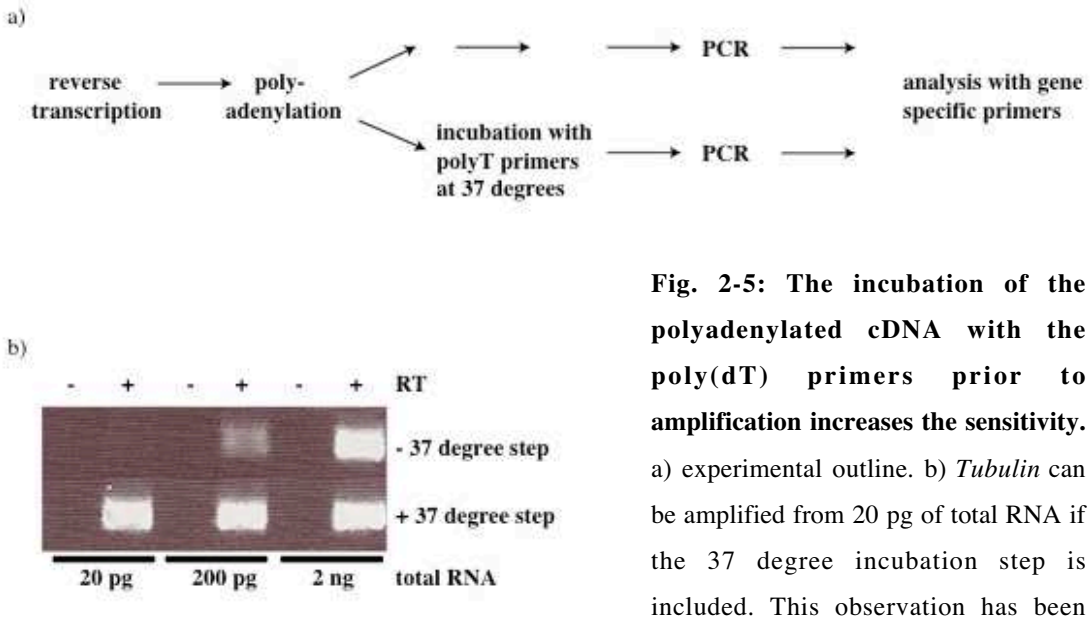

Fig. 2-5: The incubation of the polyadenylated cDNA with the poly(dT) primers prior to amplification increases the sensitivity. a) experimental outline. b) *Tubulin* can be amplified from 20 pg of total RNA if the 37 degree incubation step is included. This observation has been reproduced in 3 independent experiments.

Apart from including this step, we found that a combination of Superscript II reverse transcriptase (Invitrogen), terminal transferase (Roche) and the TAQ polymerase generated in house by the protein expression facility was optimal for the amplification process. Furthermore, we decided to perform the reverse transcription at 42 instead of 37 degrees. Although we did not see any difference in sensitivity using one or the other temperature, we think that an increase in temperature may help to improve the amplification of transcripts that contain difficult secondary structures or have a strong affinity for RNA binding proteins.

To estimate the minimal number of transcripts that we are able to detect, we spiked forelimb RNA with in vitro transcribed mRNA coding for Tbx4, which by nature is not expressed in the forelimb. The dilutions of this ectopically added transcripts were corresponding to the numbers of 100, 50 and 10 individual transcripts. In our hands, we were able to detect 50 transcripts reproducibly, and in more than 50% of the cases we reached the level of 10 transcripts. The same result was achieved when we applied a protocol established in the laboratory of Kiyokazu Agata to *Tbx4*- spiked axolotl limb RNA (in collaboration with Hiroshi Tarui).

However, we are aware that *in vitro* transcribed mRNA does not reflect the normal situation in a cell in which transcripts are covered by proteins or have started to be

degraded from their polyA tail, which may influence the efficiency of amplification. Therefore, we decided to test our protocol on dissociated single cells.

2.2.2 Single cell PCR – how do we obtain the right picture?

In the 15th century, the painter Albrecht Dürer drew a picture of a rhinoceros that reflected very well how a rhinoceros looks like. This fact would not be so amazing if he had seen such animals or at least pictures of them by his own eyes. However, he had not. He generated this great piece of art following the descriptions of a friend who had seen rhinos before.

What Dürer had achieved with drawing something that he had never seen, we want to achieve analyzing single cells of regenerating axolotl limbs. Although we do not know the complex gene expression pattern in axolotl limbs, we want to generate expression profiles of cells deriving from tissues that have been poorly characterized before. More specifically, we want to determine cell fates based on *HoxA* gene expression, and if we evaluate a cell as a proximal cell due to the absence of *HoxA13*, we need to be sure that we obtained the right information, telling us that *HoxA13* was not expressed by this cell. For our analysis, we dissociate cells from their source in which they were organized, stain them with the nuclear dye DRAQ5, FACS sort them into a 96-well plate, amplify their mRNA pool and analyze for the abundance of specific cDNAs using gene specific primers (see 4.6 and Figure 4-1). Dissociation and FACS sorting are crucial for obtaining high numbers of single cells within the shortest possible amount of time. However, each of these steps can potentially influence cells in their expression of genes. For example, cells could be damaged or induced to undergo apaptosis, or stimulated to express genes they had not expressed before. Furthermore, our method may not be sensitive enough to detect specific, low abundant transcripts. Taken together, we were aware that the result we obtain may not reflect the real picture of gene expression in cells.

We decided to establish single cell PCR on the midbud- stage blastema, as the expression patterns of *HoxA9* and *HoxA13* are already known from data obtained by whole mount in situ hybridizations. To be further confident that the results we are going to obtain by single cell PCR reflect the normal situation in the regenerate, it

would be optimal to consider low abundant genes that are expressed in every cell and whose transcripts are of similar abundance as transcripts coding for *Hox* genes.
However, no investigations directed to the characterization of the blastema on a cellular level have been taken so far. Although it has been shown that the blastema is segregated into a *HoxA13* positive and *HoxA13* negative domain, there is not much information about the expression of other genes that could be useful for our studies.
Therefore, we started to search our EST expression library (Habermann et al., 2004) aiming to identify genes from whose putative roles we could either expect their transcripts to be ubiquitously expressed, to be present at a level similar to *Hox* mRNA's, or both. From this search, a sequence putatively coding for Rp4, a component of the ribosomal complex, was found to be present in a high frequency. Another sequence putatively encoding Sec61, a component of the ER-mediated protein secretion complex, was present in two copies. We expect that both genes are expressed in every cell, as they encode essential cellular components. The different frequency in the library suggests that *Rp4* is highly expressed while transcripts of *Sec61* are less abundant.
We also decided to add the putative homologue of Twist to our set of genes. Twist is a bHLH transcription factor and in other species expressed in mesodermally specified cells during development (e.g. Quertermous et al., 1994). Information about the relative abundance of transcripts encoding HoxA proteins or Twist does not exist. However, the frequency of detecting cDNA's of *Hox* genes and *Twist* in the library were similar, suggesting that transcripts coding for Twist are present at a similar level like *Hox* genes. We therefore added *Twist* to our set of genes and believe that it is very valuable for our assessments regarding whether or not our gene expression profiles reflect the normal situation in the blastema.

2.2.3 Single cell PCR – questions concerning sensitivity and cell survival

To see how reproducibly we can amplify our set of genes from blastemas, we dissociated in three independent experiments blastemas of the midbud stage, FACS sorted their cells and generated gene expression profiles. As expected, *Rp4* was always amplified from one cell. To determine the percentages of cells expressing *Sec61*, *Twist*, *HoxA9* and *HoxA13*, we normalized against the number of wells in

which we detected these genes against the total number of wells in which we detected *Rp4*.

As it can be seen, the frequency of detecting each gene varies among the three analysis. In 80 to 95% of the rp4 expressing cells we detected *Sec61* expression. As mentioned above, we would have expected every cell to express *Sec61*, and in situ analysis have to confirm whether a few cells exist in the blastema that do not express *Sec61*.

50% to 80% of the *Rp4* expressing cells were found to express *Twist*. How can this variance be interpreted? In situ expression analyses suggest that *Twist* is not expressed in every cell of the blastema. However, we cannot exclude that cells in one experiment could have also been more seriously affected than cells in another one, for example as a result of damage and subsequent downregulation of genes.

We were most surprised by the low frequency of *HoxA9* detection. Furthermore, in many wells in which we detected *HoxA13*, *HoxA9* was absent. The whole mount in situ analyses performed by Gardiner (1995) suggests that *HoxA9* is present at higher levels, and section in situ hybridizations will have to reveal in how many cells *HoxA9* is expressed.

Taken together, from these results we do not know whether we obtained the right information regarding the expression profiles of cells that were analyzed. Variations in the detecting specific transcripts could be due to cell damage and downregulation of genes, or a lack of sensitivity of our method. We started to analyze the expression patterns of our set of genes by section in situ hybridization (Fig. 2-6) and we attempt to collect more data. However, in the following sections we want to describe the progress that we have made in addressing the sensitivity of our method on single cells and in distinguishing between damaged, unhealthy cells from those that we think were left intact.

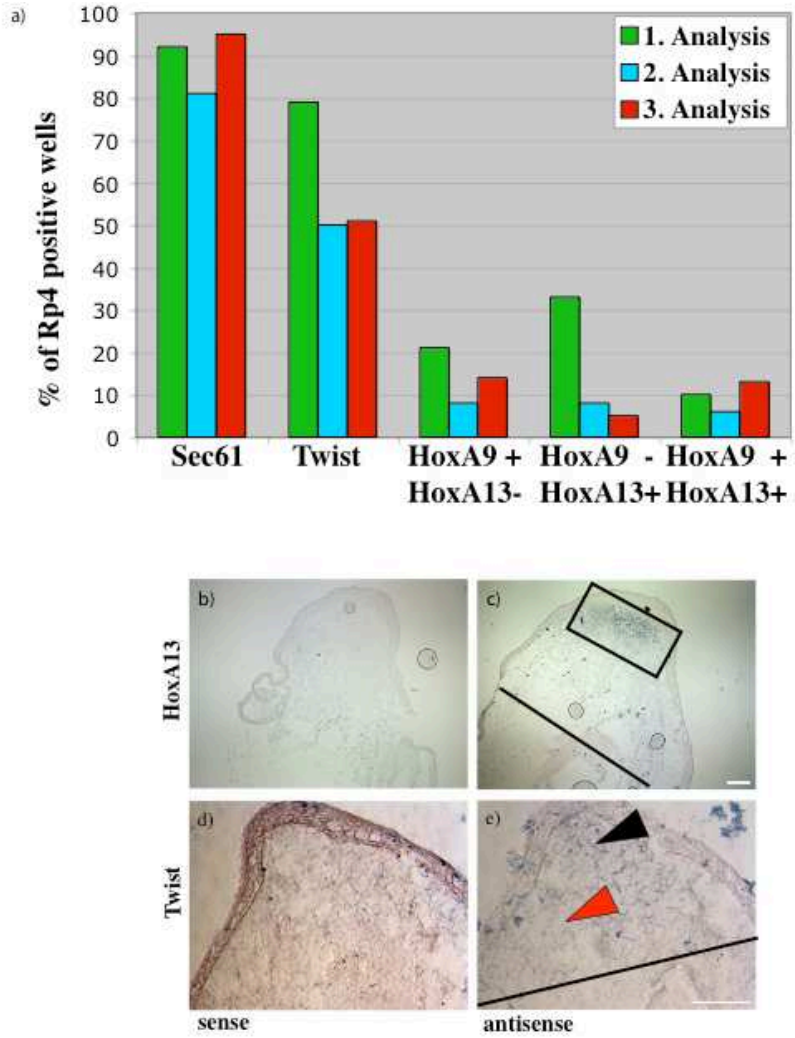

Fig. 2-6: Single cell PCR and corresponding in situ expression patterns of the midbud stage blastema. a) Percentage of wells in which *Sec61*, *Twist*, *HoxA9* and *HoxA13* were detected, normalized against the total number of wells positive for *Rp4*. Analysis 1-3 are three independent experiments. Note that only in a few wells *HoxA9* and *HoxA13* were detected in relation to the wells in which either one or the other was detected. Also, the percentage of wells in which twist was detected varies. Cell numbers: n(1)=39, n(2)=36, n(3)=37. b)-e) In situ hybridizations performed on longitudinal sections of *HoxA13* (b,c) d) and *Twist* (d,e). Not that the size of the animals used was different in both experiments. b) and d) are the respective sense controls. The expression domain of *HoxA13* is marked with a black rectangle. A white and a red arrow head point to regions in which twist is expressed or not expressed, respectively. Black lines in c) and e) indicate the plane of amputation. Distal is to the top. Bar: 500μm.

2.2.4 How reproducible is the amplification of transcripts?

We needed to be sure that the failure of detecting our set of genes is not an issue related to the sensitivity of our method. To test whether we can reproducibly amplify *Sec61*, *Twist*, *HoxA9* and *HoxA13* from single cells, we pooled cells that were dissociated from a blastema, homogenized them and split this mix into a minimum of 24 single cell equivalents (Figure 2-7). We expect each well to contain equal amounts of transcripts.

As we found that *Twist*, *HoxA13* and possibly *HoxA9* are not expressed in every cell, we were aware that the amount of mRNA in those wells is below the level of a single cell. Therefore, we also analyzed equivalents at the level of 9 cells. To get an impression where the detection limit lies, we analyzed 0.5 and 0.25 cell equivalents.

As each well contained the same amounts of transcripts, we consider our method to be reliable if we can detect the respective gene in all wells.

As shown in Figure 2-7, detection of *Sec61* and *Twist* is consistent even far below the level of one cell. *HoxA13* is detected in almost 100% of the one-cell equivalents, and considering that at this level the amount of transcript is below the amount of one cell, we consider detection of *HoxA13* by our method to be reliable. We noted, however, that its detection from equivalents below one cell equivalent is less efficient as *Twist* or *Sec61*. This could be due to several reasons like differences in cell numbers expressing these genes or different cellular levels. However, we cannot exclude that *Twist* and *HoxA13* are amplified with different efficiencies, and that these differences become most obvious at these low levels of RNA. The frequency of *HoxA9* detection never reached the level of 100%, making it difficult to judge its expression in single cells. Since we do not know whether *HoxA9* is expressed in every cell, we cannot rule out that the lower percentage in detection is a result of inefficient amplification, possibly because of a complicated secondary structure. Nevertheless, the efficiency of detecting *HoxA9* was higher from equivalents then from individual cells sorted.

Our data demonstrate that we can reproducibly amplify *Sec61*, *Twist* and *HoxA13* from mRNA levels of one cell or less, while it requires more investigations to assess whether this is also true for *HoxA9*.

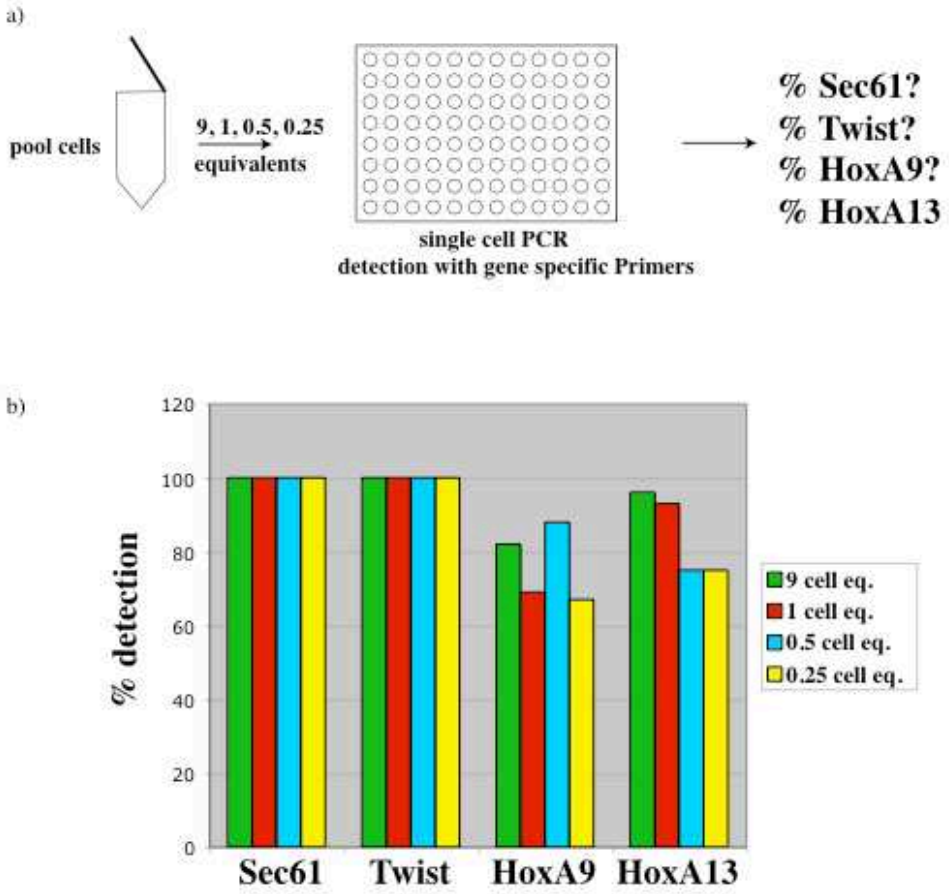

Fig. 2-7: Detection of *Sec61*, *Twist*, *HoxA9* and *HoxA13* from 9, 1, 0.5 and 0.25 cell equivalents. a) Experimental outline. b) Percentages of amplification. Results obtained from 9 and 1 cell equivalents are averages of 2 independent experiments, dilution to 0.5 and 0.25 equivalents was performed once.

2.2.5 How can we distinguish intact cells from damaged cells?

The failure of detecting transcripts from single cells could be due to damage of the cells as a result of dissociation and FACS sorting. To better assess whether cells have been affected or not, we worked with transgenic animals harboring GFP under the control of the CAGGS promotor (Sobkow et al., 2006). Damaged cells become obvious very clearly by losing their GFP signal, possibly due to leakage of cytoplasm. When we dissociated blastemas into a suspension of cells, there were no obvious signs of extensive damage and cell death. In fact, we were able perform primary culture of cells derived from both blastema and mature limb tissue and maintained cells under these conditions for several weeks. FACS analysis of blastema cells that were incubated with 7'AAD, a nuclear dye marking dead cells, showed that about 5%

of cells in the suspension had died, further suggesting that our dissociation conditions were not inducing extensive cell death. When blastema cells were FACS sorted into medium, we found bright fluorescent cells adhered to the bottom of the well after one day, further suggesting that our conditions were not toxic for them.

However, we cannot conclude from these morphological observations whether the overall gene expression had been affected during dissociation and FACS sorting, or whether certain subpopulations were affected while others were not. In a number of experiments, we tested whether protease treatment, DRAQ5 staining and FACS sorting have a negative influence on the detection of our set of genes. We did not find any obvious differences, which encouraged us to further continue using these conditions.

Figure 2-8 shows a representative expression pattern obtained from cells of the midbud stage blastema. Each cell can be assigned to the expression of a specific set of genes that was detected. The numbers shown state the Ct values as a result of the quantitative analysis using gene specific primers, with low values reflecting that the respective cDNA was abundant in the well and low values stating that it was of low abundance.

A phenomenon we always observed was that we detected the majority of *Sec61*, *Twist* and *HoxA* positive wells among the wells displaying a low Ct value of *Rp4*. We interpret that these wells represent cells that were left intact. We suggest furthermore that wells of higher rp4 values reflect a high number of cells that were affected during dissociation and FACS sorting. Therefore, we concentrate our analysis on those wells that display a low Ct value for *Rp4*. We are aware that we may bias our analysis towards certain cell types, and we cannot exclude that, among the fraction we concentrate on, some cells had already started to downregulate *HoxA* genes. However, thus far the method of excluding wells with higher Ct values of *Rp4* has served best to enrich for wells in which *HoxA* and other genes like *Twist* are detected, and we are confident that this allows us to obtain a more realistic view of gene expression profiles of cells in the regenerating limb.

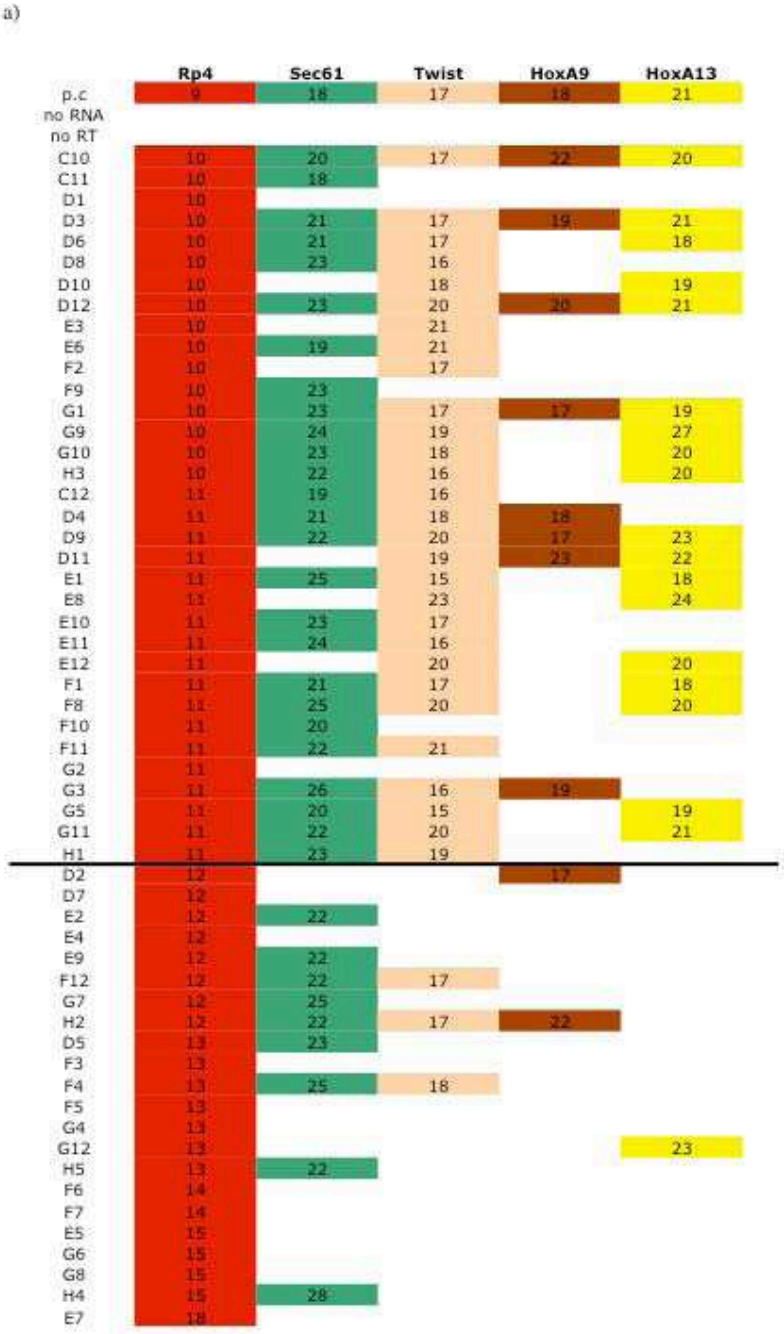

Fig. 2-8: Representative gene expression profile obtained from a midbud stage blastema. a) The first horizontal line is the positive control using purified RNA from axolotl limb tissue. The second and third horizontal lines are the "no RNA" and "no RT" control, assuring that we do not obtain signal from contaminating RNA or genomic DNA. Each further horizontal line represents a cell, and each vertical line shows the respective gene whose expression had been analyzed. Numbers indicate the Ct values, which were obtained from quantitative PCR analysis using gene specific primers. Note that most genes are detected in wells displaying a low Ct value for *Rp4*. The black line indicates until which Ct value of *Rp4* we considered cells for our analysis in this experiment.

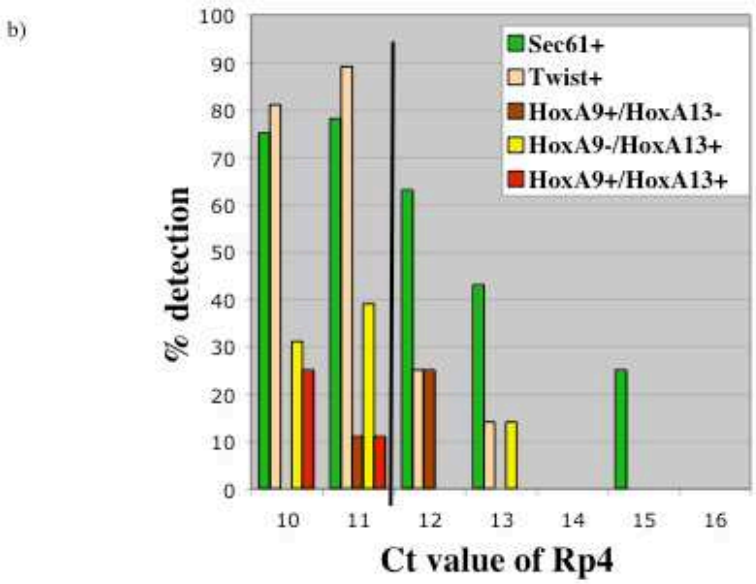

b) The same expression profile as in a). The graph shows the percentages of detecting *Sec61*, *Twist*, *HoxA9* and *HoxA13* in wells of the same Ct value for *Rp4*. As in a), the line indicates which wells we consider for our analyses (10 and 11) and which not (12-16). Note that we detect *HoxA9*$^{+}$ in wells displaying the value of 12, however, the percentage of detecting twist has dramatically decreased and we are not confident that cells sorted into these wells were not initially expressing *HoxA13* before dissociation.

2.2.6 *HoxA* gene expression at stages before blastema formation

Thus far, we demonstrated how we optimized the protocol of single cell PCR and characterized the sensitivity of the method on single cells. Furthermore, we explained the parameters used to identify cells as being intact by the time they were sorted into the reverse transcription buffer and showed that we found a reasonable number of wells in which we detected *HoxA9* and *HoxA13*. After performing these steps on the midbud stage blastema, we wanted to test whether we can detect *HoxA* expressing cells during the earliest phases of regeneration. At the moment, this is only possible for *HoxA9* and *HoxA13*, however, the 3'UTR of *HoxA11* has been isolated recently and in situ expression analysis on the blastema and the generation of gene specific primers is in progress.

To get an idea from what stage we start to detect *HoxA* genes, we decided to collect cells from upper arm mature tissue, 2 days after amputation and 5-7 days after amputation. The size of the animals was 10 cm, and in these animals the time points

chosen were before blastema formation. We are aware that we might have to collect cells from even earlier stages, however, this depends on whether we will detect *HoxA11* in these wells or not. We also collected cells 12 days after amputation when a midbud stage blastema had formed already. Cells were collected from the same batch of animals, and the amputation plane was always at the upper arm level.

Using the parameters explained above, we excluded putative damaged or dying cells based on the Ct value of *Rp4* and the expression of *Sec61* and *Twist*. In Figure 2-9 we show the percentage of *Sec61*, *HoxA9* and *HoxA13* expressing cells at the various time points. The frequency of *Sec61* detection is consistent throughout these stages. In the mature tissue, about 1% of cells were found to be *HoxA9* positive. This demonstrates the importance of determining the abundance of *HoxA11*, as we will be unable to distinguish contaminating mature proximal from dedifferentiated proximal cells.

Although at very low numbers, we can detect *HoxA9* and *HoxA13* expressing cells at the early stages. At two days after amputation, we detected 3 *HoxA13* expressing cells in one of three independent dissociations, showing that the variation at this time point is very high. Cells positive for *HoxA9* in the absence of *HoxA13* were never detected at this stage. At 5-7 days post amputation we detected populations of $HoxA9^{+}$/ $HoxA13^{-}$ and $HoxA9^{+}$/$HoxA13^{+}$ cells at low abundance. The number of wells in which we detected *HoxA* genes expressed increased when cells of the midbud stage were dissociated and sorted.

Our results show that we can detect *HoxA* expressing cells at stages before blastema formation, although at low abundance. We confirm earlier findings that $HoxA13^{+}$ cells are present at these early stages. Analysis of *HoxA11* expressions in these cDNAs will show whether progenitors of lower arm elements are present at these time points already and whether we will have to analyze cells at earlier time points.

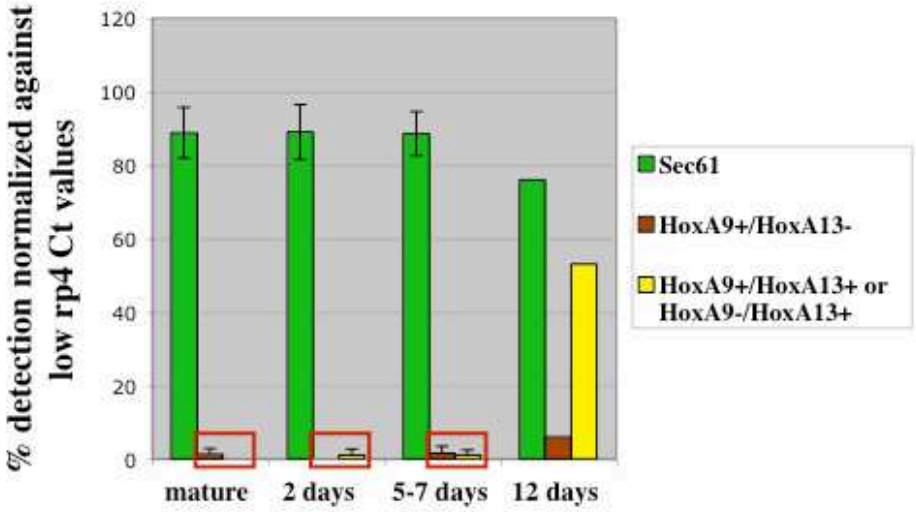

Fig. 2-9: Expression of *HoxA9* and *HoxA13* in the early regenerating limb. Tissue not further than 500 μm proximal to the amputation plane was dissociated. At low numbers, we detect *HoxA9* and *HoxA13* in wells in which cells at stages before blastema formation were sorted. Note that we can also detect *HoxA9* in the proximal mature limb, but not *HoxA13*. Thus far, we have not detected *HoxA9*$^+$/*HoxA13*$^-$ wells in which cells of a 2- day regenerate were sorted. At 5-7 days, we detect both *HoxA9*$^+$/*HoxA13*$^-$ and *HoxA9*$^+$/*HoxA13*$^+$ (or *HoxA13*$^+$ only) populations, and it will be interesting when we start to detect *HoxA11*. Error bars indicate the standard deviations obtained from at least 3 independent dissociations. Dissociation of blastema cells in this experimental row was performed once, therefore error bars are lacking. Total numbers of cells: n(mature)=232, n(2 days)=196, n(5-7 days)=240, n(12 days)=40.

2.3 Discussion

2.3.1 Investigating the early patterning events – why do we use single cell PCR?

In this work, we developed single cell PCR as a tool to study the early events and cell fate decisions regarding the reestablishment of the proximo-distal axis during regeneration. So far, investigations on the patterning of the regenerating limb were focused on the blastema stages as manipulations of the early regenerate are technically challenging.

It has been suggested that the reestablishment of the proximo-distal axis occurs by distal-most cell fates arising first, followed by the sequential intercalation of intermediate elements (for review, see e.g. Nye et al., 2003). During limb development, the expression domains of *HoxA* genes mark different domains of the future limb, and the early reexpression of the distal marker *HoxA13* demonstrates that progenitors of the future hand are among the first cells arising after amputation. However, whether all cells at this stage carry hand identities or whether progenitors of upper arm and lower arm are also present is not known. Expression analysis by RT PCR and whole mount in situ hybridizations have proven to be valuable in order to get insight into the early patterning events. However, to fully understand these processes it will be crucial to obtain single cell resolution. In our hands, expression analysis on sections of regenerating limbs of the early stages by in situ hybridization does not give satisfactory answers, and antibodies directed against axolotl Hox proteins have not been developed so far.

Single cell PCR has served to gain more insight into other developmental systems (Dulac and Axel, 1998; Chiang et al., 2003, Wardle, 2004; Hiroshi Tarui, personal communication), and we show that, in the regenerating limb, we detect populations of cells that express *HoxA* genes at stages before regeneration. This encourages us to study the early patterning events by single cell PCR

2.3.2 Sensitivity and cell damage

In our analyses, we aim to determine whether a cell obtained a hand, lower arm or upper arm fate based on the combined expression of *HoxA* genes. Hand progenitors express *HoxA13*, while lower and upper arm progenitors do not. In order to assign lower arm and upper arm fates, we need to be sure that in the case of detecting a *HoxA11* but not *HoxA13*, the lack of detecting *HoxA13* in the respective wells is not due to technical limitations.

Two critical points regarding single cell PCR are 1) the sensitivity of the technique and 2) damage of cells as a result of dissociation from their respective tissue into a cell suspension, putatively followed by downregulation of gene expression and mRNA degradation.

Sensitivity

Our analyses on cell equivalents demonstrate that we can reproducibly amplify transcripts from single cells, including *HoxA13*. However, we could not amplify *HoxA9* from wells that all contain the same amount of RNA equivalent to 9 and 1 cell. We tested several pairs of gene specific primers, which all gave the same result, and we believe that this inconsistency arises during the reverse transcription. Possible reasons are difficult secondary structures, low expression levels or a high dilution of transcripts resulting from a low number of cells expressing *HoxA9*. It will be crucial to determine the expression pattern on sections of blastemas by in situ hybridization to determine what percentage of cells expresses *HoxA9* in the blastema and whether this percentage is reflected by our analyses of single cells.

Our analyses also show that the efficiency of *HoxA13* amplification from amounts of RNA lower than 1 cell equivalent is lower than the efficiency of amplifying other transcripts. This could be due to different expression levels, different numbers of cells expressing the respective gene, or different efficiencies of amplification that become most obvious from these low amounts of RNA below the single cell level.

Exclusion of damaged cells

One step to exclude damaged cells was the usage of transgenic axolotls expressing GFP under the control of the CAGGS promotor. Analysis on sections of GFP positive axolotl limbs showed that all cells emitted at the same intensity, and using FACS we collected only those cells that were highly fluorescent. Our ability to culture mature and blastema cells and the fact that only 5% of the cells incorporated 7' AAD after dissociation suggest that our conditions were not toxic and allow us to obtain single viable cells.

After performing single cell PCR and gene specific quantitative analysis, a further step was the exclusion of wells displaying high *Rp4* Ct values. A high value reflects that the amplified cDNA is low abundant, however, one would expect an essential housekeeping gene such as *Rp4* to be abundant. We regard the cells sorted into these wells as unhealthy and damaged, supported by the fact that cDNAs of low abundant transcripts encoding transcription factors such as *HoxA* or *Twist* were primarily detected in wells displaying low Ct values for *Rp4*.

We do not rule out the possibility that our criteria favor specific subpopulations of cells and leave others out. Furthermore, we are aware that we might not entirely concentrate on wells in which undamaged cells were sorted. However, we are confident that the criteria we chose help to obtain results that reflect the *in vivo* gene expression profile of cells.

2.3.3 Time course through regeneration

To determine at what stage we can detect distally specified, *HoxA13*$^{+}$ cells, we performed single cell PCR on regenerating axolotl limbs that were cut proximally at different time points and on proximal mature tissue. From 1% of the cells in the mature limb we could amplify *HoxA9*, while *HoxA13* was never detected. We do not know in which tissue those cells were settled, but this result demonstrates that the analysis of *HoxA9* and *HoxA13* will not be sufficient for our investigations that are directed to answer whether intercalation takes place or not. *HoxA9*$^{+}$ cells present in early regenerates could have been 'de novo' specified to a proximal identity or derive from contaminating mature tissue. Therefore, it will be crucial to determine at what time *HoxA11*$^{+}$/*HoxA13*$^{-}$ cells, which mark progenitors of the lower arm, appear. The

3'UTR of the axolotl *HoxA11* has been cloned recently, and its expression analysis in the blastema as well as design of primers are under way.

We detected *HoxA13*$^+$ cells as early as 2 days post amputation, while *HoxA9*$^+$/*HoxA13*$^-$ cells were never detected at that stage. However, thus far we could not reproduce this result, and with the exception of these 3 examples, no *HoxA* genes were detected 2 days after amputation.

Although at very low numbers, we can detect *HoxA* genes more reproducibly from single cells at the amputation plane 5-7 days post amputation. In the animals we use, this corresponds to a stage in which the blastema still has not formed yet. We detect both *HoxA9*$^+$/*HoxA13*$^-$ and *HoxA9*$^+$/*HoxA13*$^+$ cells. As pointed out earlier, this could mean that progenitors of at least two different limb elements are present, or that the *HoxA9*$^+$/*HoxA13*$^-$ derive from contaminating mature upper arm tissue and points to the necessity of analyzing these cells for *HoxA11*.

Our results do not reflect the data obtained by Gardiner (1995; see Figure 2-2). A possible explanation could be the age and size of the animals we used. To obtain sufficient amounts of tissue from early regenerating limbs, we used animals of the size of 10 cm, and the bigger the animal is, the slower is the progression of regeneration. Furthermore, we are sure that the majority of cells that we collected belonged to the mature tissues of the stump with only a few cells that had undergone dedifferentiation and re-expressed *HoxA* genes at that time. Although being rather unlikely, we cannot exclude the possibility that cells at this stage of regeneration are more sensitive and thus downregulate specific genes as a result of dissociation, or that cells relevant for our analyses did not sufficiently go into suspension.

2.3.4 Future perspectives

Our results demonstrate that we can detect *HoxA13* at stages before blastema formation. It will be important to determine whether *HoxA11*$^{+}$/*HoxA13*$^{-}$ cells exist at these stages or not, reflecting whether all cells carry a distal identity or whether progenitors of the intermediate elements are present at this stage. Expression analyses of *HoxA11* and generation of optimal gene specific primers is in progress.
Our results also demonstrate that the frequency of detecting *HoxA* genes in cells of the early regenerate is very low. Therefore, it is crucial to analyze more cells in order to accumulate enough information that ultimately will allow us to interpret the early patterning mechanisms during regeneration.

—

We established a technique that allows us to study the early patterning events leading to blastema formation on a cellular level. However, we do not know where the cells that we analyze derive from. There are many different tissues and cell types in the amputated stump that all contribute progenitor cells to the blastema, and it is crucial to understand the roles of these tissues in the patterning process as well as the generation of new tissues from those resident in the stump. In the following chapter, we are going to describe and discuss work directed to understand whether blastema cells possess a specific memory regarding their tissue of origin and whether all tissues contribute equally to reconstruct the three-dimensional structure of the limb.

3. Analysis of Fate and Positional Identity during Regeneration

3.1 Introduction

3.1.1 The origin of blastema cells

The major source of cells populating the blastema is the mature local tissues at the amputation plane, and a variety of analysis has shown that progenitor cells arise from muscle tissue, chondrocytes, dermal fibroblasts and Schwann cells (Thornton, 1938, 1968; Hay and Fischman, 1961; Steen, 1968; Namenwirth, 1974; Muneoka et al., 1986; Lo et al., 1993; Kumar et al., 2000). These tissues respond to changes in their environment by losing their spatial organization, undergoing histolysis and releasing cells. By a process called dedifferentiation these cells change their cytologic characteristics and reenter the cell cycle (Chalkley, 1954). These fundamental changes in tissue organization can be best observed in multinucleated muscle fibers, which fragment and give rise to mononucleate cells that populate the blastema (Echeverri et al., 2001). Electronmicroscopical analysis revealed that, during the process of fragmentation, these fibers lose their specific localization of myofibrils in the cytoplasm resulting in cells that are indistinguishable from cells deriving from other sources (Hay, 1959).

Regardless of their origin, cells in the blastema appear indistinguishable from their morphology and display a high level of lamellipodia and plasma membrane protrusions, through which they form a network of cell/cell contacts. These dramatic changes of tissue organization to a common pool of progenitor cells with similar shape have lead to the speculation that blastema cells have obtained a state of multipotency. But, is the blastema indeed a homogeneous pool of multipotent progenitor cells, or do cells in the blastema memorize from what tissue types they derive?

3.1.2 Cell lineages during regeneration

The hypothesis that certain populations of cells can switch identity and contribute to tissues other than their origin has existed for a long time. Evidence for the fact that tissues other than skeleton can give rise to skeletal elements came from classical experiments in which salamander limbs were amputated and all skeletal material was removed from the stump (Weiss, 1925; Bischler, 1926; Thornton, 1938). Those limbs regenerated normally and contained all normal limb tissues including bone.

The question whether blastema cells retain a certain tissue specific memory or not was addressed in a number of transplantation experiments. Steen (1968) grafted labelled cartilage and muscle tissue into a host limb, amputated through the graft and analyzed labelled progeny for its contribution to other tissues. While muscle- derived cells were found in a variety of other tissues including skeleton, cartilage regenerated pure cartilage.

Marion Namenwirth (1974) took advantage of the fact that limbs that were X-irradiated lose their ability to regenerate (Trampusch, 1959; Maden, 1979; Holder et al., 1979). She grafted triploid unirradiated muscle, bone and skin (consisting of either pure epidermis or containing both dermis and epidermis) to diploid irradiated limbs and amputated through the region that received the graft (Namenwirth, 1974; Dunis and Namenwirth, 1977). Muscle, bone and skin consisting of epidermis and dermis rescued regeneration, while pure epidermis did not form any mesodermal tissue and covered the wound. The finding that epidermis does not contribute cells to the mesenchymal part of the blastema is consistent with earlier findings (Riddiford, 1960; Hay and Fischman, 1961; O'Stien and Walker, 1961).

Analyses on regenerated limbs receiving skin grafts prior to amputation revealed that cells residing in the dermis have the potential to contribute to a variety of tissues including cartilage, joint connective tissue and muscle connective tissue. Descendants of labelled dermal cells were also identified as myoblasts, however, at this time it was not clear whether this result was due to contaminating muscle attached to the graft (Namenwirth, 1974; Dunis and Namenwirth, 1977). Holder (1989) reinvestigated the role of dermis during regeneration and found 40% of limbs that regenerated from irradiated limbs receiving dermal grafts to be free of muscle, while in 60% of the limbs muscle tissue was found. The muscle-less regenerates contained skeletal

elements, tendons and dermis, demonstrating that regeneration can principally occur in the absence of muscle.

When analyzing the type of tissues that formed from bone, Namenwirth found that bone receiving limbs mainly formed new bone elements with a small percentage of cells giving rise to dermal fibroblasts. Muscle was absent from these limbs. In muscle receiving limbs, basically all cell types were present in the mature limb, agreeing with the results of Steen. However, in both experiments the authors were unable to discriminate between cells derived from muscle fibers, satellite cells and fibroblasts of the muscle connective tissue, so that it is unclear what cell types had contributed to other tissues. In this context, a recent study adressed the role of satellite cells during regeneration and suggests that these cells carry the potential to form a variety of cells including chondrocytes. However, the performed experiments involved isolation, BrdU labeling and reimplantation of the cells, and their behavior *in vivo* is unknown (Morrison et al., 2006).

Wallace (1973) transplanted unirradiated nerves into irradiated limbs and found that, when amputated through the graft, normally shaped limbs grew out that contained skeleton, connective tissue and a few muscle fibers. This effect coud be due to fibroblasts in the nerve or Schwann cells, and a phenomenon called ‘paradoxical regeneration’ suggests that Schwann cells can potentially form other tissues and rescue regeneration of an irradiated limb (Wallace, 1972; Maden, 1977). When the upper and the lower arm of a limb were irradiated while the hand was shielded and thus protected from irradiation, the limb regenerated when amputated through the upper arm, however, there needed to be a time interval between irradiation and amputation. It has been found earlier that Schwann cells can migrate along nerves in both proximal-to distal and distal-to-proximal directions (Wallace, 1972). Therefore, it was postulated that Schwann cells migrate from the intact hand along the axons to the upper arm level, rescue regeneration and contribute to mesodermal tissues (Wallace, 1972; Maden, 1977). Interestingly, Echeverri and Tanaka (2002) performed cell- labeling experiments and followed fluorescent ependymal cells of the spinal chord during tail regeneration. They showed that these cells leave their environment and contribute to muscle and cartilage, demonstrating that a switch from an ectodermal to a mesodermal fate can principally occur *in vivo*.

All these experiments suggest a certain potential of blastema cells to change identity and contribute to tissues other than their original source. However, in one way blastema cells seem to possess a tissue specific identity: Regeneration can occur in the complete absence of muscle, and it has been shown that new muscle tissue does not form from skeletal cells. We believe that this is also true for skin, however, it could never entirely be ruled out that skin- derived cells contribute to muscle, as in a reasonable amount of experiments muscle tissue formed from grafted skin, probably due to contaminating myogenic cells attached to the graft.

While at least some cell types seem to change their identity during regeneration in urodeles, this does not seem to be the case in the tadpoles of anurans, which can regenerate their limbs and tail. Already from morphological observations, the "blastema" appears to consist of heterogeneous populations of cells. To analyze the fate of the different tissue lineages during regeneration, animals with GFP labelled notochord, spinal chord and muscle tissues were generated (Gargioli et al., 2004). The result of these experiments was very clear: While regenerating notochord and spinal chord grew from their corresponding tissue, no muscle tissue was labelled in the regenerate and it turned out that it is exclusively the pool of satellite cells that gives rise to the newly forming muscle tissue (Gargioli and Slack, 2004; Chen et al., 2006).

These results point to different mechanisms between urodeles and anurans in the replacement of tissue during regeneration.

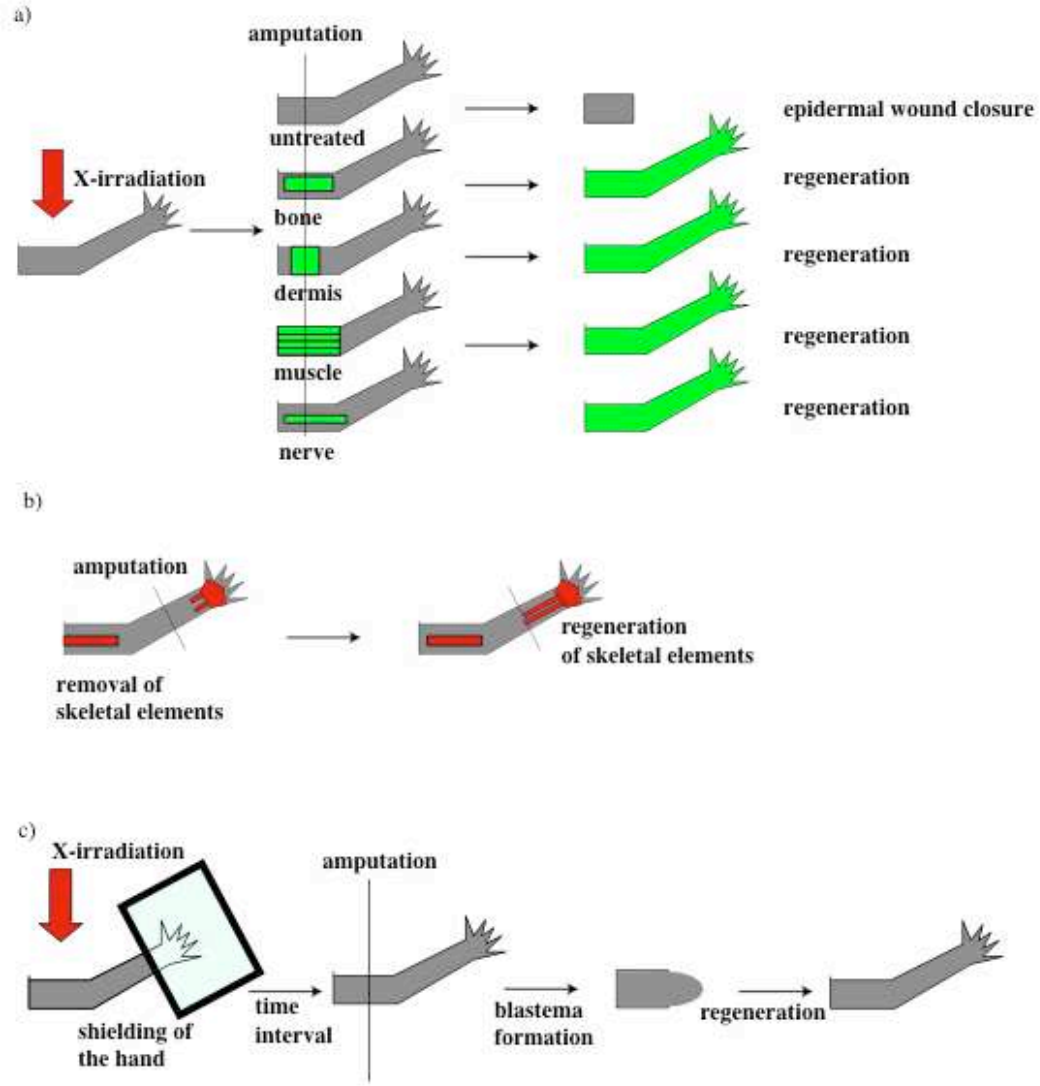

Fig. 3-1: The influence of the different tissues on regeneration. a) An X-irradiated limb looses its ability to regenerate. However, unirradiated skin, bone, muscle or nerves rescue regeneration when transplanted into an irradiated limb (Wallace and Wallace, 1973; Namenwirth, 1974; Dunis and Namenwirth, 1977. b) When bone is removed from the limb, other tissues replace it during the course of regeneration (Weiss, 1925; Bischler, 1926). c) Paradoxical regeneration. If an experiment as in a) is performed just with the difference that the hand is shielded from irradiation, this limb regenerates if a sufficient amount of time is left between irradiation and ambutation. It has been argued that within this time, unirradiated Schwann cells migrate from the hand to the upper arm level and have the potential to reconstitute the entire limb (Wallace, 1972; Maden, 1977).

3.1.3 Tissues and their impact on patterning

The results obtained from transplanting unirradiated skin, bone, muscle and nerves to irradiated limbs also illustrate another property of cells resident in these grafts: They possess information regarding the reestablishment of the proximo-distal axis, as in a reasonable number of cases well patterned limbs with upper arm, lower arm and hand elements grew out.

In particular, dermis has been shown to play a crucial role the patterning process. This has been investigated in various experiments in which the limb skin was rotated (Carlson, 1974, 1975), was made symmetrical with respect to the transverse limb axes (Tank, 1979; Maden and Mustafa, 1982; Slack, 1980, 1983) or used as positionally mismatched implants (Rollman-Dinsmore and Bryant, 1984), and as a result of manipulating the skin in all these experiments the pattern of the regenerating limb was dramatically affected. Carlson (1975) demonstrated that the effects seen are due to the dermis, while epidermis contains no patterning information. The number of experiments demonstrates that the correct spatial organization of the dermis with respect to the underlying tissues is crucial for the normal patterning of the regenerate. Furthermore, as predicted by the polar coordinate model, different positional values must be present in order to direct patterning. This is most clearly illustrated by an experiment in which a longitudinal dorsal stripe of dermis tissue was excised and grafted to a host limb in a 90° angle so that the complete circumference consisted of dorsal values. In these dorsal-only limbs, regeneration was blocked (Carlsson, 1974).

The importance of different circumferential values to be present to mediate proximo-distal outgrowth and correct patterning of the regenerate was recently revisited and further analyzed by Endo et al, who defined a step-wise model for induction of limb regeneration (Endo et al., 2004). They showed that a bump of tissue with the histological features of a blastema can be generated by inducing a lateral wound and rerouting the brachial nerve to the centre of the wound, consistent with the long-known nerve-dependence of blastema growth. However, outgrowth of an ectopic limb occurred only when a swath of full thickness skin from a 180° angle to the wound was transplanted to the denuded surface of the limb and thus created a situation in which cells from different sites of the limb circumference were juxtaposed.

Changes of the orientation of muscle in the mature limb and subsequent amputation through the manipulated region revealed that the outgrowing limb had patterning defects as well, suggesting that a part of the positional information in the limb is also encoded in muscle tissue (Carlson, 1975). There are controversial point of views about the role of bone during regeneration: Changes of orientation of bone in the mature limb such as 180° rotation and subsequent amputation through the manipulated region did not result in abnormal patterning of the regenerate (Carlson, 1975), however, Namenwirth's results show that the skeleton has the potential to form a newly patterned limb (Namenwirth, 1974).

3.1.4 Towards understanding the roles of the different tissues during regeneration

Using transgenic axolotls ubiquitously expressing GFP under the control of the CAGGS promotor in combination with molecular markers allows us to study cell fate decisions and the potential to contribute to patterning during regeneration more precisely. For our experiments, we performed transplantations of labelled skin, bone and muscle tissues as well as Schwann cells to wild type hosts.

We readdressed the question to what tissue types skin and bone contribute. In particular, we provide further evidence that skeletal or skin derived cells do not give rise to muscle during regeneration.A contribution of skin to muscle tissue could never be ruled out in the past. The role of the skin in the patterning process was extensively studied during the past decades, however, to our knowledge the fate of its cells with regard to contribution to other tissues has never been studied in intact limbs not being affected by e.g. irradiation. Therefore, the role of skin- derived cells during normal regeneration is still not known.

We furthermore tested whether our tissue transplants putatively encode information that is related to the proximo-distal patterning considering two different aspects of positional information.

The meis and HoxA genes have been shown to be crucial in controlling proximo-distal patterning (Morgan et al., 1992; Dolle et al., 1993; Small and Potter, 1993; Davis and Capecchi, 1994; Davis et al., 1995; Yokouchi et al., 1995; Fromental-Ramain et al., 1996; Zakani and Duboule, 1996; Nelson et al., 1996; Mercader et al.

1999, 2005; Boulet and Capecchi, 2004). We studied whether skin-, bone-, muscle- and Schwann cell derived progeny in the blastema upregulates these markers.

Cells derived from different proximo-distal levels exhibit different cellular behaviors involving the cell surface (Nardi and Stocum, 1983; da Silva et al., 2002). This becomes most obvious when distal blastema cells are placed into a proximal environment as during the course of regeneration the different cell populations segregate from each other and distal cells translocate back to their distal origin (Crawford and Stocum, 1988; Echeverri and Tanaka, 2005). We tested whether progeny derived from distal bone or Schwann cells exhibit such a behavior during the course of regeneration or not. Our results suggest that cells derived from skin, skeleton and muscle encode information regarding proximo-distal patterning, while Schwann cells do not. Our results furthermore support the view that a distal-to-proximal reprogramming during the earliest stages of regeneration does not occur.

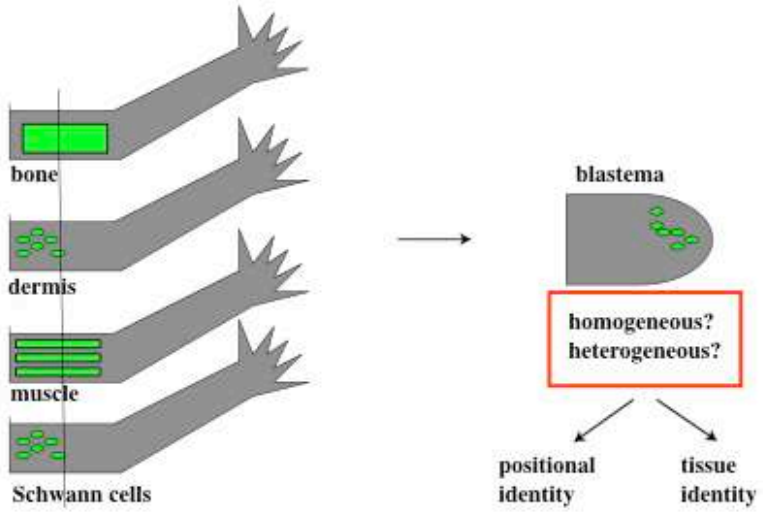

Fig. 3-2: Experimental outline and questions we aim to answer. By transplanting GFP labelled bone, dermis, muscle and Schwann cells into the mature limb and analyzing their progeny in the blastema, we want to study their plasticity regarding tissue fate. Furthermore, we want to test whether blastema cells deriving from different sources harbor positional information regarding proximo-distal identity.

3.2 Results

3.2.1 Integration of fluorescent bone, skin, muscle and Schwann cell grafts into the host tissue

To follow the fate of cells deriving from different tissue sources during the course of regeneration, we transplanted upper arm fluorescent skin, bone and muscle from donors harboring the GFP under the control of the CAGGS promotor (Sobkow et al., 2006) to the upper arm of wild type hosts. Animals specifically labeled for Schwann cells were a kind gift from Dunja Knapp and were generated during their embryogenesis by grafting the neural folds from a neurula stage transgenic embryo to a wild type host. However, the number of these animals was restricted, and we transplanted tissue that contained GFP labeled Schwann cells into wild type hosts to increase the number of animals being available for experiments.

40/40 skin-, 17/21 bone- and 10/20 Schwann cell transplants survived the grafting procedure and could be observed in the host limb 2 weeks after transplantation (Fig. 3-3). While skin transplants appeared to be integrated into the host skin without any scar formation, bone transplants did heal but remained with scars in the upper arm. Often, instead of replacing the humerus, fluorescent bone tissue was invaded by wild type cartilage cells as a healing response, resulting in a cartilageneous mass of fluorescent and non-fluorescent cells. Schwann cells integrated without any scar formation and formed a network, presumably reflecting their attachment to nerves. From the muscle transplants, only 20/52 survived the grafting procedure. 6 of those grafts formed green fluorescent fibers during the course of wound healing and were observed 4 weeks after the surgery, and one of these examples is shown in Figure 3-3. Only these grafts were considered for further analysis.

3.2.2 Bone, skin and muscle tissue harbor cells of different identities

With exception of the Schwann cell grafts, all other transplants harbored fluorescent cells of different identities, which is shown in Figure 3-3.

Skin consisted of the epidermal layer and the underlying dermal part. The fate of epidermis during regeneration is restricted to self- renewal, and it has been shown that epidermis does not contribute to pattern formation (Riddiford, 1960; Hay and Fischman, 1961; O'Steen and Walker, 1961; Namenwirth, 1974; Carlson, 1975). Therefore, when describing and discussing our results, we will refer to the dermal component of the skin hereafter. Dermal tissue is protruded by a fine meshwork of blood vessels and nerves with attaching Schwann cells, which we were unable to remove completely. Using antibodies against ß3-tubulin as a marker for axons and Myelin Basic Protein (MBP) as a marker for the myelin sheet of Schwann cells, we could detect dermal fluorescent material to be present in nerves after the tissue had integrated.

In the animals we used, cells were not ossified yet, and the three main cell types occurring in bone were cartilage, perichondrium and ligaments. Although we are lacking the respective markers, we assume that we grafted cells of all three identities.

In muscle tissue, we verified the existence of fluorescent muscle fibers by staining for Myosin Heavy Chain I (MHCI), a marker for these cells. However, we also transferred satellite cells, which are attached to the muscle fibers, as staining for the satellite cell marker Pax7 shows. In addition, we found cells lying next to nerves, presumably being Schwann cells. Although we cannot analyze with specific markers for fibroblasts, it is very likely that we also grafted these cells, as we know that fibroblasts are present in muscle tissue as well (Steen, 1968; Namenwirth, 1974).

The progeny of the transplanted neural folds produced a number of cell types including Schwann cells, oligodendrocytes, melanocytes and cells of the dorsal root ganglia (Dunja Knapp, personal communication). However, only two of these various cell types are present in the limb: Schwann cells and melanocytes. Since melanocytes of our laboratory animals are defective in migrating from the spinal chord, the only

cell type deriving from neural fold grafts are Schwann cells. In limbs with only Schwann cells labeled, fluorescent MBP positive cells attaching to nerves were detected.

We are aware that bone-, dermal- and muscle transplants did not harbor one specific cell type. However, we are studying the following questions: Do tissues other than muscle contribute cells to newly forming muscle tissue? What tissues harbor cells that putatively encode information regarding the reestablishment of the proximo-distal axis?

As we will show below, these questions are still addressable under the experimental conditions we are working with.

3.2.3 The absence of muscle tissue from skin, bone and Schwann cell grafts

Muscle tissue comprises a major part of the mature limb and attaches to bone as well as dermis. Therefore, we put an effort into the careful analysis of our transplants regarding the possibility of contamination with muscle. After wound healing, in 10% of the dermal grafts we observed the formation of long green fibers, presumably muscle deriving from dermal graft attaching myogenic cells. Any of these limbs was excluded from our further analysis. In those limbs that received fluorescent bone grafts, we did not observe any muscle fiber deriving from the graft. To further ensure that no myogenic cell was transferred along with bone or dermal tissue, a minimum of six limbs of each type of graft were analyzed for the expression of Pax7 and MHCI, and representative examples are shown in Figure 3-3. In none of the cases we could localize these markers to the grafted fluorescent cells, suggesting that we transplanted dermis and bone without attaching muscle tissue. Also, we never detected MHCI and Pax7 in fluorescent Schwann cells. While we cannot exclude nerves and Schwann cells from dermal and muscle tissue, bone does not contain nerves. Therefore, we analyzed six fluorescent bone grafts for ß3- tubulin and MBP. In none of these cases we could detect MBP positive fluorescent cells nor fluorescent cells located next to nerves, as we saw in limbs receiving dermis, muscle and Schwann cell transplants.

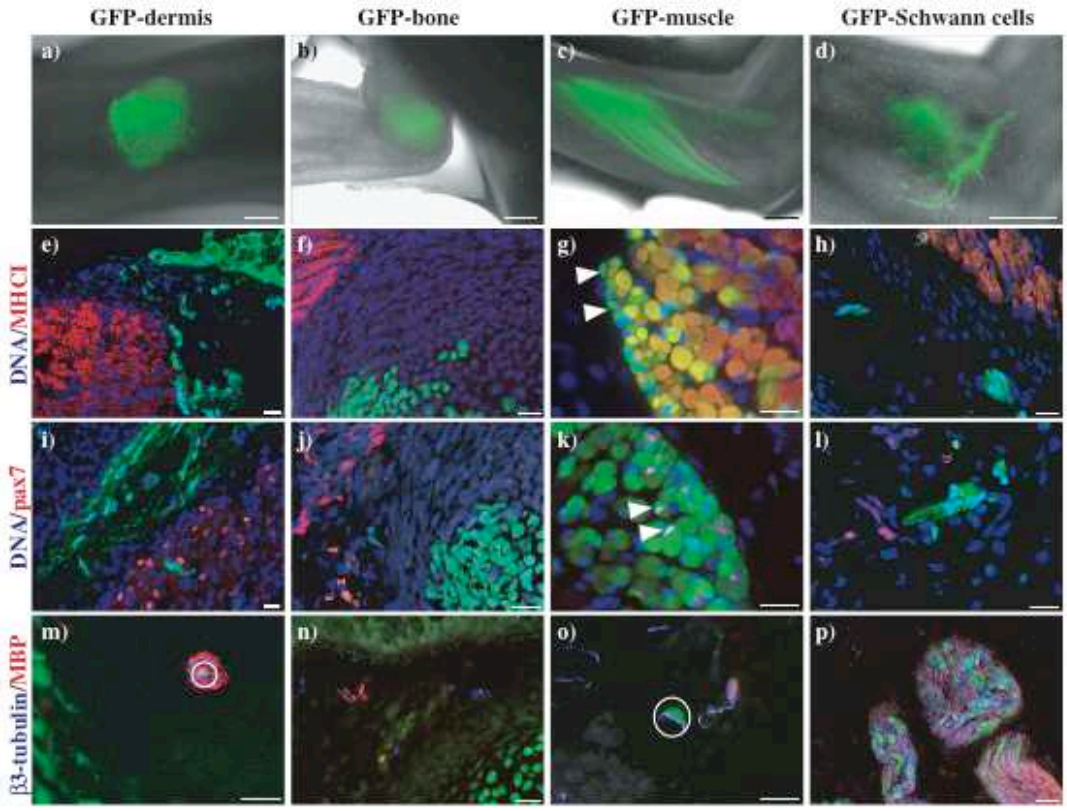

Fig. 3-3: Integration and cellular composition of fluorescent tissue grafts. Grafts of dermis (a), bone (b), muscle (c) and Schwann cells (d) integrated into the host limb. Bars: 0.5 mm. e)-p): Cross sections of limbs with integrated tissues were analyzed for MHC (e-h), Pax7 (i-l) and β3-tubulin/MBP (m-p). MHCI, Pax7 and MBP stainings are shown in the red, DAPI (e-l) and β3- tubulin (m-p) in the blue channel. We do not detect MHCI or Pax7 in cells deriving from grafts of dermis (e,i), bone (f,j) or Schwann cells (h,l), but in muscle (g,k). Arrow heads in g) indicate GFP^+/MHC^- and in k) $GFP^+/Pax7^+$ cells, showing that muscle transplants did not exclusively consist of muscle fibers. By MBP and β3-tubulin staining, we found cells in and around nerves in dermis (m; note the encircled GFP signal surrounded by MBP/β3- tubulin staining), muscle (o; encircled is a green fluorescent cell attached to a putative axon) and Schwann cells (p), but not bone (n). Bars: 50μm.

3.2.4 Progeny from all four transplantation types contribute to the blastema and the regenerate

It is known that, in the mature limb, the correct position of cells as well as a complete set of cells carrying dorsal, ventral, anterior and posterior values is crucial for the regenerative capability. To test whether our transplantations caused any defect in the ability of the limb to regenerate and to see whether progeny of each type of graft contributes to the regenerate, we amputated through the transplanted region after wound healing, followed the fluorescent cells during regeneration and examined the morphology of the regenerates. In each case, fluorescent cells entered the blastema and contributed to the formation of a new limb without any defects (Figure 3-4). This allows us to study progenitor cells derived form each graft type during and after regeneration.

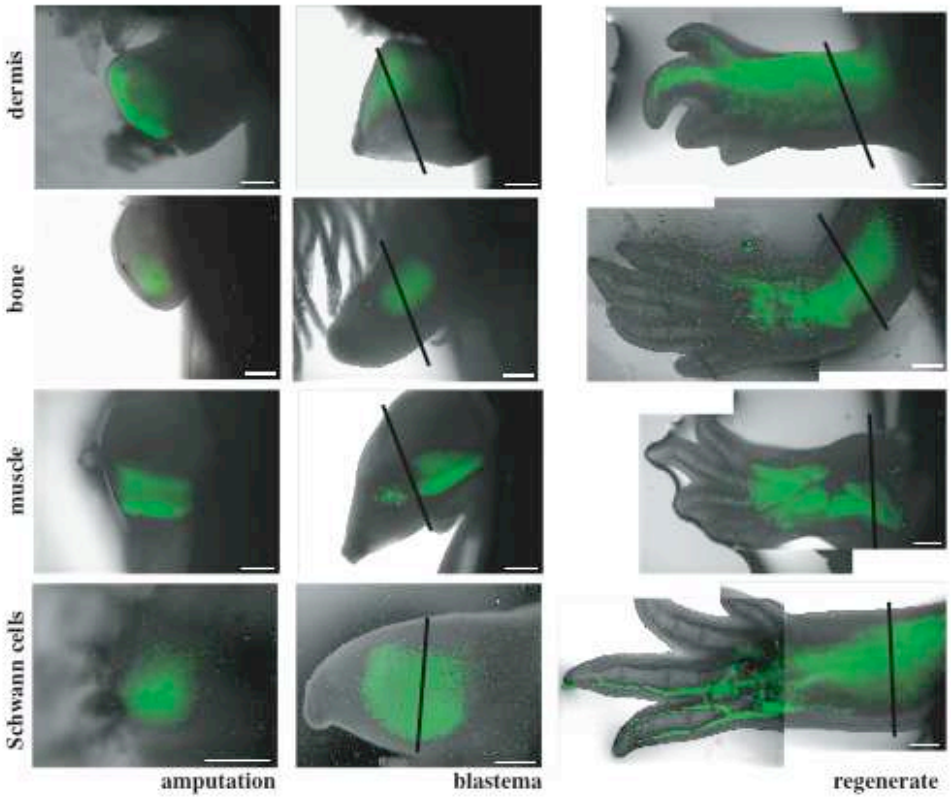

Fig. 3-4: Progenitor cells of dermis-, bone-, muscle- and Schwann cells contribute to the blastema and regenerate. In every picture, distal is to the left and proximal to the right. Black lines indicate the plane of amputation. Bars: 0.5 mm.

3.2.5 The fate of dermis- and bone derived GFP$^+$ cells

The generation of limbs labelled for dermis-, bone- and muscle tissue as well as Schwann cells provides a good opportunity to study the fate and the plasticity of cells deriving from these sources during regeneration. In our analysis addressing this question, we concentrated on the study of cells originating from the dermal and skeletal sources. The generation of animals specifically labelled for muscle fibers or satellite cells is currently ongoing (Sharyhar Khattak, personal communication) and will allow us to follow muscle derived blastema cells without contaminating fibroblasts. The fate of Schwann cells will be addressed as a separate issue (Dunja Knapp et al., personal communication).

Bone has been shown to mainly form new skeletal elements during regeneration, with a few cells contributing to connective tissue, while muscle did not form from bone (Steen, 1968; Namenwirth, 1974). In irradiated limbs, dermis has been shown to give rise to a variety of tissues, however, it has been controversial whether muscle can be formed from cells that have their origin in dermis due to contamination issues (Namenwirth, 1974; Dunis and Namenwirth, 1977; Holder, 1989). Therefore, we were curious how progeny of a muscle- free dermal tissue behaves during regeneration of limbs in which other tissues were not affected by irradiation.

3.2.6 Spatial organization of dermis- and bone derived cells in the blastema

Figure 3-5 shows representative sections of a midbud stage blastema containing progenitor cells derived from dermis and bone. As it can be seen, progeny of the bone remains in the centre of the regenerating limb, almost all dermis- derived progeny was found at the periphery. Some dermal progenitor cells are found to distribute towards the centre of the blastema. These data suggest a spatial organization of bone- and dermis derived progenitor cells in the blastema. But, are they also organized regarding their fate?

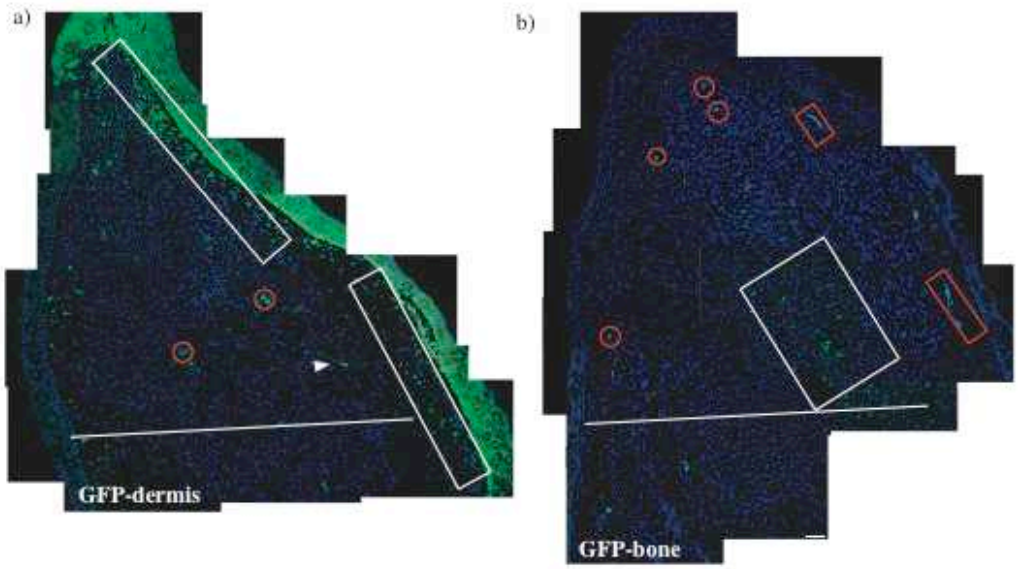

Fig. 3-5: Spatial organization of dermis- and bone- derived cells in the blastema. Longitudinal sections of midbud stage blastemas showing a) dermis- derived and b) bone- derived fluorescent progenitor cells. White rectangles highlight the domains in which fluorescent cells are found, red rectangles and circles show red blood cells, which are often found in a blastema of this stage and which are fluorescent in every channel. Note that bone- derived cells concentrate in the centre, while most of the dermis- derived blastema cells are found at the periphery. The low number of fluorescent bone-derived cells in the blastema results from the fact that after transplantation, non-fluorescent bone cells of the host populated the wound so that after two weeks of integration, the newly formed bone tissue consisted of GFP^+ and GFP^- cells. The white lines demarcate the amputation plane. Distal is to the top. Bar (for both blastemas): 100μm.

3.2.7 Dermis- and bone derived cells do not upregulate Pax7 in the blastema

As pointed out earlier, we were interested in the potential of dermis and bone derived blastema cells to contribute to other tissue types during regeneration. In particular, we wanted to test whether cells originating from both tissue types can eventually transdifferentiate into cells of the myogenic lineage.

To study this, we analyzed blastemal progenitor cells deriving either from bone, dermis or muscle for their expression of Pax7, a marker for the myogenic lineage (for review, see e.g. Buckingham et al., 2003). In Figure 3-6, we show a representative section of a midbud stage blastema stained for Pax7. As it can be seen, expression of Pax7 is restricted to the periphery of the blastema, being in one line with the mature

muscle beyond the amputation plane but absent from the outer-most cells, suggesting that it can be used as a myogenic marker during regeneration.

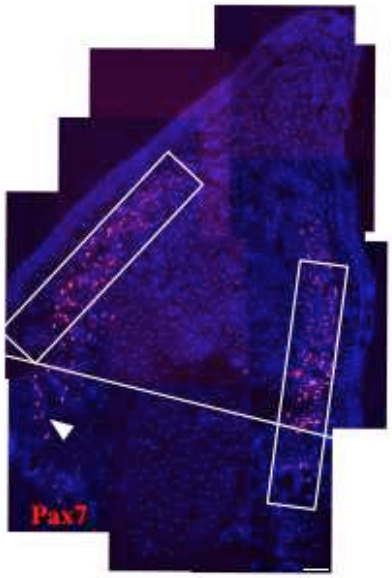

Fig. 3-6: Pax7 expression in a 12 day midbud stage blastema. Longitudinal section of a midbud stage blastema stained for Pax7. Expression domains are highlited by white rectangles, the amputation plane is depicted by a white line. Note that Pax7 expression is restricted to the periphery and starting proximal to the amputation plane (white arrow head), as amputation causes the muscle and connective tissue of the stump to contract so that some blastema cells are located next to the bone. Distal is to the top. Bar: 100µm.

Neither dermis- nor bone derived blastema cells were found to express Pax7, as shown in Figure 3-7 and summarized in Table 3-1, suggesting that cells of the dermis and bone lineage had not changed to a myogenic identity at that stage of regeneration. In contrast, between 12.5% and 75% of those progenitor cells originating from muscle expressed Pax7. This variety of $Pax7^{+}$ cells might be due to different percentages of myogenic cells transferred with each individual graft.

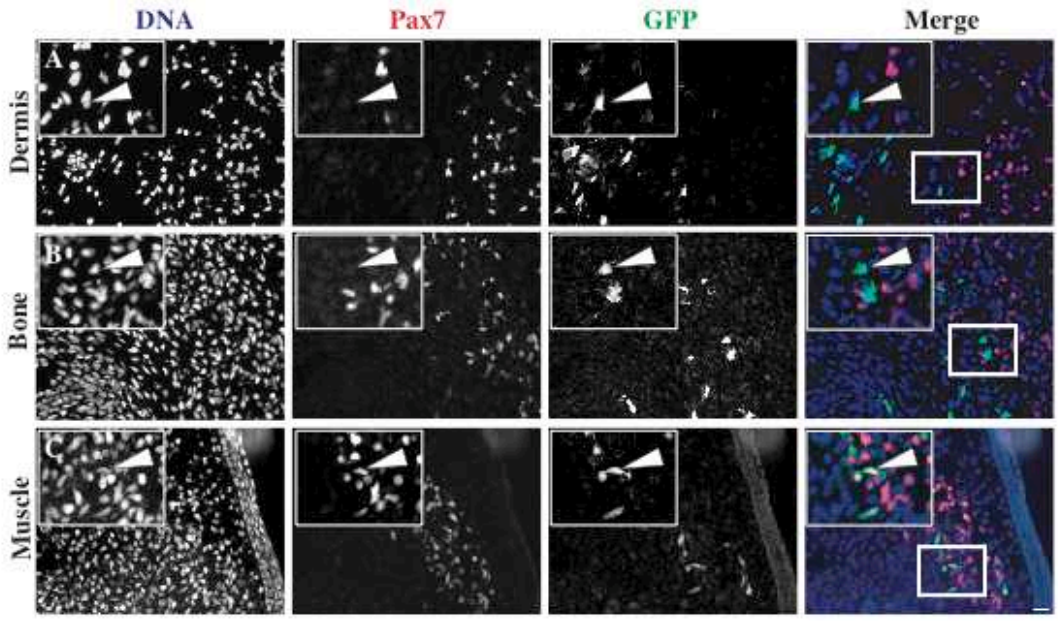

Fig. 3-7: Pax7 is not upregulated in blastema cells derived from dermis and bone, but is expressed in muscle derived progenitors. Pax7 staining of longitudinal sections of midbud stage blastemas harboring dermis- (A), bone- (B) or muscle- (C) derived fluorescent progenitor cells. White arrow heads indicate GFP positive cells, whose nuclei do not colocalize with Pax7 when deriving from dermis and bone, but do colocalize with Pax7 when deriving from muscle tissue. Bar: 50µm.

Table 3-1*: Dermis- and bone derived cells do not upregulate Pax7 in the blastema

sample	GFP+/Pax7-	GFP-/Pax7+	GFP+/Pax7+
dermis 1	49	83	0
dermis 2	11	15	0
dermis 3	16	30	0
dermis 4	79	250	0
dermis 5	115	118	0
bone 1	84	130	0
bone 2	40	64	0
muscle 1	10	68	22
muscle 2	14	55	2
muscle 3	6	47	19

*In blastemas harboring descendants of bone and dermis, domains of GFP^+ cells and $Pax7^+$ cells were often spatially segregated from each other, and numbers in this table represent only those cells that are located in overlapping regions.

3.2.8 Dermis- and bone derived cells do not contribute to muscle tissue after regeneration

From looking at the blastema stage, we cannot exclude that a subset of myogenic progenitor cells does not express Pax7 or that bone and dermis derived blastema cells could switch their identity after the blastema stage.

Therefore, we examined whether we could find evidence for a contribution of dermis and bone derived cells to muscle tissue in the regenerated limbs, using MHCI as a marker for muscle fibers and Pax7 as a marker for satellite cells. As shown in Figures 3-8 and 3-10 and summarized in Table 3-2 and 3-3, we never found any indication that cells deriving from those tissues had ultimately changed their identity to form a satellite cell or to contribute to muscle fibers, suggesting that bone and dermis do not contribute to rebuild muscle tissue during the course of regeneration. In contrast, we find that muscle derived cells contribute to muscle fibers after regeneration and upregulate MHCI (Figure 3-8).

Table 3-2*: Dermal progeny does not express Pax7 and MHCI after regeneration

sample	$GFP^+/Pax7^-$	$GFP^-/Pax7^+$	$GFP^+/Pax7^+$	$MHCI^+/GFP^+$?
1	10	65	0	No
2	40	20	0	No
3	115	18	0	No
4	10	1	0	No
5	60	47	0	No
6	59	55	0	No

*We scored only those GFP^+ cells that were located in the muscle tissue

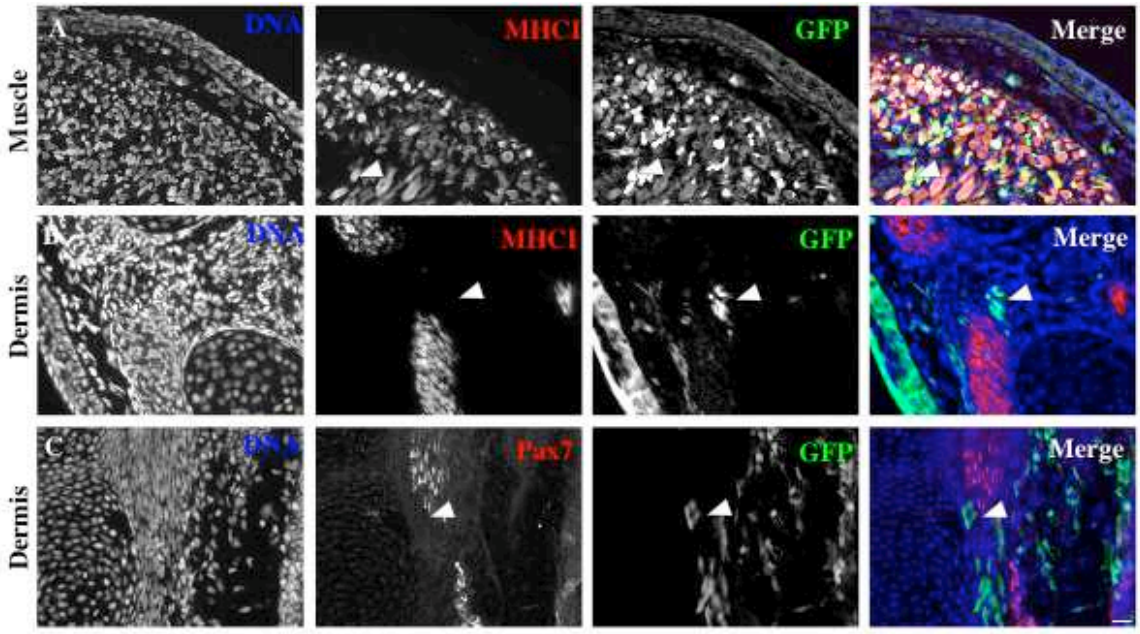

Fig. 3-8: Progeny of dermis does not contribute to muscle fibers and satellite cells after regeneration. A-C: Cross sections of regenerated limbs harboring muscle- derived (A) or dermis-derived (B, C) fluorescent progeny. A: In some cells, colocalization of GFP and MHCI can be detected (arrow head), illustrating that progeny had contributed to muscle tissue. B and C: No colocalization of GFP and MHCI (B) or Pax7 (C) can be detected in dermis- derived fluorescent progeny (compare arrow heads). Note that the thickness of the muscle fibers is different in A and B. Differently sized muscle fibers have also been observed in muscle tissue of the tail. Bar (for all panels): 50 µm

However, we found dermis- derived cells to take a variety of other cell fates, which is shown in Figure 3-9. Although respective markers are lacking, morphological observations suggest that cartilage and perichondrial cells as well as fibroblasts of the muscle connective tissue and tendons are among dermis-derived progeny. By staining with MBP, we identified Schwann cells, which possibly derived from contaminating Schwann cells that were transferred during the grafting procedure (data not shown).

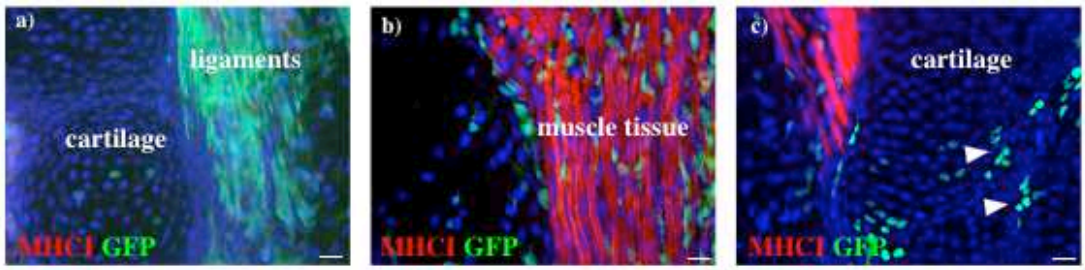

Fig. 3-9: Dermal progeny is found in a variety of non-dermal tissues after regeneration. a)-c) are longitudinal sections of regenerated limbs harboring fluorescent dermal progeny. Sections were stained for MHCI, and location of the cells was determined by morphological observations. a) Contribution to long fibers that are negative for MHCI. These could be tendons or ligaments. b) Dermal progeny is also found in muscle tissue where cells possibly contribute to connective tissue. c) Fluorescent dermal progeny in skeletal elements, where cells contributed to cartilage (white arrow heads). Bars: 50 μm.

In contrast to dermis, bone derived cells were found to be mainly restricted to renew the skeletal tissue. 90% of the bone derived cells or more had either contributed to cartilage, perichondrium or ligaments (Table 3-3). A small subset of cells was either found to be present around the elbow joint, between radius and ulna or in the connective tissue next to the digits. As mentioned earlier, none of the bone derived cells expressed Pax7 and gave rise to muscle fibers. To test whether those cells that were found outside the bone gave rise to Schwann cells, we also tested whether they expressed MBP or were located next to the nerves (Figure 3-10). We did not find any evidence, however, that those cells had formed Schwann cells and assume that they are fibroblasts and part of the connective tissue.

Table 3-3: Progeny of bone mainly contributes to skeletal elements and does not upregulate MHCI and Pax7

example	cells in skeletal structures	Cells outside skeletal structures	$Pax7^+/MBP^+$?	MHC^+?
1	253	10	no	no
2	757	20	no	no
3	3338	327	no	no

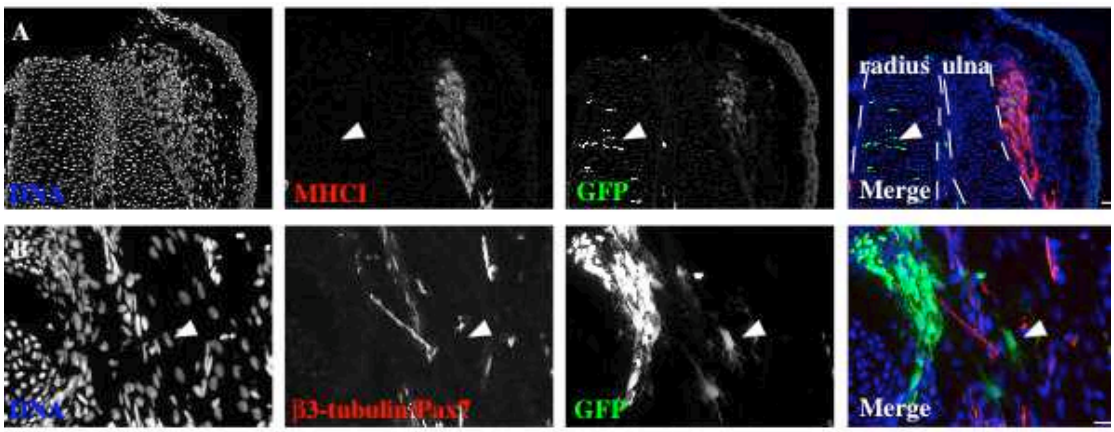

Fig. 3-10: Progeny of bone does not contribute to muscle tissue and mainly gives rise to new skeletal elements. A and B are longitudinal sections of regenerated limbs which received fluorescent bone grafts prior to amputation. A: Representative example of bone-derived cells contributing to newly formed bone, stained for MHCI. The lower arm region is shown. Dashed white lines in the Merge panel indicate the two skeletal elements of the lower arm, radius and ulna. Most fluorescent cells are found within skeletal structures (white arrow head). Note that there is some background signal in the MHCI positive region. B) the elbow region of a regenerate. Most fluorescent cells shown here contributed to the ligaments of the joint. Those few cells located outside the skeletal structures (white arrow head) were double stained for β3-tubulin and Pax7. In the example shown here as in all other fluorescent cells, there is no colocalization with β3-tubulin and Pax7. Bars: 50μm.

Our results demonstrate that normally, neither dermis nor bone derived cells contribute to muscle tissue during regeneration. However, we can confirm earlier findings in that we found that dermis derived cells contribute to a variety of non-dermal tissues. We do not know the specific cell types that harbor this potential to change their fate. We also confirm that the majority of bone- derived progeny gives rise to the newly- forming skeletal elements.

3.2.9 Do blastema cells deriving from different sources differ in their expression of genes associated with proximo-distal identity?

The midbud stage blastema is a self operating system and contains all the information to fully reconstitute the regenerating limb. However, it is not known whether all cells in the blastema contribute equally to the reconstruction of this complex structure. It is widely accepted that dermal- and muscle tissue possess information to rebuild the limb (e.g., Carlson, 1974, 1975). The role of bone- derived cells in the patterning

process has been controversial (compare Namenwirth, 1974 to Carlson, 1975 and Muneoka et al., 1986), and there is little information about the patterning activity of Schwann cells. However, it has been suggested that they have the potential to reconstitute a fully patterned limb (Wallace, 1972; Wallace and Wallace, 1973; Maden, 1977).

We decided to investigate whether dermis-, bone-, muscle- and Schwann cell derived progeny upregulates *Meis* and *HoxA* genes, which both play a crucial role in the reestablishment of the proximo-distal axis (Figure 3-11). We interpret upregulation of these markers as an indication that the respective tissue possesses information regarding the reconstitution of the proximo-distal axis. Although it has never been shown explicitely that the patterning information harbored by dermis and muscle tissue is of proximo-distal nature, we found it very likely that at least subpopulations of their progeny express *Meis* or *HoxA* genes.

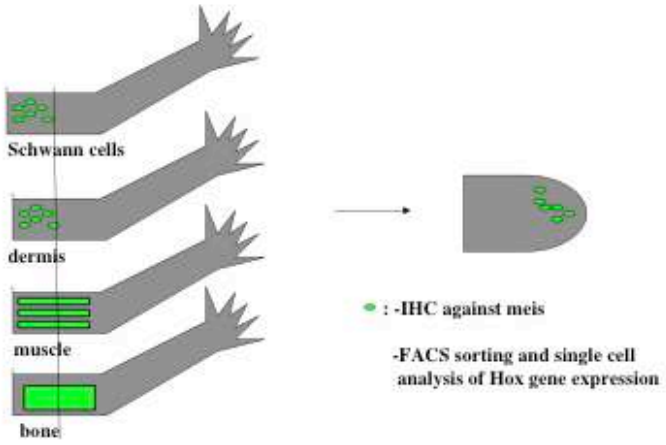

Fig. 3.11: Experimental outline to investigate which of the tissues possesses information that is related to proximo-diatal patterning.

3.2.10 Meis expression and nuclear localization in descendants of bone, dermis, muscle and Schwann cells

Meis genes encode homeodomain transcription factors that act through DNA binding. Therefore, we expect that in a proximally specified cell Meis localizes to the nucleus. Furthermore, the meis domain in the developing limb is restricted to the proximal region of the limb bud and extends distally only when the limb bud had been treated with retinoic acid.

We purchased a commercially available antibody directed against the C-terminal domain of the mouse homologues of Meis1/2/3. Figure 3-12 shows a representative section of a midbud stage blastema, and it can be seen that Meis expression and nuclear localization is restricted to the proximal region of the blastema. It is absent from mature tissue and cells of the distal region of the blastema.

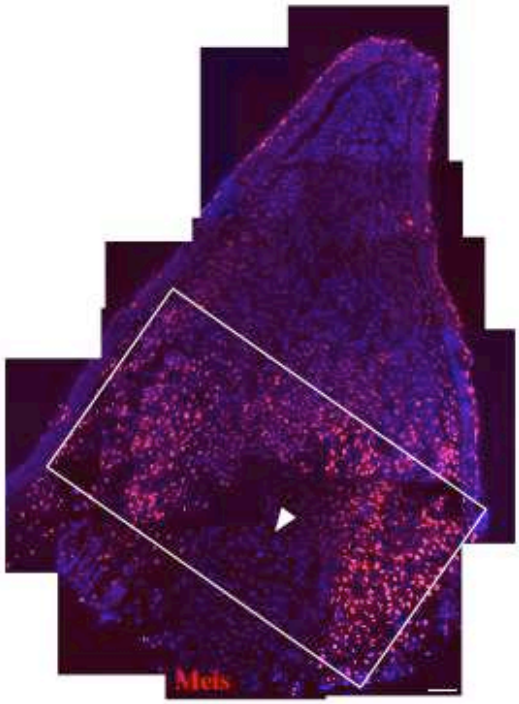

Fig. 3-12: Meis expression in the blastema. Longitudinal section of a midbud stage blastema stained for Meis. The expression domain in the proximal part of the blastema is highlited by a white rectangle. Note that meis staining is absent from mature bone (white arrow head). Also note that some nuclei of the epidermis are positive for Meis. This is most likely unspecific binding, as we also observe this cell layer to trap other antibodies. Bar: 100µm.

When analyzing whether GFP labelled cells displayed nuclear Meis staining, we only took cells into account that were clearly located in the proximal domain, with more distal neighbor cells showing nuclear localization of meis. In Figure 3-13, we show that Meis positive nuclei are present among progenitor cells originating from bone, dermis and muscle. In contrast, none of the Schwann cell progeny in the proximal region of the blastema displayed nuclei that were positive for Meis.

As summarized in Table 3-4, the highest percentage (70%- 100%) of Meis being located nuclear was found among the bone derived progenitors, while expression in progenitor cells of muscle and dermis origin appeared to be weaker, and the percentage of Meis positive nuclei varied from 5% to 100% among the different grafts.

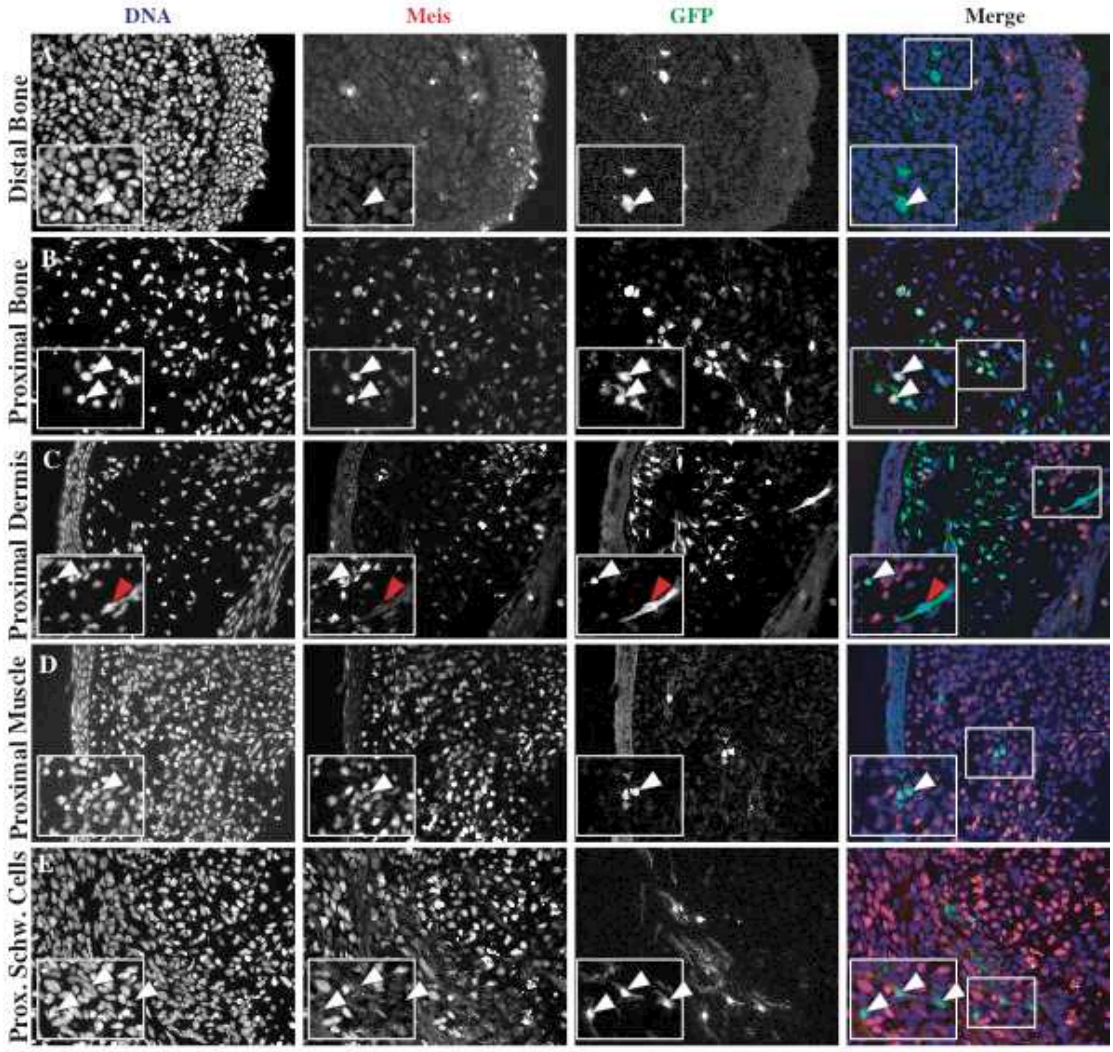

Fig. 3-13: Expression and nuclear localization of Meis in bone-, dermis-, muscle- and Schwann cell derived, GFP+ progenitor cells. Antibody staining against Meis on sections of blastemas harboring bone-, dermis-, muscle- or Schwann cell- derived fluorescent progenitor cells. Insets show an enlargment of the area marked by a white rectangle. A: Bone- derived cells are shown in the distal region of a blastema (white arrow head). We detect a cytoplasmic background, however, Meis is clearly absent from the nucleus. B: In contrast, bone-derived cells in the proximal part of the blastema are positive for Meis (white arrow heads). C: Cells in the proximal dermis showed a weaker signal for Meis (white arrow head). The red arrow head points to a cell that we scored as negative, as no nuclear Meis staining is obvious. D: Muscle- derived progenitors (white arrow head) showing nuclear localization of Meis. E: Schwann cell- derived progenitor cells in the proximal blastema (white arrow heads), no nuclear Meis staining is obvious. Bar (for all panels): 50 μm.

Table 3-4*: Expression and nuclear localization of Meis in bone-, dermis-, muscle- and Schwann cell derived progenitor cells in the blastema

example	$GFP^+/Meis^+$	$GFP^+/Meis^-$	% $GFP^+/Meis^+$
dermis 1	7	14	33
dermis 2	0	7	0
dermis 3	7	12	37
dermis 4	8	103	7
dermis 5	1	9	10
dermis 6	17	14	55
dermis 7	2	2	50
dermis 8	5	1	83
dermis 9	4	9	31
dermis 10	11	1	92
bone 1	12	5	71
bone 2	82	0	100
bone 3	32	2	94
bone 4	12	0	100
bone 5	43	2	96
bone 6	12	1	92
muscle 1	23	2	92
muscle 2	1	4	20
muscle 3	1	18	5
Schwann cell 1	0	7	0
Schwann cell 2	0	34	0
Schwann cell 3	0	13	0
Schwann cell 4	0	3	0
Schwann cell 5	0	8	0

*In all examples, only cells that were located in the proximal region were scored. Note that bone derived cells show the highest percentage of meis expression and nuclear localization. Variations among dermis- and muscle derived cells may reflect variations in the cellular composition of individual transplants.

As we could detect Meis positive nuclei among cells derived from bone, dermis and muscle grafts, we suggest that that in these tissues a subset of cells encodes positional information related to proximo-distal patterning. With regard to Meis expression and localization, progenitors derived from Schwann cells may behave differently in the patterning process.

3.2.11 Expression of *HoxA* genes in descendants of bone, dermis, muscle and Schwann cells

In contrast to Meis, antibodies against HoxA proteins were not available for axolotl cells. In chapter 2, we described the establishment of the single cell PCR method and showed that we can detect *HoxA9* and *HoxA13* in cells of the blastema. Therefore, we dissociated midbud stage blastemas harboring the respective labelled cells of different origin, sorted them by their GFP signal and analyzed the generated cDNA pool using gene specific primers as described in chapter 2.

Figure 3-14 shows the percentages of cells expressing *HoxA* genes depending on where they originate from. In 30% of the bone-, 50% of the muscle- and 60% of the dermis- derived cells expression of *HoxA9*, *HoxA13* or both was detected. In contrast, none of the Schwann cells was found to express *HoxA9* or *HoxA13*.

We also analyzed expression of the lineage markers *Myf5*, *Sox9* and *Sox10*.

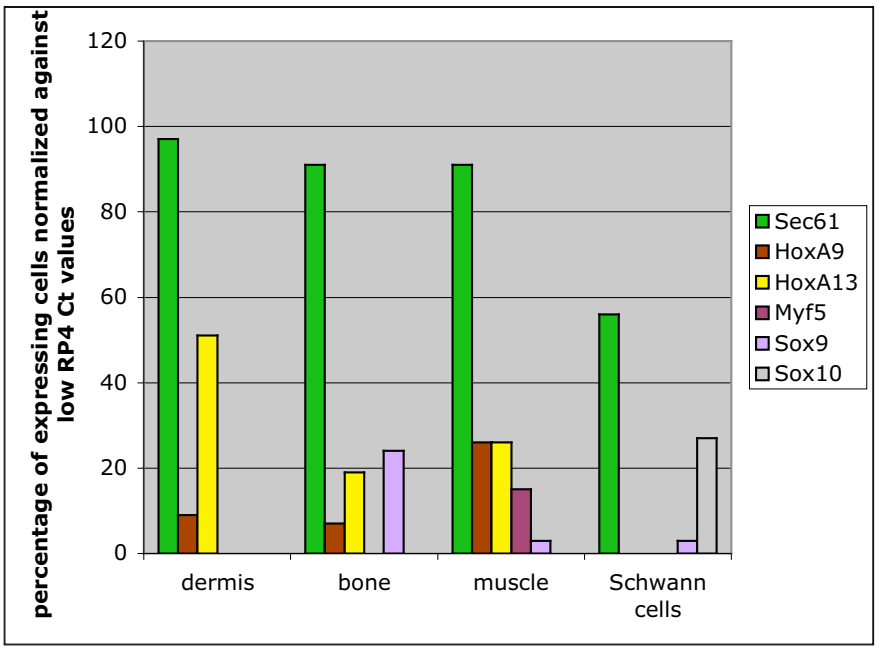

Fig. 3-14: Expression of *HoxA* genes and lineage markers in cells deriving from dermis, skeleton, muscle or Schwann cells. The graph shown here reflects the average value obtained from 2 independent experiments except muscle, whose progeny was collected once. Total numbers of cells: n(dermis)=44, n(bone)=44, n(muscle)=40, n(Schwann cells)=38.

In Figure 3-15, expression patterns of *Myf5* and *Sox9* in the midbud stage blastema are shown. *Myf5* is a marker for myogenic cells Buckingham et al., 2003), and we expected to detect it in a subpopulation of cells derived muscle grafts. Our analysis show that we detected *Myf5* in 16% of the muscle- derived cells. *Sox9* is a marker for cells of the chondrogenic lineage during development (for review, see e.g. Kawakami et al., 2006). As dermis, bone and muscle tissue contribute cells to the regenerating cartilage, and we expect it to be expressed by subpopulations of cells deriving from these tissues. Indeed, we found that 25% of the bone- derived cells and 3% of the muscle derived cells expressed *Sox9*, however, none of dermis- derived cells was found to express *Sox9* thus far. *Sox10* is expressed neural crest derived cells during development (for review, see Kelsh, 2006), and we found it to be expressed in 26% of the Schwann cell derived progeny in the blastema. As it is obvious from Figure 3-14, we did not find evidence for $HoxA^{+}/Sox10^{+}$ coexpressing cells, but we detected coexpression of *Myf5*/*HoxA* genes and *Sox9*/*HoxA* genes in blastema cells (Figure 3-15).

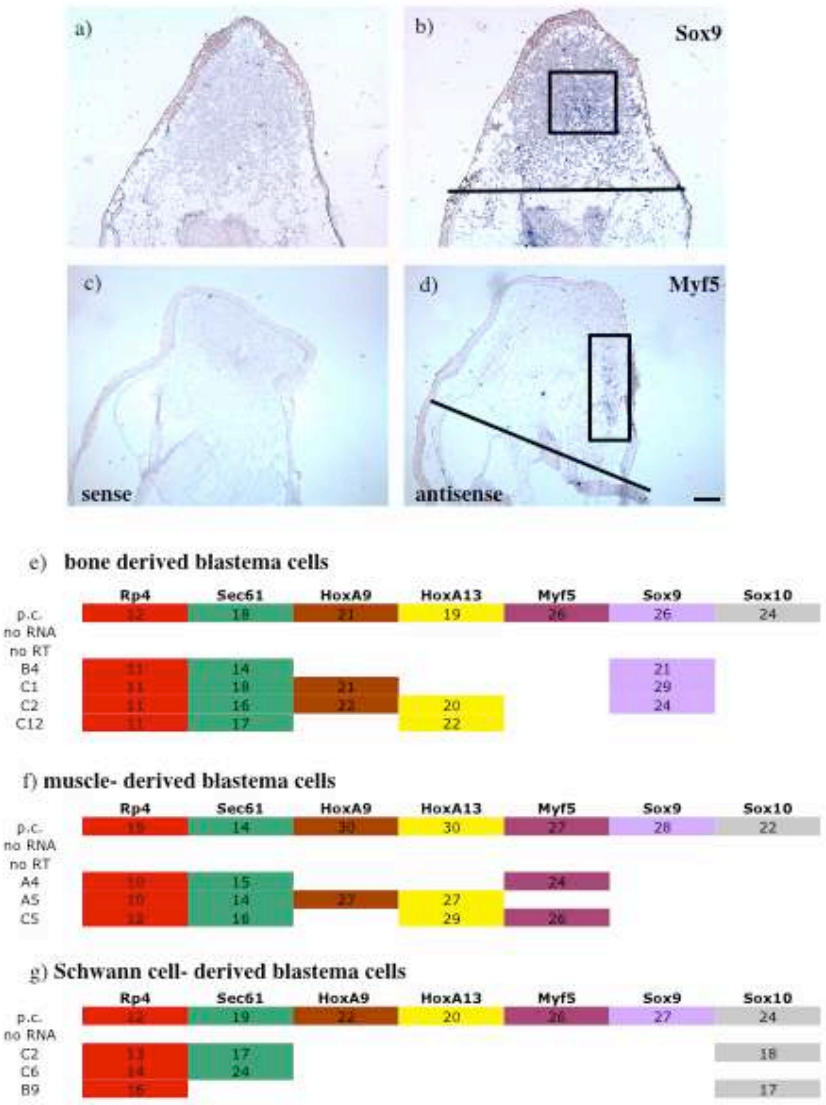

Fig. 3-15: Expression of *Myf5* and *Sox9* in the midbud stage blastema and their coexpression with *HoxA* genes. The *Sox9* expression domain (b) is in the centre of the blastema, the *Myf5* expression domain (d) is found at the periphery. Expression domains are highlited by a black rectangle. a) and c) are the respective sense controls on consecutive sections. Amputation planes are marked by a black line. Distal is to the top. Bar: 0.5 mm. e-g) Examples of our analyses on single cells, showing that different subpopulations of cells regarding lineage marker and *HoxA* gene expression exist. e) bone-derived, f) muscle-derived and g) Schwann cell- derived blastema cells. We find *Sox9* expression mainly among the bone-derived, *Myf5* expression exclusively among the muscle-derived and *Sox10* expression exclusively among the Schwann cell-derived blastema cells. We detect *Sox9*/*HoxA* and *Myf5*/*HoxA* coexpression, and we detect expression of either *HoxA* genes or the lineage markers *Myf5* and *Sox9*. We never detect coexpression of *Sox10* and *HoxA* genes. Interestingly, in a significant number of cases we can detect *Sox10* but not *Sec61* in Schwann cell- derived blastema cells.

The graph in Figure 3-14 also shows that in only 55% of the wells in which Schwann cells were sorted, *Sec61* was detected. This is contrasted by 90% of detection in wells containing cDNAs of cells derived from bone, dermis or muscle, and one could assume that Schwann cells are more affected by dissociation and FACS sorting. In fact, dermal- and bone- derived cells dissociated more easily from their corresponding tissue than Schwann cells. To test whether there is evidence for dying Schwann cells as a result of cell dissociation, we incubated them with 7'AAD, a nuclear dye that intercalates into the DNA of dead cells exclusively. We found 2% dead cells among the dissociated Schwann cell population, suggesting that Schwann cells were left intact. In addition, we sorted fluorescent Schwann cells into medium and could still observe some of these cells attached to the bottom of the well 24 hours after sorting. Furthermore, we detected transcripts encoding the transcription factor Sox10 in 26% of the cDNAs generated from single Schwann cells, showing that putatively low abundant transcripts can be amplified from dissociated Schwann cells. These experiments suggest that Schwann cell derived progenitors were not more affected than cells of other tissues.

Our data show that, among progeny of skeletal-, dermal- and muscle tissue in the blastema, cells express *HoxA* genes, while progeny of Schwann cells does not. This coincides with our previous findings regarding the expression and localization of Meis proteins in progenitor cells of different origin and suggests that skeletal-, dermal- and muscle tissue possess proximo-distal information, while Schwann cells do not.

3.2.12 Distal bone cells stably retain their distal character during regeneration while distal Schwann cells do not

It has been shown *in vivo* and *in vitro* that blastema cells deriving from different levels along the proximo-distal axis behave different in their adhesiveness and segregate from each other, and it is widely accepted that these properties of the cells are part of the mechanism that leads to the reestablishment of the proximo-distal axis. However, experiments addressing these questions were directed to the blastema as a whole tissue, so that it is not known whether all cell types in the blastema harbor this ability to segregate from cells of different proximo-distal levels. Furthermore, at the

blastema stage cells have already obtained their positional values and it has never been investigated whether they stably retain their identity or whether there is a time point before blastema formation in which cells can be potentially reprogrammed in a distal to proximal direction.

A change in proximo-distal identity is most obvious in the skeletal pattern, therefore we transplanted fluorescent bone tissue of one digit to the mature upper arm, thus replacing the humerus with a finger bone element. As a control, we replaced the humerus of wild type hosts with a fluorescent donor humerus. Figure 3-16 shows representative examples of a distal and a proximal graft followed through the course of regeneration. After allowing the wounds to heal, we amputated through the implant and followed the fluorescent cells during the course of regeneration. After the completion of regeneration, the majority of distally derived cells was found in the hand. In1/13 cases, fluorescence was found distributed equally between lower arm and hand. In contrast, all limbs (15/15) that were harboring a grafted humerus showed fluorescence to be concentrated in the upper and lower arm after regeneration, and only a few cells were detected in the hand.

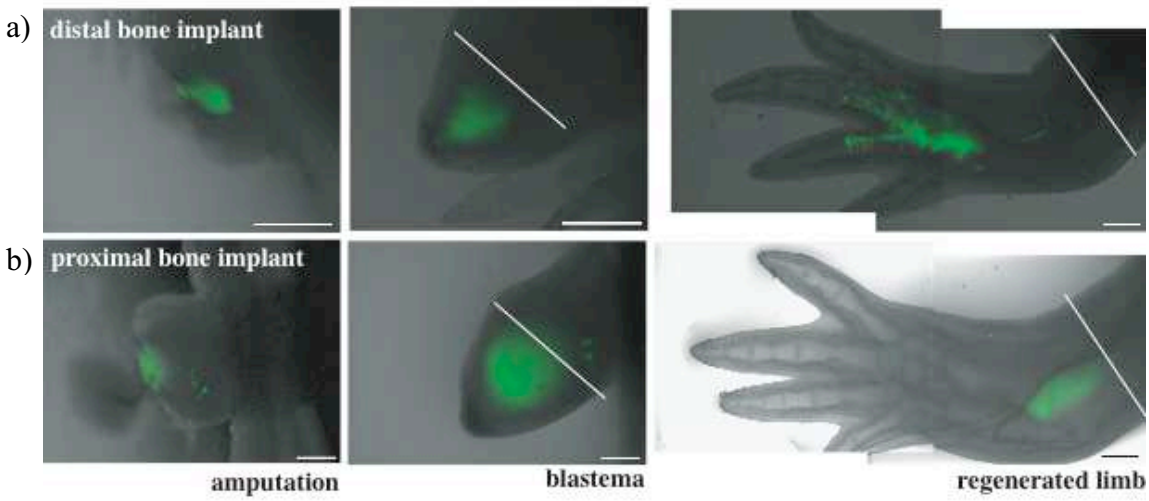

Fig. 3-16: Distal bone- derived cells stably retain their distal identity. a) Distal translocation of distally derived fluorescent progeny of bone cells that were implanted into the upper arm, thereby replacing the humerus 2 weeks before amputation. Note that fluorescent cells are found in the hand after regeneration. In comparison, we show in b) the behavior of proximally derived fluorescent bone that was transplanted in the same way. In contrast, fluorescent cells are found concentrated in the upper and lower arm after regeneration. Pictures are representatives of 13 distal and 15 proximal bone implants. White lines mark the amputation plane. Distal is to the left. Bars: 0.5 mm.

To quantify this difference of cell localization after regeneration, we sectioned through 3 representative regenerates that received digit- and humerus graft prior to amputation, respectively, and counted the number of fluorescent cells found in the hand versus the number of those found in the lower arm. In addition, we also analyzed the regenerate in that we found distally derived cells equally distributed between hand and lower arm. In each case, we did not count cells in the upper arm, since it was not possible to detect the amputation plane and thus to differentiate between those cells that dedifferentiated and contributed to the regenerate from those that did not. In those regenerates that received a distal graft, 70% to 93% of the progeny was found in the hand after regeneration, and in that case in which digit derived cells distributed equally between hand and lower arm, 40% of the fluorescent derivatives were found in the hand. In contrast, only 17% to 23% of the cells deriving from the humerus implant were found in the hand and the majority of cells was detected in the lower arm.

Table 3-5*: Translocation of proximal versus distal bone derived cells after implantation in the upper arm, amputation and regeneration

sample	Cells in hand	Cells in lower arm	% cells distal
Proximal implant 1	42	211	17
Proximal implant 2	122	587	17
Proximal implant 3	973	2365	29
Distal implant 1	176	75	70
Distal implant 2	2624	197	93
Distal implant 3	1070	91	92
Distal implant – exceptional case	85	121	41

*We scored only cells of upper arm and hand, as we were unable to identify the exact location of the amputation plane. Therefore, we were were unable to distinguish between cells belonging to the regenerated part of the upper arm versus those belonging to the stump.

This difference in translocation of distal bone versus proximal bone derived cells suggests that cells of this lineage keep their positional memory and segregate from those cells that carry more proximal values. In addition, our data support the hypothesis that cells do not proximalize during the earliest stages of regeneration.

Although we do not know the genetic network that controls the maintenance of positional identity, we have shown that bone derived blastema cells contain Meis in their nucleus and express *HoxA* genes, which are both implicated in proximo-distal patterning. In contrast, we did not find any evidence for Schwann cells expressing these regulators. We wanted to investigate whether the lack of these positional markers in the Schwann cell progeny correlates with their ability to maintain their proximo-distal identity during regeneration. Therefore, we transplanted mature hand derived fluorescent Schwann cells to the mature upper arm of a wild type host, allowed the wounds to heal and amputated through the graft. In all 15 cases we found fluorescent progeny deriving from these distal grafts evenly distributed along the proximo-distal axis (Figure 3-17). We reamputated 5 limbs through the regenerated part of the upper arm, and in each case fluorescent cells populated the entire regenerate.

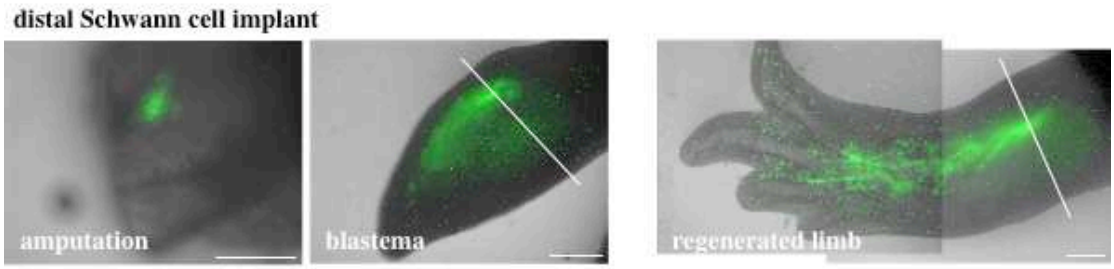

Fig. 3-17: Translocation of distally derived fluorescent progeny of Schwann cells that were implanted into the upper arm. Note the difference to distally derived progeny of bone (Fig. 3-16). The example shown represents the result obtained from 15 distal Schwann cell implants. The white line shows the amputation level. Distal is to the left. Bars: 0.5 mm.

The different behavior of distal bone versus distal Schwann cell progeny regarding the maintenance of their positional value correlates with the nuclear localization of Mei*s* and expression of *HoxA* genes in these cells. All together, these data suggest that Schwann cells do not encode information that leads promotes the reestablishment of the proximo-distal axis.

3.3 Discussion

3.3.1 Experimental conditions and composition of the transplants

We followed the fate of GFP labelled cells deriving from different tissues and investigated their ability to transdifferentiate and reestablish the proximo-distal axis of the limb. Previous studies addressed these questions without using molecular markers, and all experiments investigating the role of dermis and nerves in contributing to other tissues were performed on irradiated limbs (Namenwirth, 1974; Dunis and Namenwirth, 1977; Maden, 1977; Holder, 1989). In contrast, we chose experimental conditions that allow us to track cells in unaffected limbs, and our analyses were supported using molecular markers.

For our experiments, we transplanted fluorescent upper arm skin, skeletal and muscle tissue as well as grafts containing fluorescent Schwann cells to the upper arm of a wild type host. With the exception of the Schwann cell grafts, all other transplants harbored several labeled cell types. Skin contains the epidermal layer, dermal fibroblasts, blood vessels and nerve sheaths with Schwann cells attached. Besides muscle fibers and satellite cells, muscle grafts contained fibroblasts, nerve sheaths and blood vessels as well. Skeletal grafts contained cartilage, perichondrium and presumably also cells of the ligaments/joint connective tissue.

Thus, we are aware that these transplants harbored a variety of different cell identities. However, as we discuss below, these conditions allowed us to address and answer fundamental questions concerning the heterogeneity of the blastema.

3.3.2 Cells of skeletal- and dermal origin do not give rise to muscle

Is the blastema a homogeneous pool of pluripotent cells, or do blastema cells possess a tissue specific memory? More specifically, can all blastema cells potentially form muscle, or is this ability restricted to a subset of cells?

Previous studies elucidated that cells of the skeleton do not give rise to myogenic cells (Steen, 1968; Namenwirth, 1974), and limb regeneration can occur in the complete absence of muscle (Holder, 1989). However, none of these studies could exclude the possibility that a subset of cells originating from dermis forms myogenic

cells during regeneration, due to putative contamination in dermal grafts and the difficulty to distinguish myogenic cells from fibroblasts resident in muscle tissue at that time.

We readdressed this question using Pax7 and MHCI as markers for the myogenic line to investigate whether any fluorescent bone- or dermis- derived cell upregulates these markers during regeneration. Using GFP labelled bone and skin grafts enabled us to immediately identify those limbs in which fluorescent muscle fibers formed after integration and exclude those from our analysis.

We did not find any evidence for either bone- or dermis-derived cells to upregulate these markers either during or after regeneration, demonstrating that neither skeletal nor dermal cells normally contribute to muscle tissue. This confirms earlier findings investigating the fate of skeletal cells and further strengthens the hypothesis that muscle does not form from skin tissue. However, we cannot rule out that specific cells in the skin have the potential to form muscle, which may become most obvious under conditions where all other stump tissue had been affected by irradiation. Nevertheless, we find this possibility rather unlikely.

3.3.3 The fate of muscle- derived blastema cells

Since neither bone nor skin contribute to muscle during regeneration, what tissue gives rise to the newly forming muscle? We found that new muscle fibers and satellite cells form exclusively from preexisting muscle tissue. Therefore, dedifferentiating muscle fibers, satellite cells or fibroblasts of muscle connective tissue are candidates to form new myogenic tissue. Whether fibroblasts can switch their lineage and in which way cells of dedifferentiated muscle fibers and satellite cells contribute has to be addressed with promoter specific labeling of these various cell types.

From some implants of muscle tissue, fluorescent progeny was found in the skeletal elements. This finding is consistent with earlier work showing that implants of muscle gave rise to basically all tissue types of the regenerate, including cartilage (Steen, 1968; Namenwirth, 1974). However, neither this work nor our study can discriminate myogenic cells from other, non-myogenic cells in the tissue graft. Recently, it has been shown that purified and BrDU labelled satellite cells, when implanted into a blastema, are found in cartilage and epidermis after regeneration was complete

(Morrison et al., 2006). While we cannot exclude that fluorescent cells in the skeleton could possibly derive from satellite cells, we did not find any evidence that descendants from muscle implants contribute to epidermis.

3.3.4 The fate of bone-derived blastema cells

In line with previous findings, we found cells of skeletal origin to give rise mainly to the skeleton including cartilage, perichondrium and ligaments. Only a small number of cells were found located outside the bone tissue, distributed either between radius and ulna in the lower arm, in muscle or dermal tissue. Marker specific analysis showed that these cells were neither Schwann cells nor myogenic, and morphologically they resembled fibroblasts. This finding is consistent with what has been described before (Namenwirth, 1975; Steen, 1968). Interestingly, in these studies more fibroblasts formed from skeletal elements in the background of an irradiated limb, suggesting that bone tissue has a limited capacity to compensate for the loss of connective tissue. However, neither those nor our studies can exclude that contaminating fibroblasts were transferred along the skeletal grafts and that bone exclusively gives rise to bone during the course of regeneration.

3.3.5 The fate of dermis derived blastema cells

Descendants from the skin gave rise to a variety of tissues and, based on morphological observations, were found to be present in tendons, skeletal elements and connective tissue in the muscle. These cells are very likely to derive from the dermal component of the skin. In irradiated limbs, it has been shown that epidermal cells cover the wound after amputation without regenerating new mesodermal tissue (Namenwirth, 1974), and there is no reason to assume that this situation could be different in our experimental system. Our results are consistent with earlier studies, however, in this work dermis was transplanted to irradiated limbs, and the contribution to various other cell types could be due to a compensation for the damaged tissue in the stump (Namenwirth, 1974; Dunis and Namenwirth, 1977, Holder, 1989). Here, we show that the contribution of dermal cells to skeleton,

tendons and various connective tissues reflects the normal situation during regeneration.

The major component of the dermis are the fibroblasts, and it is not known whether and how these cells differ from other fibroblasts, for example those being resident in muscle tissue. Since dermis and muscle tissue both contain fibroblasts and both contribute to skeletal elements, are these changes due to fibroblasts? It has been shown that the various kinds of connective tissue fibroblasts and cartilage cells synthesize a somewhat similar assortment of cell products (Thorp and Dorfman, 1967). Therefore it may not require drastic changes when a dermal or connective tissue fibroblast converts into a cartilage cell, or vice versa. In contrast, myogenic cells drive a completely different genetic program, and it may be less likely that a fibroblast starts to produce various types of myosins and contributes to a muscle fiber or a satellite cell. From our studies we can exclude dermal fibroblasts to take a myogenic fate. Whether this is also true for fibroblasts in the muscle tissue and in which way myogenic cells behave regarding the change of identities will be the goal of future investigations using promotor specific labeling of cells. In our laboratory, the isolation of different cell type specific promoters and the development of the tools to label specific cell types are in progress (Sharyhar Khattak, personal communication).

3.3.6 Tissue lineage specific organization of the blastema

A blastema of the midbud stage is a self operating system (Stocum, 1968) and divides into at least 3 domains consisting either of upper arm, lower arm or hand progenitors (Echeverri and Tanaka, 2005). In this regard, we found it interesting to note that the blastema at that stage is also organized in a tissue specific manner (Figures 3-5, 3-6 and 3-15). We found that the blastema divides into a central domain containing bone-derived and a peripheral domain containing dermis-derived progenitors, with a few cells of dermal origin spreading towards the centre of the blastema. Those are probably cells giving rise to skeletal elements, tendons or muscle connective tissue. We can observe lineage specific organization also at the level of marker gene expression: Chondrogenic, sox9^{+} cells concentrate in the centre of the blastema, however, this domain does not connect with the mature bone of the stump and leaves

a sox9$^-$ domain inbetween, suggesting that chondrogenic specification does not start in dedifferentiated cells that are located next to the bone. As both antibody staining against pax7 and in situ hybridizations for myf5 show, myogenic cells are located at the periphery of the blastema, however, they do not mix with the outer-most cells.
The distribution of differently originating blastema cells and the well defined expression of lineage markers in specific domains of the blastema provide further evidence that, despite morphologically appearing as a homogeneous pool, blastema cells bear fundamental differences depending on their origin and fate.

3.3.7 Expression of the lineage markers *Sox9*, *Sox10* and *Myf5* in descendants of bone, dermis, muscle and Schwann cells

The fact that new muscle tissue arsises from muscle implants implies that descendants of these grafts express the myogenic lineage markers *Myf5* and Pax7 (Buckingham et al., 2003). Consistent with this, we found Pax7$^+$ and *Myf5*$^+$ cells in blastema cells deriving from muscle tissue (Figures 3-6 and 3-15). The presence of *Myf5*$^-$ and Pax7$^-$ cells is not surprising for us as descendants of these muscle grafts give also rise to a variety of other tissues. Progeny of the bone-, dermis- or Schwann cell grafts did not express these markers, showing that none of these graft type gives rise to myogenic cells and confirming what we had found earlier.
Cartilage arises from descendants of bone, dermis and muscle tissue, and we expect cells of all three types of grafts to express the chondrogenic marker *Sox9* in the blastema. We detected *Sox9*$^+$ cells among progeny of skeleton and muscle, but so far not of dermis. However, this is very likely to be due to the fact that only a very small fraction of the dermal cells switches to the chondrogenic lineage, so that the accumulation of more cells will allow us to detect *Sox9*$^+$ cells among dermal progenitors. The low number of *Sox9* expressing cells (25%) deriving from bone may reflect that only these cells truly form cartilage, while the rest gives rise to perichondrium and joint connective tissue. Furthermore, we are aware that we are looking at ‘snapshots’, and it is possible that the respective *Sox9*$^-$ cells would start expression minutes, hours or days later as a result of cell cycle dependent transcription or differences in the differentiation state, respectively. Sox10 is a transcription factor that marks neural crest derived cells (Kelsh et al., 2006), and so

far there is no information about its expression in any tissue of the axolotl. In the search for a marker that allows us to specifically detect progeny of Schwann cells in the blastema, by analyses of cDNAs generated from single cells we found this gene to be expressed by 25% of descendants of Schwann cells. So far, we did not detect *Sox10* expressing cells among the progeny of all other tissue types, suggesting that we found a marker specific for Schwann cells. The fact that we detected *Sox10* in only 25% of the cells may reflect dynamics in gene expression, such as cell cycle dependent transcription. Expression analysis using in situ hybridization is in progress.

3.3.8 Tissue architecture – who can build a limb?

So far, it had not been investigated whether all cells in the blastema are equally involved in the proximo-distal patterning. In studies transplanting distal blastemas to proximal stumps, we noticed that not all distally- derived cells were displaced to the hand (Stocum, 1975; Pecorino et al., 1996), however, this issue was not included into the authors's discussion. Assuming that all cells that carry positional information adhere to the 'rule of distal transformation' (Rose, 1962; Stocum, 1975) and do not become reprogrammed in a distal-to-proximal way, we wanted to examine whether there is a population of cells in the blastema that does not carry positional identity.

How can we study whether cells contain the information where to place tissues of a finger, a lower arm, an upper arm? The mechanisms by which the complex three-dimensional structure of the limb forms during the course of regeneration are largely unknown.

To assess whether a cell carries positional identity, we chose criteria that are based on studies identifying Meis and *HoxA* as important genes controlling proximo-distal patterning (Morgan et al., 1992; Dolle et al., 1993; Small and Potter, 1993; Davis and Capecchi, 1994; Davis et al., 1995; Yokouchi et al., 1995; Fromental-Ramain et al., 1996; Zakani and Duboule, 1996; Nelson et al., 1996; Mercader et al. 1999, 2005; Boulet and Capecchi, 2004) or revealed cell surface based properties related to positional information. This becomes most obvious when distal blastema cells are grafted to a more proximal location of the blastema. Following the rule of distal transformation, the majority of these cells translocated to their original level during the course of regeneration (Crawford and Stocum, 1988; Echeverri and Tanaka,

2005). To us, a tissue either possesses positional information when at least some cells of its progeny in the blastema express *HoxA* genes or localize Meis proteins to their nucleus. Alternatively, distal translocation of distally derived cells is a strong indication that the respective tissue harbors retains its positional identity, and we investigated this by transplanting respective tissues derived from the hand to the upper arm level, following their progeny through the course of regeneration after amputating through the transplant.

It is known that dermis plays a major role in the patterning process (Carlson, 1974, 1975; Tank, 1979, 1981; Maden and Mustafa, 1982; Slack, 1980, 1983; Rollmann-Dinsmore and Bryant, 1984; Holder, 1989). Furthermore, skeletal elements show a characteristic pattern in the limb, with different morphologies in the hand versus the arm. As progeny of dermis, bone and muscle contribute to bone, one would expect descendants of these tissues to fulfil atleast one of our criteria. But, does this also apply to Schwann cells?

3.3.9 Schwann cells do not express positional markers and do not adhere to the 'rule of distal transformation'

Progeny of Schwann cells was neither found to express *HoxA* genes, locate Meis to the nucleus nor showed the characteristic distal translocation. The distribution of distally derived Schwann cells along the entire arm could also suggest that cells became respecified to a more proximal fate during the earliest phases, possibly by retinoic acid. However, this is very unlikely as it has been shown that meis is an essential component in proximalization and responds to retinoic acid, but we did not find any evidence for meis signalling in these cells.

We are aware that other positional markers may exist and other, yet unknown cellular properties may lead to the reestablishment of the proximo-distal axis. However, the correlation between not expressing two important positional markers and the failure of distal translocation strongly suggests that Schwann cells are not part of that mechanism which leads to the reestablishment of the proximo-distal axis.

From the data obtained by single cell analysis, one could argue that Schwann cells were not left intact during the dissociation and, as a result, downregulated their genes. Indeed, we detected *Sec61* in only 56% of the cells, although we expect it to be

present in every cell. Analysis by FACS did not show any evidence for these cells being damaged, and we could sort and culture some of them for at least 24 hours. Furthermore, the detection of transcripts coding for Sox10, which we expect to be abundant at a similar level like transcripts coding for HoxA proteins, suggests that not all cells were affected in their transcription. Furthermore, analysis of nuclear Meis localization and the grafting experiment strengthen our finding that Schwann cells do not actively contribute to pattern the regenerating limb.

3.3.10 Bone-, dermis- and muscle derived progenitor cells express positional markers

Consistent with our expectations, we found both nuclear Meis localization and *HoxA* gene expression in bone-, dermis- and muscle- derived blastema cells, suggesting that these tissues potentially contribute to the patterning process.

While nearly all descendants of bone displayed a strong meis staining in their nucleus, this number was lower in progeny of dermal and muscle origin and varied from graft to graft. This may result from the fact that the transplants consisted of cells carrying different identities, and the numbers of those cell types expressing the marker genes we were analyzing for may have varied in each individual transplantation. To be able to perform statistical analysis on *Hox* gene expression of progenitors derived from all four different types of grafts and compare the percentages of cells, more cells have to dissociated and analyzed by single cell PCR.

As *HoxA9* expression in the absence of *HoxA13* marks future upper arm and lower arm cells, it was interesting to note that more bone derived cells express and localize Meis in comparison to *HoxA9* expression. However, in situ hybridizations on *HoxA9* will have to confirm that the data we obtain using single cell PCR reflect the normal situation.

Apart from differences in the nuclear localization of Meis and the expression of *HoxA* genes, these data suggest that progeny of bone, dermis takes part in the processes that lead to the reestablishment of the proximo-distal axis of the limb.

3.3.11 Bone- derived cells adhere to the 'rule of distal transformation'

The finding that bone derived cells possess positional information is further strengthened by the fact that the vast majority of distal bone descendants translocate to their level of origin during the course of regeneration when transplanted more proximally before. We noted that not all cells derived from distal bone grafts translocated to the hand region after amputation. Whether this is due to experimental conditions or represents those cells that do not express *HoxA* genes is not clear.
We would have liked to perform this transplantation assay also on distal dermis and muscle tissues, however, this turned out to be experimentally challenging. Both tissue types are protruded by a fine meshwork of nerves, and we showed that distally derived Schwann cell progeny distributes along the entire arm under these conditions. Therefore, it is difficult to determine whether all fibroblasts or myogenic cells translocate to their distal origin.

3.3.12 The expression of positional markers correlates with the (in)ability of distal translocation in grafts of bone and Schwann cells

Our experiments demonstrate that the behaviour of distal bone and Schwann cell grafts regarding their translocation during regeneration correlates with the expression of patterning relevant genes in progeny of these tissues. We do not know how both issues are linked. It has been shown that retinoic acid regulates Meis (Mercader et al., 2005) and Prod1, a molecule being involved in proximalization and cell surface mediated recognition of positional identity (da Silva et al., Echeverri and Tanaka, 2005). We would expect the effect of distal translocation to be blocked if we either incubated distal bone grafts in retinoic acid prior to transplantation and amputation, or overexpressed Meis or Prod1 in distal bone cells.
Using this transplantation assay, it would be interesting to determine what factors are sufficient to induce positional memory in putative neutral cells, such as Schwann cells. Does ectopic expression of Prod1 or meis keep the entire cell population at upper and lower arm levels? Conversely, would overexpression of HoxA13 in Schwann cells lead to their distalization? However, whether such an assay is realistic

or not largely depends on other factors, for example the state off differentiation/dedifferentiation of Schwann cells in the blastema.

3.3.13 The coexpression of *HoxA* genes with *Myf5*, *Sox9* and *Sox10*

So far, we showed that cells deriving from muscle possess positional information, but we could not satisfactory show that dedifferentiating myofibers or satellite cells express marker genes associated with proximo-distal identity.
Using single cell PCR, we showed that 25% myf5 expressing cells also express *HoxA* genes, suggesting that future muscle fibers or satellite cells possess positional identity. It remains unknown whether *Myf5*$^{+}$/*HoxA9*/*13*$^{-}$ cells represent specific subpopulations of *Myf5* expressing cells. For example, positional information might be required for future muscle fibers, but not satellite cells. It is also not clear whether cells coexpressing *Myf5* and *HoxA* genes derive from dedifferentiating muscle fibers, satellite cells or transdifferentiating fibroblasts of the muscle connective tissue.
Our results are consistent with data obtained from the developing limb bud, in which myogenic cells have been shown to express *HoxA* genes (Yamamoto et al., 1998), suggesting that myogenic cells are involved in patterning the developing limb.
We also detected *Sox9*$^{+}$/*HoxA9*/*13*$^{+}$ cells, a result that we expected as *HoxA* genes are involved in adhesion and differentiation of cartilage during development (Morgan et al., 1992; Dolle et al., 1993; Small and Potter, 1993; Davis and Capecchi, 1994; Davis et al., 1995; Yokouchi et al., 1995; Fromental-Ramain et al., 1996; Zakani and Duboule, 1996; Boulet and Capecchi, 2004).
Therefore, our analyses on single cells suggest that, during regeneration, myogenic and chondrogenic cells possess positional information and supplement data obtained from the developing limb demonstrating the same phenomenon during limb development.

3.3.14 Is there a proximalizing factor during the earliest stages?

It has been speculated whether RA acts as a proximalizing morphogen, and Echeverri and Tanaka (2005) showed that distal blastema cells do not become reprogrammed when transplanted to a more proximal region of the blastema, they retain their identity

and contribute to hand tissue in the regenerated limb. However, the earliest stages of regeneration immediately after wounding, when only a few dedifferentiating cells are present and the regenerate presumably consists of a few layers of cells, have not been considered. We show for the first time that also during the earliest stages cells adhere to the 'rule of distal transformation' and do not become reprogrammed in a distal-to-proximal manner. Therefore, our results strongly suggest that it is rather unlikely that retinoic acid acts on proximo-distal patterning during regeneration.

3.3.15 Our results in the context of previous findings

In our work, we reinvestigated important questions concerning cell plasticity and positional information using the power of molecular markers. It has always been unclear whether dermis- derived progenitors contribute to muscle tissue during regeneration (Namenwirth, 1974; Dunis and Namenwirth, 1977; Holder, 1989), and we show for the first time that this is clearly not the case. Since earlier studies addressed this study on irradiated limbs, it is possible that under such conditions specific cells in the dermis are forced to change their identity to a myogenic fate. However, since we observed dermal cells to give rise to a variety of other tissues including cartilage, tendons and connective tissue under normal conditions, we find this possibility very unlikely that. The formation of skeletal elements and connective tissue from dermis is consistent with earlier results, and we can also confirm that the majority of bone- derived blastema cells gives rise to newly forming bone during regeneration.

Using Meis and *HoxA* as molecular markers for positional information, we confirmed earlier studies suggesting that dermal and muscle tissue harbor information regarding the patterning of the regenerate (e.g. Carlson, 1974, 1975). Descendants of both tissues were shown to express HoxA or localize Meis to their nucleus, strongly suggesting that they have an impact on proximo-distal patterning. Bone has been thought to not play a role in the patterning (Carlson, 1975, Muneoka et al., 1986), although paradoxically unirradiated bone can rescue regeneration in irradiated limbs, forming a limb that is patterned in its proximo-distal axis (Namenwirth, 1974). We provide evidence that bone- derived cells harbor positional information. First, we also found Meis and *HoxA* to be expressed. Second, distally derived bone cells recognized

when they were grafted more proximally and translocated back to their level of origin during regeneration.

The role of Schwann cells has been poorly investigated, although three studies taken 30 years ago suggest that Schwann cells could potentially form a normally patterned limb (Wallace, 1972, 1973; Maden, 1977). We suggest here that Schwann cells do not play any role in proximo-distal patterning, as they neither express important key regulators of positional identity nor harbor the ability to retain the information regarding what proximo-distal level they derive from.

Research on regeneration aims to identify molecules and networks that can be used for tissue engineering and the regrowth of defective or damaged tissues. In this regard, it will be certainly an advantage to know what cell types play a major role in establishing a specific pattern and which cell types do not.

3.3.16 Future perspectives

Future studies will have to address the fate and potential to pattern the regenerate on specific cell types. Do fibroblasts in the muscle contribute to muscle fibers or satellite cells during regeneration? Do cartilage cells form perichondrial cells during regeneration? Which types of cells such as satellite cells, dedifferentiating muscle fibers, endothelial cells, cartilage cells, perichondrial cells, muscle resident and dermal fibroblasts express *Meis* or *HoxA* genes, and which of these cell types adheres to the rule of distal transformation? These and other questions will be answered using promotor specific cell labeling, and the isolation of promotor sequences and the development of the appropriate genetic tools are in progress (Sharyhar Khattak, personal communication).

4. Materials and Methods

4.1 Axolotl care

Ambystoma mexicanum (axolotls) were bred in our facility where they were kept at 18°C in Dresden tap water. Small animals (2-5 cm) were fed daily with artemia, larger animals (5-10 cm) were fed 2-3 times per week with fish pellets. For surgery and live microscopy, animals were anesthesized in 0.01% ethyl-p-benzoate (Sigma). The experiments described here were performed 3-10 cm long larval axolotls. White strain axolotls were used that contain negligible skin pigmentation.

4.2 Microscopy

4.2.1 Fluorescent live microscopy

Fluorescent cells in either mature tissue or different blastema stages were imaged live through the axolotl skin that is only several cell layers thick in larval axolotls. The cells were imaged using a 25x or 50x planeofluar objective on a Zeiss Axiovert 200 system with a Spot digital camera, controlled by MetaMorph image acquisition software.

4.2.2 Fluorescent microscopy on tissue sections

To visualize fluorescence and meis antibody staining and GFP, digital images of axolotl limb blastema longitudinal sections were taken on an upright Olympus BX61 microscope using a camera purchased from Diagnostic Instruments Inc. under the control of the Spot Advanced program.
The images were taken with using the 4x, 10x and 20x objectives.

4.3 Immunohistochemistry

Limbs were fixed in freshly made 4% paraformaldehyde (Riedel-de-Haen) overnight at 4°C. After washing in PBS, limbs were equilibrated in 30% sucrose (Applichem) and frozen in Tissuetek (O.C.T. compound; Sakura). 18 m thick cryosections were prepared, washed in TBS/0.3% Tween (Sigma), blocked in TBS+20% goat serum (Gibco) and stained with primary antibodies over night at 4°C. After several washing steps in TBS/0.3% Tween, sections were incubated with the secondary antibody for 1 hour at room temperature. The sections were then washed and incubated with Hoechst (Sigm; 1 g/ml), washed again and mounted in TBS/glycerol.
Primary and secondary antibodies used are listed in Table 4-1.

Table 4-1: Antibodies used in this study

Primary antibodies

name of antibody	obtained from	species	dilution
anti-Meis 1/2/3, clone 9.2.7	Upstate cell signalling solutions	mouse	1:200
anti-Pax7	Generated from hybridoma cell lines in the lab by Anja Telzerow	axolotl	supernatant of cells
anti-MHC	Gene Tex Industries	mouse	1:1000
anti-MBP	Gene tex Industries	rat	1:100
anti-β3-tubulin	R&D systems	mouse	1:1000

Secondary antibodies

anti-mouse Cy5	Chemicon	goat	1:200
anti-rat Cy3	Chemicon	rabbit	1:100

4.4 Molecular Biology

4.4.1 RNA extraction from axolotl tissue

To extract total RNA, 1 ml of Trizol (Invitrogen) was added to 50-100mg of deep frozen axolotl tissue that had been grinded to a powder in liquid nitrogen before. The tissue was homogenized by passing it multiple times through a syringe with a 25 guage needle and incubated for 5 min at room temperature. 0.2 ml of chloroform (Merck) was added per ml of Trizol and the tube was shaken vigorously for 15 sec. After a 5 min incubation at room temperature, the mixture was centrifuged at 4°C and 13,000 rpm for 10 min. The aqueous phase was removed afterwards and 0.25 ml of isopropanol (Merck) and 0.25 ml of RNA precipitation solution (0.8 M citrate and 1.2 M NaCl) were added. Everything was mixed well, incubated at room temperature for 10 min and centrifuged again at 4°C and 13,000 rpm. The supernatant was discarded and the pellet washed in 75% and 100% Ethanol (Merck). After the pellet had dried, it was dissolved in RNase free water (Gibco). RNA concentrations were measured using an Ultrospec 2100 pro spectrometer (Amersham Biosciences). Stocks were kept in liquid nitrogen.

4.4.2 cDNA preparation from total RNA

1 µg of total RNA was mixed with 500 ng poly d(T) primer (Bioline), 1 µl of 10 mM dNTP's (Sigma) and water to a volume of 13 µl. The tube was heated for 5 min at 65°C and dropped to 42°C. 4 µl of 5x first strand buffer were mixed with 2 µl of 100 mM DTT (both Invitrogen) and added to the tube. After a 2 min incubation at 42°C, 1 µl of SSII reverse transcriptase (Invitrogen) was added to the mixture. Reverse transcription was performed at 42°C for 50 min. The reverse transcriptase was heat inactivated at 70°C for 10 min afterwards. CDNA was stored at -20°C.

4.4.3 PCR

PCR reactions were performed in a total volume of 50µl containing 0.2 M of each dNTP, reaction buffer (protein expression facility), 0.2 M of each primer (Sigma) and 5 units of TAQ polymerase (protein expression facility). Either 1-2 µl of cDNA or 200 ng of plasmid DNA were used as a template. Depending on the annealing temperature of the primers and the length of the generated product, 35 cycles with 15 s at 95°C, 30 s at 55-60°C and 30-90 s at 72°C were performed. The PCR products were analyzed on a 1% agarose gel containing 1.3 µl Ethidiumbromide and, if necessary, purified using the purification kit (Quiagen) following the manufacturer's instructions.

4.4.4 Cloning of *Sox9*

A partial *Sox9* sequence was cloned using degenerate primers whose forward and reverse primer sequences can be seen in Table 4-2. PCR reactions were performed as described above. The reaction product was purified from a 1% agarose gel and cloned into the pCRII vector (sequence available at www.invitrogen.com) using the TA cloning kit (Invitrogen), following the instructions by the manufacturer. Transformation was performed using the F' bacteria that were provided along with the TA cloning kit, following the manual. The plasmids were purified using the Miniprep kit (Quiagen), following the manufacturer's manual and given for sequencing of the insert using the in house service. The insert was sequenced using the T7 and SP6 primers (provided by the service), for which the pCRII vector provides binding sites 3' and 5' to the multiple cloning site, respectively. Sequences were analyzed and blasted using the following website: www.ncbi.nlm.nih.gov/BLAST/.

4.4.5 3' RACE of sox9 and HoxA13

Based on the published *HoxA13* sequence (Gardiner et al., 1995) and on the cloned *Sox9* sequence, 3' RACE was performed on cDNA prepared from a midbud stage blastema using the Smart II RACE kit (BD Bioscience), following the instructions given by the manufactorer. The respective sets of primers as well as the primer set used to extend *HoxA13* is seen in Table 4-2. After purification and sequencing of the reaction products, the correct sequence was verified by performing a PCR in which the primers were designed so that the forward primer would hybridize 5' to the binding sites of the RACE primers, while the reverse primer would hybridize in the region that was amplified by RACE, as close as possible to the 3' end of the sequence.
In both cases, a band of the correct size was obtained that was purified and verified by sequencing.

Table 4-2: Primers used to clone and extend *Sox9* and *HoxA13*

Cloning of *Sox9* using degenerate primers

gene	forward	reverse
Sox9	CACATCAARACVGAGCARCTGAG	GTGTASACKGGYTGYTCCCAGTG

3'RACE of *HoxA13* and *Sox9*

gene	RACE primer	nested primer
HoxA13	CTCAAGACCACCAGCTAATGGACTCCC	GGTCTCAACAAAAACCTAAGCCGAAGC
Sox9	CCTATCGCAGACACGACGGGC	CCAGCACTGGGAACAACCCGTCTAC

Cloning of *HoxA13* and *Sox9*

gene	forward	reverse
HoxA13	TGGAATGGGCAAGTGTACTG	CACGGCGGTATTTTATGGTG
Sox9	TCAACCTGCAGCAGCACTAC	GGCACAGAGAAAAGACACTTG

4.4.6 *Ambystoma mexicanum* genes used in this study

Sequences of *Rp4*, *Sec61*, *Twist* and *HoxA9* were obtained from our EST library (accession numbers Am 2630, Am 1372 and Am 588, respectively). *HoxA9* was identified using primers directed against the well conserved homeobox domain by Frank Martin). The sequence of *Myf5* was a kind gift of Karen Echeverri, the sequence of *Sox10* was a kind gift by Akira Tazaki. The cloned sequence of *Sox9* can be accessed from the website http://www.ncbi.nlm.nih.gov/ using the accession number AY894689.

4.5 In situ hybridization

4.5.1 Probe preparation

DNA templates for sense and antisense probes were prepared by PCR from the respective genes using primers with SP6 and T7 polymerase promoter overhangs. The primers were designed so that the entire sequence was amplified, and depending on the length of the known sequence, the length of the products ranged from 500-1500 bp, Transcription was performed from the purified PCR product at 37°C for 2 hours with the DIG RNA labeling kit (Roche), following the manual provided by rhe manufacturer. Probes were purified by precipitation with 100% Ethanol plus 4M LiCl in TE at -20°C for 1 hour to overnight and dissolved in 100 µl of Rnase free water. 1-2 µl of probe was used per 100 µl of hybridization buffer.

4.5.2 Section In situ hybridization

Axolotl limb tissue was fixed in 4% fresh paraformaldehyde overnight at 4°C, washed in PBS, equilibrated in 30% sucrose and embedded in tissue tek.
16 µm thick sections were mounted on Superfrost adhesive slides and dried at RT for several hours. The sections were quickly washed in PBS and treated with denaturation mix (2% SDS, 100 mM DTT in 1x PBS) for 20 min at RT. After 3 washes with PBS/0.1% tween the sections were digested with Proteinase K (1 µg/ml) in PBS/tween for 10 min at 37°C and post-fixed directly afterwards with 4% PFA at RT.

Slides were washed in PBS/tween and incubated at RT for 15 min in triethanolamine with 0.25% acetic anhydride. After several washes in PBS/tween, slides were prehybridized in hybridization buffer (50% formamide, 5x SSC, 5x Denhardts, 750 µg/µl yeast RNA, 0.1% tween) for 1 hour at 70°C and then hybridized over night at 70°C with the DIG labeled probe in hybridization buffer. Slides were then washed twice an hour at 70°C in post-hybridization buffer (50% formamide, 2x SSC, 0.1% tween) and then three times for 10 min in maleic acid buffer (100 mM maleic acid at pH 7.5, 150 mM NaCl, 0.1% tween). Sections were then incubated in blocking buffer (maleic acid buffer plus 10% goat serum) for 1 hr at RT and then incubated overnight at 4°C in blocking buffer plus alkaline phosphatase conjugated anti-DIG antibody (diluted 1:2000). Slides were washed twice in maleic acid buffer and twice in alkaline phosphatase buffer (100 mM Tris-Cl at pH 9.5, 50 mM $MgCl_2$, 100 mM NaCl, 0.1% tween). Each slide was overlayed with filtered NBT-BCIP (Sigma) for 1-2 days at RT. The staining reaction was stopped with PBS/tween and the slides mounted in 90% glycerol.

4.6 Cell dissociation and FACS sorting

For cell dissociation and subsequent FACS sorting, our GFP transgenic line (Sobkow et al., 2006) was used, with the advantage that non-green red blood cells and, based on the brightness of the GFP signal, damaged and leaking cells could be sorted out.
Axolotl limb blastemas or mature tissue were manually dissected in papain based dissociation solution (100 U/ml Dnase IV (Roche), 10 µg /ml cystein (Sigma), 30 U/ml papain (Sigma) in 65% L-15 medium (Gibco)) or liberase based dissociation solution (100 U/ml Dnase IV, 0.35 mg/ml liberase blendzyme (Roche) in 80% PBS. Depending on the tissue (dermis-, muscle- or Schwann cell derived blastema cells, entire blastemas or mature tissue) to be dissociated and on the size of the blastemas, 1-4 blastemas or 1-2 mature limbs per ml dissociation solution were dissected until a single cell suspension was visible. Liberase dissociates under mild conditions, however, the dissociation is very ineffective and especially single cells of the myogenic lineage are underrepresented. Using papain, more cells are lyzed, but dissociation with this enzyme results in a higher yield of single cells, and myogenic cells are less underrepresented.

After the dissociation, the cell suspension was transferred into a new tube so that large tissue pieces were left behind. When dissociated with papain, cells were washed and incubated with DRAQ5 (Axxora) at 4°C for 20 min. When dissociated with liberase, cells were incubated with DRAQ5 directly without prior washing.

Cells were then passed through a 22 µm filter and FACS sorted into reverse transcription buffer. Only bright green and single cells were sorted. Our gating strategy can be seen seen from Figure 4-1.

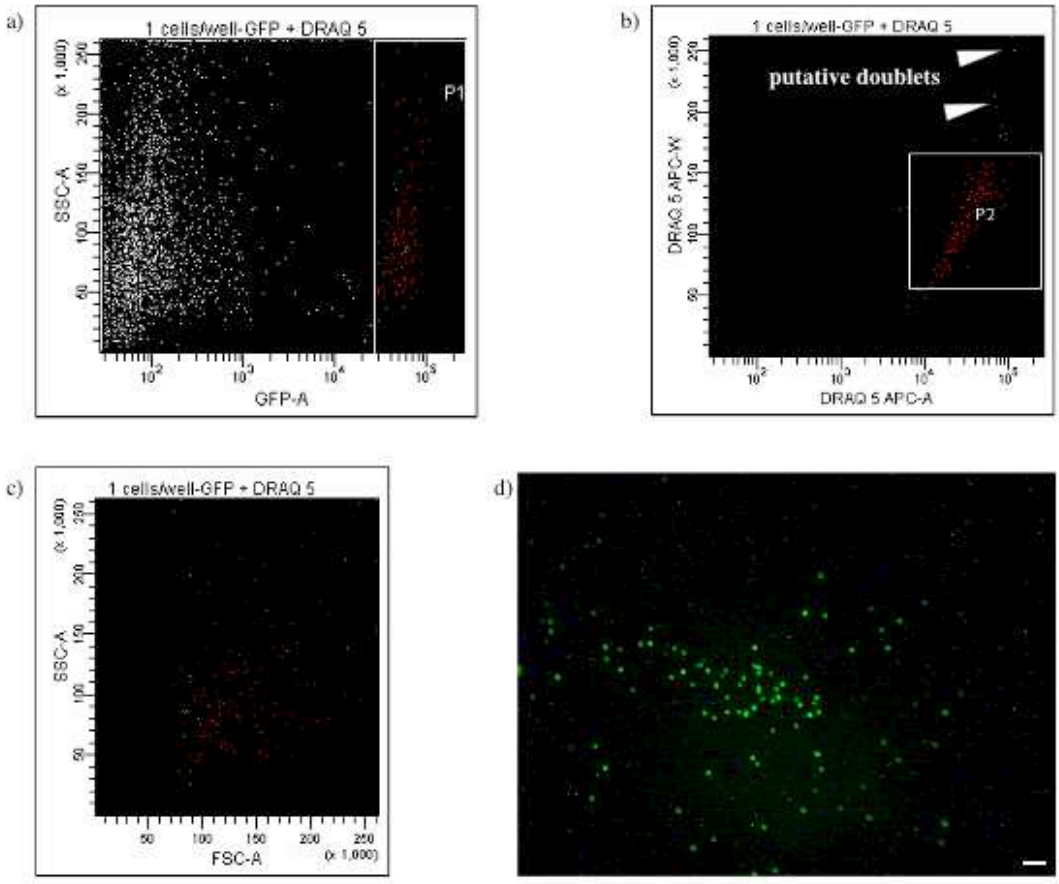

Fig. 4-1: Gating strategy of sorting single cells. a) We dissociated tissues of transgenic animals harboring GFP under the control of the CAGGS promotor. The white line marks until what intensity (x-axis) background fluorescence is detected, and fluorescent counts are found at the right side of that line (P1 fraction). On the left are putative red blood cells and putative damaged GFP+ cells detected b) P1 fraction displayed based on DRAQ5 staining, which allows distinction of singlets from doublets based on detecting area and width. High width signals reflect doublets, at lower signals are the singlets. The scatter suggests that doublets in our cell suspension are found at an approximate signal of 250 (arrow heads), the majority of events is found at signals between 75 and 150, possibly due to cell and nucleus size and the orientation of the cell when moving through detection. We sorted putative single cells from widths until 170 (P2 fraction) to be sure to not sort doublets. c) The P2 fraction scattered by

FSC (size) and SSC (granulation and surface characteristic, demonstrating that this population is very divergent with respect to these parameters. d) Sorting of the P2 fraction and microscopical analysis show that we obtain single fluorescent cells. Bar: 100µm.

4.7 Single cell PCR

4.7.1 Reverse Transcription

Cells were sorted into a 96 well plate in which each well contained 5µl reverse transcription buffer centrifuged and incubated for 1 min at 65°C and 3 min at 22°C. 2.6 µl RNase free water and 0.4 µl SSII reverse transcriptase (Invitrogen) were then added to each well so that the reverse transcription buffer reached a final volume of 8 µl containing 50 mM Tris-Cl pH 8.3, 75 mM KCl, 0.1 ng/µl RT primer (sequence: TGG ACT AAC TAT GAA TTC TTT TTT TTT TTT TTT TTT TTT V), 2 µM dNTP's, 0.5% NP40 (Fluka), 0.08 µl RNAguard (GE Healthcare) and 0.27 µl Prime RNase inhibitor (VWR). For reverse transcription, the plate was incubated at 42°C for 15 min and 70°C for 10 min.

4.7.2 Poly A tailing

To each reaction well, 8 µl polyadenylation solution was added to reach a final concentration of 100 mM of potassium cacodylate (Roche), 2 mM of $CoCl_2$ (Roche), 0.2 mM of DTT, 100µM of dATP and 0.2 µl terminal transferase (Roche) were added to reach a final volume of 16 µl. The plate was incubated at 37°C for 15 min and at 65°C for 10 min.

4.7.3 PCR

The reaction volume was increased to 50 µl for PCR amplification to reach a final concentration of 1x reaction buffer (protein expression facility), 1 mM dNTP's, 0.07 µg/µl PCR primer (sequence: CAT GTC GTC CAG GCC GCT CTG GGA CAA AAT ATG AAT TC TTT TTT TTT TTT TTT TTT TTT TTT) and 0.1 U/µl TAQ polymerase (protein expression facility). After one complete run (1 cycle of 37°C for

5 min and 72°C for 20 min; 25 cycles of 94°C for 1 min, 42°C for 2 min and 72°C for 6 min plus 10 sec extension/cycle), fresh TAQ polymerase was supplied along with buffer, dNTP's and PCR primer to a final volume of 60 µl and maintaining the final concentrations of each component. After the addition of the fresh components, the amplification reaction was repeated. After the completion of the second run, we normally generated a total amount of 8-10 µg cDNA which was analyzed subsequently in a quantitative PCR using gene specific primers.

4.7.4 Real time PCR on cDNA generated by single cell PCR

The cDNAs obtained from single cell PCR were used as a template to perform quantitative PCR at a final dilution of 1:1000. Reactions were performed in a total volume of 10 µl using the SYBR Green kit from Stratagene and following the instructions given by the manufacturer. We used the recommended final primer concentration of 300 nm. Sequences of gene specific primers are seen in Table 4-3.

Table 4-3 Gene specific primers used on axolotl cDNAs generated from single cells

gene	forward	reverse
Rp4	TGAAGAACTTGAGGGTCATGG	CTTGGCGTCTGCAGATTTTTT
Sec61	CTGGTGAATGCTGCCATC	CACTGTTCCGCAGGAAAGATA
HoxA9	TGCTGGACAGTGGCTATCAC	CAACGAGCATGAAAGGAGGT
HoxA13	GGGCACACTAAAAAGGTTAAA	GCAGGGTTTACGACAATGTAC
Twist	ACATTGCCCACACTCCATTT	TAGACACCGGATCCATCAGC
Myf5	AGCAGATTCCTGCGATGTTT	GCACCACATGACAAAACACA
Sox9	CCCCCAGAAAGCAAAACTGT	GGCACAGAGAAAAGACACTG
Sox10	CATCCAGCCAGGAAAGAAGA	AATGGGCGAAGTATGGAGTG

4.8 Axolotl surgery

In each case, the respective tissue was grafted to a wild type host from a transgenic donor of the same size, expressing GFP under the control of the CAGGS promotor (Sobkov et al., 2005). Transplantation of dermal, muscle and cartilage tissue was performed on 5-8 cm big animals. Special care was taken to transfer tissues from left hindlimb to left hindlimb, left forelimb to left forelimb, a.s.o.

4.8.1 Skin

For grafting fluorescent skin, a large piece of the dorsal upper arm host skin was removed and replaced by a smaller square of donor tissue. Before transplanting, the grafts were carefully checked for underlying muscle tissue and, if necessary, cleaned. The anterior-posterior orientation was kept.
The skin flaps were washed and attached nerves were, if possible, removed. At the same location, skin was removed from the host to place the graft. The anterior/posterior orientation was kept in order to avoid any abnormalities during regeneration. After 2 weeks, grafts were found integrated into the host limb without scar formation.

4.8.2 Muscle

The proximal limb of a donor animal was amputated and transferred into APBS. After removal of bone and dermal tissue, muscle tissue was inserted into a host limb. Host muscle tissue was removed and minced to increase the chance of integration and formation of fluorescent muscle fibers. After 4 weeks, fluorescent muscle fibers could be observed in about 5% of the cases, and amputation was performed slightly proximal to the area of transplantation.

4.8.3 Bone

The humerus of a donor was removed and placed into APBS, where it was cleaned from contaminating muscle. The bone was then placed into papain mix (see 4.6) for 30 min to digest contaminating cells. The humerus was then placed into a host limb whose humerus had been removed before.The limb was amputated through the region of the graft 2-4 weeks after transplantation.

5. References

Agata, K., and Watanabe, K. (1999). Molecular and cellular aspects of planarian regeneration. Semin Cell Dev Biol 10, 377-83.

Becker, T., Wullimann, M. F., Becker, C. G., Bernhardt, R. R., and Schachner, M. (1997). Axonal regrowth after spinal cord transection in adult zebrafish. J Comp Neurol 377, 577-95.

Bischler, V. (1926). L'influence du squellette dans la regeneration, et les potentialities des divers terrotoires du member chez *Triton cristatus*. *Rev. Suisse Zool.*, 33, 431-560.

Boilly, B., Cavanaugh, K. P., Thomas, D., Hondermarck, H., Bryant, S. V., and Bradshaw, R. A. (1991). Acidic fibroblast growth factor is present in regenerating limb blastemas of axolotls and binds specifically to blastema tissues. Dev Biol 145, 302-10.

Boulet, A. M., and Capecchi, M. R. (2004). Multiple roles of Hoxa11 and Hoxd11 in the formation of the mammalian forelimb zeugopod. Development 131, 299-309.

Brady, G., and Iscove, N. N. (1993). Construction of cDNA libraries from single cells. Methods Enzymol 225, 611-23.

Buckingham, M., Bajard, L., Chang, T., Daubas, P., Hadchouel, J., Meilhac, S., Montarras, D., Rocancourt, D., and Relaix, F. (2003). The formation of skeletal muscle: from somite to limb. J Anat 202, 59-68.

Butler, E.G., and O'Brien, J.P. (1942). Effects of localized x-radiation on regeneration of
the urodele limb. Anat Rec. 84, 407-413

Carlson, B. M. (1974). Morphogenetic interactions between rotated skin cuffs and underlying stump tissues in regenerating axolotl forelimbs. Dev Biol 39, 263-85.

Carlson, B. M. (1975). The effects of rotation and positional change of stump tissues upon morphogenesis of the regenerating axolotl limb. Dev Biol 47, 269-91.

Carlson, B. M. (1975). Multiple regeneration from axolotl limb stumps bearing cross-transplanted minced muscle regenerates. Dev Biol 45, 203-8.

Cebria, F., Kobayashi, C., Umesono, Y., Nakazawa, M., Mineta, K., Ikeo, K., Gojobori, T., Itoh, M., Taira, M., Sanchez Alvarado, A., and Agata, K. (2002). FGFR-related gene nou-darake restricts brain tissues to the head region of planarians. Nature 419, 620-4.

Chalkeley, D.T. (1954). A quantitative histological analysis of forelimb regeneration in *Triturus viridescens, J. Morphol*. 94, 21-70.

Chen, Y., Lin, G., and Slack, J. M. (2006). Control of muscle regeneration in the Xenopus tadpole tail by Pax7. Development 133, 2303-13.

Chiang, M. K., and Melton, D. A. (2003). Single-cell transcript analysis of pancreas development. Dev Cell 4, 383-93.

Christensen, R. N., and Tassava, R. A. (2000). Apical epithelial cap morphology and fibronectin gene expression in regenerating axolotl limbs. Dev Dyn 217, 216-24.

Christensen, R. N., Weinstein, M., and Tassava, R. A. (2001). Fibroblast growth factors in regenerating limbs of Ambystoma: cloning and semi-quantitative RT-PCR expression studies. J Exp Zool 290, 529-40.

Christensen, R. N., Weinstein, M., and Tassava, R. A. (2002). Expression of fibroblast growth factors 4, 8, and 10 in limbs, flanks, and blastemas of Ambystoma. Dev Dyn 223, 193-203.

Cohen, S. M., Bronner, G., Kuttner, F., Jurgens, G., and Jackle, H. (1989). Distal-less encodes a homoeodomain protein required for limb development in Drosophila. Nature 338, 432-4.

Cohen, S. M., and Jurgens, G. (1989). Proximal-distal pattern formation in Drosophila: cell autonomous requirement for Distal-less gene activity in limb development. Embo J 8, 2045-2055.

Crawford, K., and Stocum, D. L. (1988). Retinoic acid coordinately proximalizes regenerate pattern and blastema differential affinity in axolotl limbs. Development 102, 687-98.

da Silva, S. M., Gates, P. B., and Brockes, J. P. (2002). The newt ortholog of CD59 is implicated in proximodistal identity during amphibian limb regeneration. Dev Cell 3, 547-55.

Davies, A., Simmons, D. L., Hale, G., Harrison, R. A., Tighe, H., Lachmann, P. J., and Waldmann, H. (1989). CD59, an LY-6-like protein expressed in human lymphoid cells, regulates the action of the complement membrane attack complex on homologous cells. J Exp Med 170, 637-54.

Davis, A. P., and Capecchi, M. R. (1994). Axial homeosis and appendicular skeleton defects in mice with a targeted disruption of hoxd-11. Development 120, 2187-98.

Davis, A. P., Witte, D. P., Hsieh-Li, H. M., Potter, S. S., and Capecchi, M. R. (1995). Absence of radius and ulna in mice lacking hoxa-11 and hoxd-11. Nature 375, 791-5.

Dearlove, G. E., and Stocum, D. L. (1974). Denervation-induced changes in soluble protein content during forelimb regeneration in the adult newt, Notophthalmus viridescens. J Exp Zool 190, 317-28.

Dolle, P., Izpisua-Belmonte, J. C., Brown, J., Tickle, C., and Duboule, D. (1993). Hox genes and the morphogenesis of the vertebrate limb. Prog Clin Biol Res 383A, 11-20.

Dulac, C., and Axel, R. (1998). Expression of candidate pheromone receptor genes in vomeronasal neurons. Chem Senses 23, 467-75.

Dungan, K. M., Wei, T. Y., Nace, J. D., Poulin, M. L., Chiu, I. M., Lang, J. C., and Tassava, R. A. (2002). Expression and biological effect of urodele fibroblast growth factor 1: relationship to limb regeneration. J Exp Zool 292, 540-54.

Dunis, D. A., and Namenwirth, M. (1977). The role of grafted skin in the regeneration of x-irradiated axolotl limbs. Dev Biol 56, 97-109.

Echeverri, K., Clarke, J. D., and Tanaka, E. M. (2001). In vivo imaging indicates muscle fiber dedifferentiation is a major contributor to the regenerating tail blastema. Dev Biol 236, 151-64.

Echeverri, K., and Tanaka, E. M. (2002). Ectoderm to mesoderm lineage switching during axolotl tail regeneration. Science 298, 1993-6.

Echeverri, K., and Tanaka, E. M. (2005). Proximodistal patterning during limb regeneration. Dev Biol 279, 391-401.

Endo, T., Bryant, S. V., and Gardiner, D. M. (2004). A stepwise model system for limb regeneration. Dev Biol 270, 135-45.

French, V., Bryant, P. J., and Bryant, S. V. (1976). Pattern regulation in epimorphic fields. Science 193, 969-81.

Fromental-Ramain, C., Warot, X., Messadecq, N., LeMeur, M., Dolle, P., and Chambon, P. (1996). Hoxa-13 and Hoxd-13 play a crucial role in the patterning of the limb autopod. Development 122, 2997-3011.

Gann, A. A., Gates, P. B., Stark, D., and Brockes, J. P. (1996). Receptor isoform specificity in a cellular response to retinoic acid. Proc Biol Sci 263, 729-34.

Gardiner, D. M., Blumberg, B., Komine, Y., and Bryant, S. V. (1995). Regulation of HoxA expression in developing and regenerating axolotl limbs. Development 121, 1731-41.

Gardiner, D. M., and Bryant, S. V. (1996). Molecular mechanisms in the control of limb regeneration: the role of homeobox genes. Int J Dev Biol 40, 797-805.

Gargioli, C., and Slack, J. M. (2004). Cell lineage tracing during Xenopus tail regeneration. Development 131, 2669-79.

Habermann, B., Bebin, A. G., Herklotz, S., Volkmer, M., Eckelt, K., Pehlke, K., Epperlein, H. H., Schackert, H. K., Wiebe, G., and Tanaka, E. M. (2004). An Ambystoma mexicanum EST sequencing project: analysis of 17,352 expressed sequence tags from embryonic and regenerating blastema cDNA libraries. Genome Biol 5, R67.

Globus, M. (1988). A neuromitogenic role for substance P in urodele limb regeneration.
In: Inoue S, Shirai T, Egar M, Aiyama S, Geraudie J, Nobunaga T, Sato NL (eds). Regeneration and development. Okada Printing & Publishing, Maebashi, pp 675-685.

Hartmann, C. H., and Klein, C. A. (2006). Gene expression profiling of single cells on large-scale oligonucleotide arrays. Nucleic Acids Res 34, e143.

Hata, S., Namae, M., and Nishina, H. (2007). Liver development and regeneration: from laboratory study to clinical therapy. Dev Growth Differ 49, 163-70.

Hay, E.D. (1959). Electron microscopic observations of muscle dedifferentiation in regenerating *Amblystoma* limbs. *Dev Biol* 3: 26-59.

Hay, E. D., and Fischman, D. A. (1961). Origin of the blastema in regenerating limbs of the newt Triturus viridescens. An autoradiographic study using tritiated thymidine to follow cell proliferation and migration. Dev Biol 3, 26-59.

Holder, N. (1989). Organization of connective tissue patterns by dermal fibroblasts in the regenerating axolotl limb. Development 105, 585-93.

Holder, N., Bryant, S. V., and Tank, P. W. (1979). Interactions between irradiated and unirradiated tissues during supernumerary limb formation in the newt. J Exp Zool 208, 303-10.

Iten, L. E., and Bryant, S. V. (1975). The interaction between the blastema and stump in the establishment of the anterior--posterior and proximal--distal organization of the limb regenerate. Dev Biol 44, 119-47.

Kawakami, Y., Rodriguez-Leon, J., and Belmonte, J. C. (2006). The role of TGFbetas and Sox9 during limb chondrogenesis. Curr Opin Cell Biol 18, 723-9.

Kelsh, R. N. (2006). Sorting out Sox10 functions in neural crest development. Bioessays 28, 788-98.

Kim, W. S., and Stocum, D. L. (1986). Retinoic acid modifies positional memory in the anteroposterior axis of regenerating axolotl limbs. Dev Biol 114, 170-9.

Kumar, A., Velloso, C. P., Imokawa, Y., and Brockes, J. P. (2000). Plasticity of retrovirus-labelled myotubes in the newt limb regeneration blastema. Dev Biol 218, 125-36.

Lo, D. C., Allen, F., and Brockes, J. P. (1993). Reversal of muscle differentiation during urodele limb regeneration. Proc Natl Acad Sci U S A 90, 7230-4.

Loyd, R. M., and Tassava, R. A. (1980). DNA synthesis and mitosis in adult newt limbs following amputation and insertion into the body cavity. J Exp Zool 214, 61-9.

Maden, M. (1977). The regeneration of positional information in the amphibian limb. J Theor Biol 69, 735-53.

Maden, M. (1977). The role of Schwann cells in paradoxical regeneration in the axolotl. J Embryol Exp Morphol 41, 1-13.

Maden, M. (1979). The role of irradiated tissue during pattern formation in the regenerating limb. J Embryol Exp Morphol 50, 235-42.

Maden, M. (1980). Intercalary regeneration in the amphibian limb and the rule of distal transformation. J Embryol Exp Morphol 56, 201-9.

Maden, M. (1983). The effect of vitamin A on the regenerating axolotl limb. J Embryol Exp Morphol 77, 273-95.

Maden, M. (1983). A test of the predictions of the boundary model regarding supernumerary limb structure. J Embryol Exp Morphol 76, 147-55.

Maden, M. (1985). Retinoids and the control of pattern in regenerating limbs. Ciba Found Symp 113, 132-55.

Maden, M., and Goodwin, B. C. (1980). Experiments on developing limb buds of the axolotl Ambystoma mexicanum. J Embryol Exp Morphol 57, 177-87.

Maden, M., and Mustafa, K. (1982). The structure of 180 degrees supernumerary limbs and a hypothesis of their formation. Dev Biol 93, 257-65.

Meinhardt, H. (1983). A boundary model for pattern formation in vertebrate limbs. J Embryol Exp Morphol 76, 115-37.

Mercader, N., Leonardo, E., Azpiazu, N., Serrano, A., Morata, G., Martinez, C., and Torres, M. (1999). Conserved regulation of proximodistal limb axis development by Meis1/Hth. Nature 402, 425-9.

Mercader, N., Leonardo, E., Piedra, M. E., Martinez, A. C., Ros, M. A., and Torres, M. (2000). Opposing RA and FGF signals control proximodistal vertebrate limb development through regulation of Meis genes. Development 127, 3961-70.

Mercader, N., Tanaka, E. M., and Torres, M. (2005). Proximodistal identity during vertebrate limb regeneration is regulated by Meis homeodomain proteins. Development 132, 4131-42.

Mescher, A. L. (1976). Effects on adult newt limb regeneration of partial and complete skin flaps over the amputation surface. J Exp Zool 195, 117-28.

Mescher, A. L. (1996). The cellular basis of limb regeneration in urodeles. Int J Dev Biol 40, 785-95.

Michael, M. I., and Faber, J. (1961). The self-differentiation of the paddle-shaped limb regenerate, transplanted with normal and reversed proximo-distal orientation after removal of the digital plate (Ambystoma mexicanum). Arch Biol (Liege) 72, 301-30.

Morgan, B. A., Izpisua-Belmonte, J. C., Duboule, D., and Tabin, C. J. (1992). Targeted misexpression of Hox-4.6 in the avian limb bud causes apparent homeotic transformations. Nature 358, 236-9.

Morrison, J. I., Loof, S., He, P., and Simon, A. (2006). Salamander limb regeneration involves the activation of a multipotent skeletal muscle satellite cell population. J Cell Biol 172, 433-40.

Mullen, L. M., Bryant, S. V., Torok, M. A., Blumberg, B., and Gardiner, D. M. (1996). Nerve dependency of regeneration: the role of Distal-less and FGF signaling in amphibian limb regeneration. Development 122, 3487-97.

Muneoka, K., Fox, W. F., and Bryant, S. V. (1986). Cellular contribution from dermis and cartilage to the regenerating limb blastema in axolotls. Dev Biol 116, 256-60.

Namenwirth, M. (1974). The inheritance of cell differentiation during limb regeneration in the axolotl. Dev Biol 41, 42-56.

Nardi, J. B., and Stocum, D. L. (1983). Surface properties of regenerating limb cells: evidence for gradation along the proximodistal axis. *Differentiation* 25, 27-31

Nelson, C. E., Morgan, B. A., Burke, A. C., Laufer, E., DiMambro, E., Murtaugh, L. C., Gonzales, E., Tessarollo, L., Parada, L. F., and Tabin, C. (1996). Analysis of Hox gene expression in the chick limb bud. Development 122, 1449-66.

Niazi, I. A., and Saxena, S. (1978). Abnormal hindlimb regeneration in tadpoles of the
toad *Bufo andersoni*, exposed to vitamin A. *Folia Biol* (Krakow) 26, 3-11

Niswander, L., Tickle, C., Vogel, A., Booth, I., and Martin, G. R. (1993). FGF-4 replaces the apical ectodermal ridge and directs outgrowth and patterning of the limb. Cell 75, 579-87.

Nye, H. L., Cameron, J. A., Chernoff, E. A., and Stocum, D. L. (2003). Regeneration of the urodele limb: a review. Dev Dyn 226, 280-94.

O'Steen, W.R., and Walker, B.E. (1961). Radioautographic studies of regeneration in the
common newt. II. Regeneration of the forelimb. *Anat. Rec.* 142, 179-188

Otteson, D.C., and Hitchcock, P.F (2003). Stem cells in the teleost retina: persistent neurogenesis and injury-induced regeneration. *Vision Res* 43(8): 927-36

Papageorgiou, S., and Holder, N. (1983). The structure of supernumerary limbs formed after 180 degrees blastemal rotation in the newt Triturus cristatus. J Embryol Exp Morphol 74, 143-58.

Pecorino, L. T., Entwistle, A., and Brockes, J. P. (1996). Activation of a single retinoic acid receptor isoform mediates proximodistal respecification. Curr Biol 6, 563-9.

Pescitelli, M. J., Jr., and Stocum, D. L. (1980). The origin of skeletal structures during intercalary regeneration of larval Ambystoma limbs. Dev Biol 79, 255-75.

Poss, K. D. (2007). Getting to the heart of regeneration in zebrafish. Semin Cell Dev Biol 18, 36-45.

Poss, K. D., Shen, J., and Keating, M. T. (2000). Induction of lef1 during zebrafish fin regeneration. Dev Dyn 219, 282-6.

Quertermous, E. E., Hidai, H., Blanar, M. A., and Quertermous, T. (1994). Cloning and characterization of a basic helix-loop-helix protein expressed in early mesoderm and the developing somites. Proc Natl Acad Sci U S A 91, 7066-70.

Reddien, P. W., Bermange, A. L., Murfitt, K. J., Jennings, J. R., and Sanchez Alvarado, A. (2005). Identification of genes needed for regeneration, stem cell function, and tissue homeostasis by systematic gene perturbation in planaria. Dev Cell 8, 635-49.

Reddien, P. W., Bermange, A. L., Murfitt, K. J., Jennings, J. R., and Sanchez Alvarado, A. (2005). Identification of genes needed for regeneration, stem cell function, and tissue homeostasis by systematic gene perturbation in planaria. Dev Cell 8, 635-49.

Reddien, P. W., Oviedo, N. J., Jennings, J. R., Jenkin, J. C., and Sanchez Alvarado, A. (2005). SMEDWI-2 is a PIWI-like protein that regulates planarian stem cells. Science 310, 1327-30.

Repesh, L.A., and Oberpriller, J.C. (1978). Scanning electron microscopy of epidermal cell migration in wound healing during limb regeneration in the adult newt *Notophthalmus viridescens*. *Am J Anat* 151: 539-556.

Riddiford, L. M. (1960). Autoradiographic studies of tritiated thymidine infused into the blastema of the early regenerate in the adult newt, Triturus. J Exp Zool 144, 25-31.

Rollman-Dinsmore, C., and Bryant, S. V. (1984). The distribution of marked dermal cells from small localized implants in limb regenerates. Dev Biol 106, 275-81.

Rose, S. M. (1962). Tissue-arc control of regeneration in the amphibian limb. *Symp. Soc. Study Develop. Growth* 20, 153-176

Sanchez Alvarado, A., Newmark, P. A., Robb, S. M., and Juste, R. (2002). The Schmidtea mediterranea database as a molecular resource for studying platyhelminthes, stem cells and regeneration. Development 129, 5659-65.

Saunders, J.W. Jr (1948). The proximo-distal sequence of the origin of the parts of the chick wing and the role of the ectoderm. *J. Exp. Zool.* 108, 363-403

Schilthuis, J. G., Gann, A. A., and Brockes, J. P. (1993). Chimeric retinoic acid/thyroid hormone receptors implicate RAR-alpha 1 as mediating growth inhibition by retinoic acid. Embo J 12, 3459-66.

Slack, J. M. (1983). Positional information in the forelimb of the axolotl: properties of the posterior skin. J Embryol Exp Morphol 73, 233-47.

Slack, J. M. (2003). Regeneration research today. Dev Dyn 226, 162-6.

Slack, M. J. (1980). Morphogenetic properties of the skin in axolotl limb regeneration. J Embryol Exp Morphol 58, 265-88.

Small, K. M., and Potter, S. S. (1993). Homeotic transformations and limb defects in Hox A11 mutant mice. Genes Dev 7, 2318-28.

Sobkow, L., Epperlein, H. H., Herklotz, S., Straube, W. L., and Tanaka, E. M. (2006). A germline GFP transgenic axolotl and its use to track cell fate: dual origin of the fin mesenchyme during development and the fate of blood cells during regeneration. Dev Biol 290, 386-97.

Steen, T. P. (1968). Stability of chondrocyte differentiation and contribution of muscle to cartilage during limb regeneration in the axolotl (Siredon mexicanum). J Exp Zool 167, 49-78.

Stocum, D. L. (1968). The urodele limb regeneration blastema: a self-organizing system. I. Morphogenesis and differentiation of autografted whole and fractional blastemas. Dev Biol 18, 457-80.

Stocum, D. L. (1968). The urodele limb regeneration blastema: a self-organizing system. i. Differentiation in vitro. Dev Biol 18, 441-56.

Stocum, D. L. (1975). Regulation after proximal or distal transposition of limb regeneration blastemas and determination of the proximal boundary of the regenerate. Dev Biol 45, 112-36.

Stocum, D. L. (1980). Intercalary regeneration of symmetrical thighs in the axolotl, Ambystoma mexicanum. Dev Biol 79, 276-95.

Stocum, D. L. (1982). Determination of axial polarity in the urodele limb regeneration blastema. J Embryol Exp Morphol 71, 193-214.

Stocum, D. L., and Melton, D. A. (1977). Self-organizational capacity of distally transplanted limb regeneration blastemas in larval salamanders. J Exp Zool 201, 451-61.

Stoick-Cooper, C. L., Moon, R. T., and Weidinger, G. (2007). Advances in signaling in vertebrate regeneration as a prelude to regenerative medicine. Genes Dev 21, 1292-315.

Takano, T., Pulvers, J. N., Inoue, T., Tarui, H., Sakamoto, H., Agata, K., and Umesono, Y. (2007). Regeneration-dependent conditional gene knockdown (Readyknock) in planarian: Demonstration of requirement for Djsnap-25 expression in the brain for negative phototactic behavior. Dev Growth Differ 49, 383-94.

Tank, P. W. (1978). The occurrence of supernumerary limbs following blastemal transplantation in the regenerating forelimb of the axolotl, Ambystoma mexicanum. Dev Biol 62, 143-61.

Tank, P. W. (1979). Positional information in the forelimb of the axolotl: experiments with double-half tissues. Dev Biol 73, 11-24.

Tassava, R. A., and Garling, D. J. (1979). Regenerative responses in larval axolotl limbs with skin grafts over the amputation surface. J Exp Zool 208, 97-110.

Thornton, C.S. (1938). The histogenesis of the regenerating fore limb of larval *Amblystoma* after exarticulation of the humerus. *J Morph* 62, 219-235

Thornton, C. S. (1968). Amphibian limb regeneration. Adv Morphog 7, 205-49.

Thorp, F.K., and Dorfman, A. (1967). Differentiation of connective tissues. In: "Current topics in Developmental Biology". (A. A. Moscona and A. Monroy, eds., pp. 151-190. Academic Press, New York.

Trampusch, H. A. (1959). [Recent tests determining the effects of x-rays on morphogenesis.]. Ned Tijdschr Geneeskd 103, 695-6.

Wallace, B. M., and Wallace, H. (1973). Participation of grafted nerves in amphibian limb regeneration. J Embryol Exp Morphol 29, 559-70.
Wallace, H. (1972). The components of regrowing nerves which support the regeneration of irradiated salamander limbs. J Embryol Exp Morphol 28, 419-35.

Wang, L., Marchionni, M.A., and Tassava, R.A. (2000). Cloning and neuronal expression
of a type III newt neuregulin and rescue of denervated nerve-dependent newt limb blastemas by rhGGF2. *J. Neurobiol.* 43, 150-158.

Wardle, F. C., and Smith, J. C. (2004). Refinement of gene expression patterns in the early Xenopus embryo. Development 131, 4687-96.

Weiss, P. (1925). Unabhängigkeit der Extremitätenregeneration vom Skelett (bei *Triton cristatus). Wilhelm Roux' Arch. Entwicklungsmech. Organ.*, 104, 359-394.

Whitehead, G. G., Makino, S., Lien, C. L., and Keating, M. T. (2005). fgf20 is essential for initiating zebrafish fin regeneration. Science 310, 1957-60.

Wolpert, L. (1969). Positional information and the spatial pattern of cellular differentiation. J Theor Biol 25, 1-47.

Yokouchi, Y., Nakazato, S., Yamamoto, M., Goto, Y., Kameda, T., Iba, H., and Kuroiwa, A. (1995). Misexpression of Hoxa-13 induces cartilage homeotic transformation and changes cell adhesiveness in chick limb buds. Genes Dev 9, 2509-22.

Yoshizato, K. (2007). Growth potential of adult hepatocytes in mammals: highly replicative small hepatocytes with liver progenitor-like traits. Dev Growth Differ 49, 171-84.

Zakany, J., Gerard, M., Favier, B., Potter, S. S., and Duboule, D. (1996). Functional equivalence and rescue among group 11 Hox gene products in vertebral patterning. Dev Biol 176, 325-8.